AN UPDATED GPS VELOCITY FIELD FOR PUERTO RICO AND THE VIRGIN ISLANDS: CONSTRAINTS ON TECTONIC SETTING AND INTERNAL-DEFORMATION

By

Desmond Kelvin Ihemedu

Presented to the Faculty of the Graduate School of

The University of Texas at Arlington in Partial Fulfillment

of the Requirements

for the Degree of

MASTER OF SCIENCE IN GEOLOGY

THE UNIVERSITY OF TEXAS AT ARLINGTON

December 2011

DEDICATION

To God Almighty and to my sweet mother Celestina Ihemedu

ACKNOWLEDGEMENTS

I am heartily thankful to my supervisor, Prof. Glen Mattioli, whose encouragement, guidance, invaluable advice and huge academic support have made it possible for me to complete this research thesis. I will also like to show my gratitude to my thesis committee members (Prof. John Wickham, Prof. Pamela Jansma and Prof. Christopher Scotese) for giving me some time out of their busy schedules to advise me while writing my thesis.

I am highly indebted to my (field) data acquisition team members while I was in the field for data collection in Puerto Rico. In particular, I would like to thank Stephanie Quintana and her step-dad. I also owe my deepest gratitude to my colleague Joseph Salazar; I really appreciate his support while we worked and studied together trying to understand the GIPSY-OASIS II software.

Finally, I would like to express my appreciation to my dear wife Adaobi Desmond and my Arlington friends, Amos Komolafe and Niyi Adedeji for their moral, spiritual and mental support during my studies. I am extremely grateful to you all.

November 18, 2011

ABSTRACT

AN UPDATED GPS VELOCITY FIELD FOR PUERTO RICO
AND THE VIRGIN ISLANDS: CONSTRAINTS
ON TECTONIC SETTING AND
INTERNAL-DEFORMATION

DESMOND KELVIN IHEMEDU, M.S

The University of Texas at Arlington, 2011

Supervising Professor: Glen S. Mattioli

Puerto Rico and the northern Virgin Islands define the eastern end of the Greater Antilles, while the Puerto Rico trench and the Muertos Trough define the northern and the southern limits of the North American – Caribbean plate boundary zone. Three microplates have been defined: (1) Gonave, to the west; (2) Hispaniola, at the center; and (3) Puerto Rico and the northern Virgin Islands (PRVI) at the eastern end. Global Positioning System (GPS) geodesy was previously conducted in this region from 1994 to 2003. It was concluded that the locus of the highest permissible on-surface deformation in Puerto Rico and the northern Virgin Island is within the Lajas Valley, in southeastern Puerto Rico. This thesis presents 32 updated and reprocessed (IGS05) GPS velocities from 32 different sites and locations in the PRVI block. Data were collected and analyzed from 11 newly installed continuous GPS stations. 11 campaign stations were re-occupied while another 10 campaign stations, which could not be re-occupied in 2011 were simply reprocessed in IGS05 with the other 22 stations. The goal was to rigorously test for the magnitude and location of internal deformation within the PRVI microplate.

TABLE OF CONTENTS

LIST OF ILLUSTRATIONS

Figure Page

LIST OF TABLES

CHAPTER 1

INTRODUCTION

1.1 Introduction

Tectonic models for the northern Caribbean (e.g., Byrne et al., 1985; Mann et al., 1995) proposed several microplates within the boundary zone on the basis of geologic and earthquake evidence. It has been suggested that within plate boundary zones, larger earthquakes are more likely to occur along a few major faults or narrow belts of deformation separating discrete crustal blocks, whereas smaller earthquake events may be distributed over a broad region. The controversy as to how the Puerto Rico-Virgin Islands (PRVI) microplate is categorized has been put to partial rest by previous Global Positioning System (GPS) geodetic data analysis. Recent results from GPS geodesy proposed upper bounds on the potential intrablock displacement within the Puerto Rico and the northern Virgin Islands (Jansma et al., 2000; Jansma and Mattioli, 2005). Seismicity along the EW-trending boundary between the North America and Caribbean plates is consistent with evolution of the boundary zone from a relatively simple set of transform faults in the west to a more complex deformation zone ~250 km wide in the east as shown in Fig. 1.1. Motion along the predominantly east-west striking major structures of the northern Caribbean is primarily left-lateral. Fig. 1.2 shows three microplates within the diffuse boundary zone: (1) the Gonave in the west (Mann et al., 1995); (2) the Hispaniola in the center (Byrne et al., 1985); and (3) the Puerto Rico–northern Virgin Islands in the east (Masson and Scanlon, 1991). The Puerto Rico trench and the Muertos trough define the northern and southern limits of the plate boundary zone, respectively. In the west, the Swan and Oriente transform faults define the EW-trending Cayman trough and bound the short (~100 km), NS-trending Mid-Cayman spreading center.

The proposed microplate model assumes that nearly all of the deformation associated with North America–Caribbean motion is concentrated along the faults that bound the three rigid blocks. These are: the Oriente; Septentrional; Enriquillo-Plantain Garden; and Anegada faults; the Muertos trough and North Hispaniola deformed belt; and the Mona rift faults northwest of Puerto Rico as shown in Fig. 1.2.

Jansma et al. (2000) proposed an independently translating Puerto Rico–northern Virgin Islands microplate within the northeastern Caribbean. Previous analysis of sparse GPS geodetic data does not support models that proposed either: (i) counterclockwise rotation of the Puerto Rico–northern Virgin Islands about a nearby vertical axis (Masson and Scanlon, 1991; Reid et al., 1991) or (ii) eastward tectonic escape of the block within the Caribbean–North America plate boundary zone (Jany et al., 1987). Rather Jansma et al. (2000) favored NE - translation of the PRVI block relative to North America, and a relatively simple, monotonic increase in velocity across the PRVI block from east to west. This thesis is focused on updating the geodetic analysis of Jansma et al. (2000) and Jansma and Mattioli (2005) with the inclusion of the most recent geodetic data from both previously established (c.1998-2000) and newly installed (c. 2008) continuous and campaign GPS sites in the Puerto Rico–northern Virgin Islands block. The results were analyzed with respect to ITRF05/IG05 (International Terrestrial Frame 2005) defined by the International GPS Service (IGS) center of the Jet propulsion Laboratory (NASA) together with a refined Caribbean reference frame (DeMets et al., 2000, 2007).

The aim of this thesis is to use updated and recent geodetic data to: (i) refine the velocity of the Puerto Rico–northern Virgin Islands block with respect to the Caribbean plate; (ii) constrain maximum permissible displacements along potentially active faults on the island of Puerto Rico and immediately offshore; and (iii) re-examine potential diffuse extension between the Virgin Islands and eastern Puerto Rico.

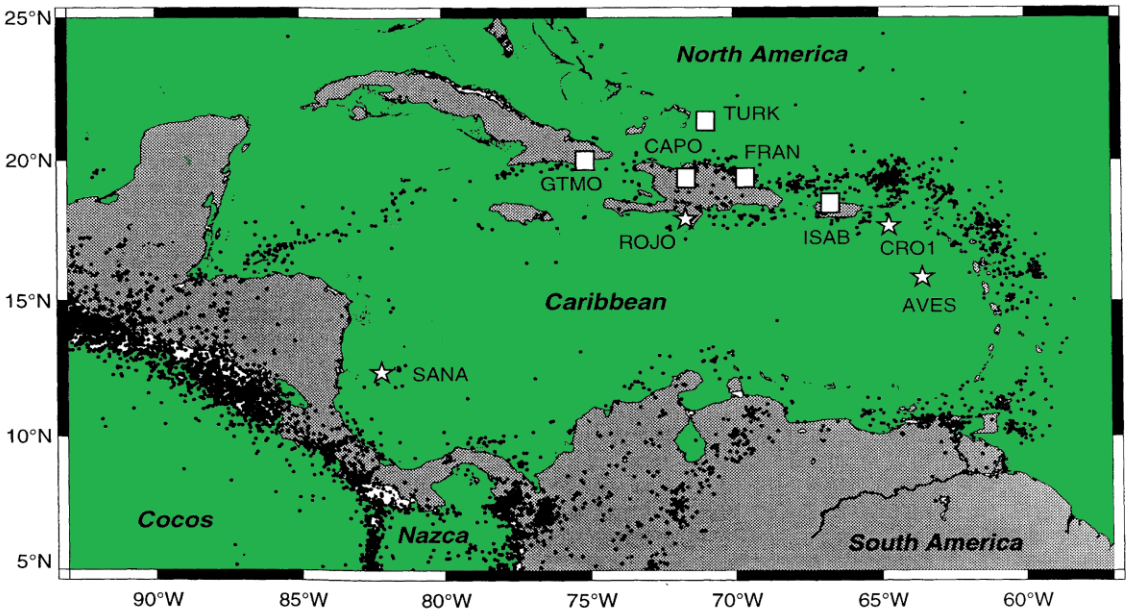

Figure 1.1 Map of Caribbean plate and regional seismicity.

Regional seismicity epicenters for earthquakes above depths of 60 km with magnitudes >3.5 from 1st January 1967 until 28th April 1999 (U.S. Geological Survey) The five GPS sites initially used to constrain Caribbean reference frame are plotted as stars: SANA—San Andres Island; ROJO—Cabo Rojo, Dominican Republic; CRO1—St. Croix, U.S. Virgin Islands; AVES—Aves Island; and BARB—Barbados. Original CANAPE Global Positioning System sites are ROJO and CRO1 plus the squares: CAPO—Capotillo, Dominican Republic; FRAN—Cabo Frances Viejo, Dominican Republic; GORD—Virgin Gorda; GTMO—Guantanamo Bay, Cuba; ISAB—Isabela, Puerto Rico; and TURK—Grand Turk, Turks and Caicos. Figure modified from Jansma et al., 2000.

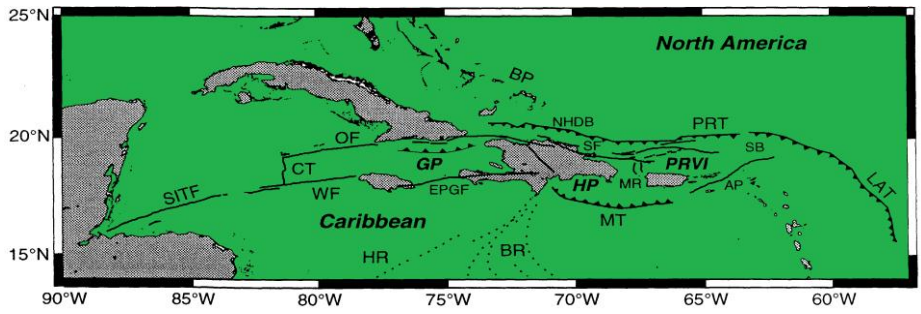

Figure 1.2 Map of northern Caribbean plate boundary, microplates and structures.

AP—Anegada Passage; BP—Bahamas Platform; BR—Beata Ridge; CT—Cayman trough spreading center; EPGF—Enriquillo- Plantain Garden fault; GP—Gonave platelet; HP—Hispaniola platelet; HR— Hess Rise; LAT—Lesser Antilles Trench; MR—Mona Rift; MT—Muertos trough; NHDB—North Hispaniola deformed belt; OF—Oriente fault; PRT—Puerto Rico Trench; PRVI—Puerto Rico–Virgin Islands block; SB—Sombrero Basin; SITF—Swan Islands transform fault; SF—Septentrional fault; WF—Walton fault. Figure from Jansma et al., 2000.

1.2 Geology and Tectonic Setting

Puerto Rico and the northern Virgin Islands represent the eastern edge of the ancestral Greater Antilles island arc. Arc volcanism here was associated with subduction from the north, which commenced in the Cretaceous and continued until the Eocene and Oligocene (Cox et al., 1977; Lewis et al., 1990). Ceasation of arc volcanism was accompanied by orogenesis, folding, faulting and local uplift. It is believed that termination of arc volcanism may be related to: (1) collision of the western Greater Antilles with the Bahama Bank (Pridell and Barrett, 1990); (2) subduction of the Bahama Bank beneath Puerto Rico (Erickson et al., 1989); or (3) subduction of buoyant oceanic crust (Larue et al., 1990).

The summary of the nine phases of geologic evolution of PRVI are: (1) oceanic crustal development in the late Jurassic; (2) early volcanic arc build up in the early Cretaceous; (3) early arc volcanism disruption as indicated by the unconformity in the Bermeja Complex in the early Cretaceous; (4) renewed volcanic arc build up in the late Cretaceous, as indicated by the thick volcanic pile; (5) localized late Maastrichtian arc disruption in St. Croix; (6) renewed volcanic arc build up in the early Tertiary; (7) cessation of volcanism, uplift of several kilometers, and deformation of the arc massif, (late Eocene – mid Oligocene); (8) development of a carbonate platform (late Oligocene – Miocene); and (9) deformation events, both local and tectonic subsidence, local extension and contractional tectonism, accompanied by anticlockwise rotation, which was proposed to have stopped 4.5 Myr ago (Mid Miocene – Recent) (Reid et al., 1991).

The main tectonic features/boundaries of Puerto Rico and the Virgin Islands are discussed in turn below. Each is highlighted under a different subsection and all the features are shown in Fig. 1.3.

1.2.1 The Puerto Rico trench and Muertos trough

These features are EW-striking, and define the northern and southern boundaries of the PRVI block; both are characterized by diffuse zones of earthquakes that dip below the island of Puerto Rico (McCann and Pennington, 1990; McCann, 2002).

1.2.2 The Puerto Rico trench

The trench lies ~100 km offshore and reaches a water depth >8 km. In contrast, the depth in the Muertos trough is ~5 km. The Puerto Rico trench and the offshore South Puerto Rico Slope fault (Grindlay et al., 1997) accommodate ~85% of the current highly oblique North America–Caribbean relative plate motion (Jansma and Mattioli, 2005). The remaining 15% must be taken up along subaerial faults in Puerto Rico or along the Muertos trough.

1.2.3 Muertos trough

The Muertos trough has ongoing deformation with seismicity and the existence of an accretionary prism along the lower slope south of southeastern Hispaniola and southwestern Puerto Rico, along which 40 km of underthrusting is thought to have occurred (Ladd et al., 1977; Ladd and Watkins, 1978; Byrne et al., 1985; Larue and Ryan, 1990). The bathymetric expression of the Muertos trough disappears near 65°W, southwest of St. Croix (McCann and Pennington, 1990; Masson and Scanlon, 1991; Deng and Sykes, 1995). The relationship with the Anagada passage farther east is poorly defined.

1.2.4 The Mona Passage

This feature bounds the Puerto Rico–northern Virgin Islands microplate to the west and contains the NS-trending Mona rift in the north and the similarly oriented Yuma rift in the south. The Mona rift was formed as a result of east-west extension between Puerto Rico and Hispaniola during the last few million years (Larue and Ryan, 1990, 1998; Van Gestel et al., 1998).

1.2.5 Yuma rift

The kinematics of this feature are not well constrained, and thus the nature of the boundary between the Puerto Rico–northern Virgin Islands and Hispaniola microplates south of the Mona rift is currently unclear.

1.2.6 Anegada passage

The eastern boundary of PRVI is marked by this ENE-trending feature, which connects the Neogene Virgin Island and Whiting basins in the southwest with the Sombrero basin in the northeast (Fig. 2). Transtension is likely, which is dominated by northeast-southwest–striking and east-west–striking faults (Jany et al., 1987; Holcombe et al., 1989; Masson and Scanlon, 1991).

1.2.7 Lajas Valley

The Lajas Valley is the zone of highest onshore seismicity. It is an EW-trending feature in southwestern Puerto Rico, which continues offshore to the west and passes south of the southern termination of the Mona Canyon as shown in Figure 1.3. Several workers have proposed active deformation here and some have mapped onshore surface expressions of Holocene faults (Mann and Prentice, 2005; Mann et al., 2005)

1.2.8 The Great Northern Puerto Rico fault zone and the Great Southern Puerto Rico fault zone

Puerto Rico is traversed by two northwest-southeast striking fault zones: (1) the Great Northern Puerto Rico fault zone; and (2) the Great Southern Puerto Rico fault zone. The fault zones were active during the Eocene and record predominant thrust and left-lateral displacement in response to amalgamation of discrete island arc terrains at the leading edge of the Caribbean plate (Glover and Mattson, 1960; Glover, 1971; Erikson et al., 1990, 1991).

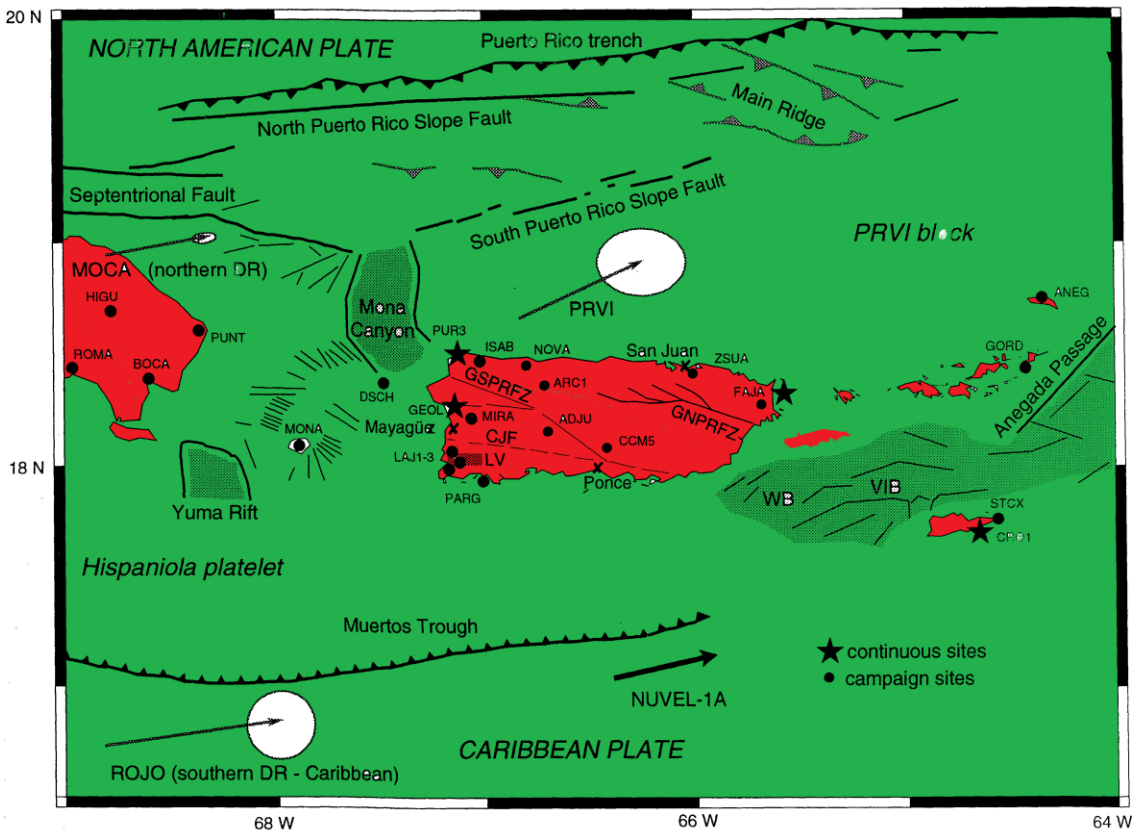

Figure 1.3 Mixed-mode for Global Positioning System geodetic network in the northeastern Caribbean, along with prominent tectonic and structural features.

GNPRFZ—Great Northern Puerto Rico fault zone; GSPRFZ—Great Southern Puerto Rico fault zone; CJF—postulated Cordillera-Joyuda faults; LV—Lajas Valley (medium gray shaded rectangle in southwestern Puerto Rico). Major offshore structures also are shown. Light gray shaded regions are zones of inferred extension. WB—Whiting Basin; VIB—Virgin Islands Basin. Arrows are GPS-derived velocities relative to North America and the NUVEL-1A velocity, derived from global plate motions, of the Caribbean with respect to North America. Length of NUVEL-1A arrow corresponds to a rate of 11 ± 3 mm/yr. Circles are 95% confidence limits. Fig. modified from Jansma et al., 2000.

1.3 Prior GPS Results for Puerto Rico and Virgin Islands

Below, I discuss the few previous studies that I deem to be of great importance to my thesis.

1.3.1 Analysis of GPS geodetic data collected on PRVI block from (1994 - 1999)

Jansma et al. (2000) proposed an independently translating Puerto Rico–northern Virgin Islands block within the northeastern Caribbean boundary zone with ~85% of the relative motion occurring between the Puerto Rico–northern Virgin Islands block and North American plate and ~15% between the Puerto Rico–northern Virgin Islands and the Caribbean plate. Relative motion of western Puerto Rico with respect to the Caribbean, as constrained by GPS geodetic data, was estimated as 2.4 ± 1.4 mm/yr to the west, and derived velocities of western Puerto Rico with respect to North America are consistent with oblique convergence across the western Puerto Rico trench, supported by earthquake slip vectors and low-angle thrusts imaged in seismic profiles. The Jansma et al. (2000) model defines the distribution of interplate slip, but lacks rigorous quantitative mechanical modeling, and two GPS sites (ZSUA in San Juan and GORD in Virgin Gorda), were not included in the analysis. The Jansma et al. (2000) model focused more on the western half of the PRVI block because the geodetic data were not evenly distributed over the microplate. The slow velocity of Puerto Rico with respect to the Caribbean has led some authors to assume that Puerto Rico is part of the Caribbean plate and to include sites in Puerto Rico in the formulation of the Caribbean reference frame (Weber et al., 2001). This is clearly incorrect as demonstrated by the rigorous statistical tests used by Jansma and Mattioli (2005). I address this further below.

1.3.2 Analysis of GPS geodetic data collected on PRVI block from (1994-2005)

Jansma and Mattioli (2005) confirmed the existence of an independent Puerto Rico–northern Virgin Islands microplate and demonstrated that it exists at the 99.9% confidence level. At a location near the center of Puerto Rico (18.25°N, 66.5°W), motion of the Puerto Rico–northern Virgin Islands microplate with respect to the Caribbean is 2.6 ± 2.0 mm/yr (95%) directed toward N82.5°W ± 34° (95%). This result also supports east-west extension of several mm/yr in the boundary zone between the North America and Caribbean plates from eastern Hispaniola to the eastern Virgin Islands. Extension increases westward with most of the extension

accommodated in the Mona rift. East-west extension of 1.5–3.9 mm/yr across the island of Puerto Rico is permitted by the sparse GPS data (Jansma and Mattioli, 2005). A zone of east-west extension of 1–2 mm/yr also exists between eastern Puerto Rico and Virgin Gorda, where it is either attached to the Caribbean plate or simply moves within error at the same rate. Motions along or across any of the subaerial structures of Puerto Rico were constrained to be ≤ 2 mm/yr. In addition, NW-SE to E-W extension of 2.0 ± 2.3 mm/yr was observed across the Anegada Passage. The results of Jansma and Mattioli (2005) updated and refined the geodetic velocity analysis by Jansma et al. (2000) by including datasets from four continuous sites: PUR3, GEOL, FAJA, and CRO1 together with seven campaign GPS sites: ISAB, PARG, ADJN, ARC2, ZSUB, SALN and GORD. Their analysis included observations from 1994 to 2001. One important goal of this thesis was to update the geodetic velocity field of the previous work of Jansma and Mattioli (2005) by including and analyzing an enhanced data set from eleven newly established continuous GPS sites and the twenty-one (previously established) campaign sites.

1.4 Aims and Objectives

The original aim of this study was to determine the precise tectonic motion of the Puerto Rico–northern Virgin Islands microplate with respect to the larger North American and Caribbean plates. The original plan includes updating velocity fields from eleven GPS continuous sites and re-occupying twenty-one campaign sites. However, only eleven campaign sites were recovered and re-observed during my field work in the summer of 2011. The overall goal was to refine the findings of Jansma and Mattioli (2005), with specific emphasis on: (i) constraining maximum permissible displacements along potentially active faults on the island of Puerto Rico and immediately offshore; and (ii) re-examining potential diffuse extension between the northern Virgin Islands and eastern Puerto Rico.

CHAPTER 2

METHODS – GPS GEODESY

2.1 GPS Data Acquisition

In the 1990's GPS became the primary tool for geodetic investigations. A permanent IGS (International GPS Service) station was established in St. Croix in 1995 (CRO1) and a vector tie to the original 1986 site, STCX, was established (Dixon et al., 1998), which extended the time series by nearly a decade and therefore improved the CRO1 velocity estimate. Previous analysis used data from continuous GPS sites: PUR3, GEOL, FAJA and CRO1, and campaign GPS sites: ISAB, PARG, ADJN, ARC2, ZSUA, SALN, and GORD (see Table 3.1, 3.2 and 3.3). All campaign observations after 1999 were obtained with the following hardware: Trimble 4000 SSi 12-channel, dual-frequency, code-phase receivers and Dorn-Margolin type choke ring antennae. Data from campaign stations were collected using either 0.5 m spike mounts or standard tripods with rotating optical plummet setups using a 30 second observation epoch and 10° elevation mask. Individual campaign occupations were normally obtained with 10–24 h of continuous data over 2–3 consecutive observation days. Observations that are less than 8 hours were not included in the time series (Jansma and Mattioli, 2005) and these are also excluded here.

This thesis uses GPS measurements collected from eleven newly installed continuous sites obtained from the www.UNAVCO.org data archive (G. Wang, PI) and twenty-one campaign sites of which eleven out of the twenty-one were recovered and re-observed during the May/June 2011 campaign. Out of the total 32 GPS sites analyzed, 15 sites have not been previously included in any kinematic analysis.

2.1.1 Field Procedure for campaign site data acquisition

The following field procedures were used for all campaign sites: (1) antenna was oriented to the true North using a compass; (2) antenna was leveled using a precision spirit level; (3) receiver was programmed to collect one epoch of raw data transmitted by tracked GPS satellite at 30 second interval using an elevation mask of 7°; and (4) each daily session was programmed to begin at 00:00 UTC and to end at 23:59 UTC. At the completion of the 2011 campaign, the raw GPS observation files were downloaded, backed up and merged into a single daily file (if there are multiple sessions) with a file name designated for that site, which was then transferred to a UNIX work station for further processing (see below).

The basic equipment tools used during my GPS geodetic data acquisition processes on campaign sites include the following: (1) 12V battery, which is usually the main power supply; (2) receiver; (3) antenna; (4) AC power, used as the main power supply if available; (5) and solar panel used as a power backup or to charge the battery. Figure 2.1 – 2.4 shows some typical geodetic instrument setups, which I used during my data acquisitions in 2011.

Figure 2.1 Power generating source used on a campaign site - AC power and DC backup.

(a)

(b)

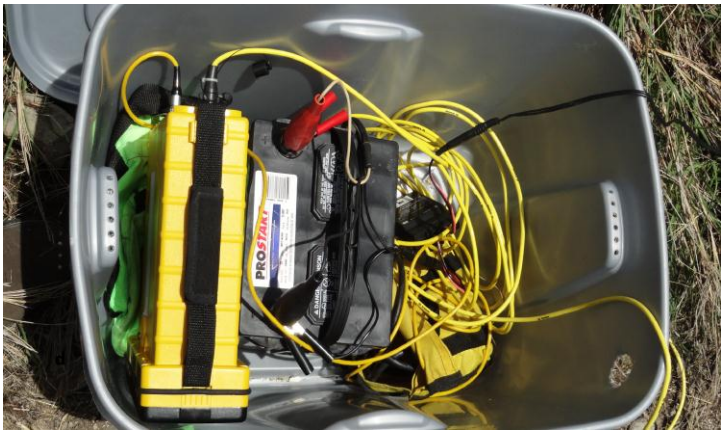

(c)

Figure 2.2 Typical geodetic instrument setups used on a campaign site (a) a spike mounted antenna; (b) a geodetic pin epoxied into concrete; (c) a receiver connected to battery and antenna.

Figure 2.3 GPS geodetic antenna - standard tetrapod with choke ring antenna.

Figure 2.4 Geodetic setup with a solar backup on the campaign site LAJ1.

2.2 GPS Data Processing

The raw data, i.e. GPS observables, were converted from the receiver's binary proprietary format to RINEX format (i.e. Receiver Independent Exchange Format; Gurtner and Estey, 2006) and renamed according to the GIPSY convention before the data were processed. GIPSY-GPS Inferred Position System Orbit Analysis & Simulation Software (GIPSY – OASIS II), a collection of UNIX based software programs developed at the Jet Propulsion Laboratory (JPL), was used to solve for precise positions from raw GPS data (Lichten and Border, 1987; Heflin et al., 1992; Blewit et al., 1992; Webb and Zumberge, 1995; Zumberge et al., 1997). The GPS data were analyzed in a semi-automated fashion using UNIX scripts provided by JPL, or authored by Charles DeMets (U. Wisconsin), and modified or independently written by Glen S. Mattioli. In this research I used gd2p.pl script from JPL to process my obsevations. Turner (2003) presents a detailed step by step description on how to use GIPSY – OASIS software to process GPS data. The discussion below is taken from Turner (2003) and reproduced here with minor modification.

1. The *program Ninja* translates the rinex files into a FORTRAN binary file, removes outliers and detects cycle slips. Data for each satellite are merged into a *qm* file and decimated into 300 second intervals

2. Individual qm files are merged into a single file, and a name list is created from the *QMfile* called qregress.nml

3. The *qregress.nml* namelist drives *qregress*, which does the physical modeling of the receiver measurements. qregress applies the physical models (receiver location, tidal effects, polar motion, perturbation rotation, precession, nutation and earth rotation) to the orbits and observations and gives the output *rgfile*

4. The *rgfile* is used by the program wash_nml to create a wash.nml file, both of which are the input for the preprefilter, prefilter, and filter modules (which runs the

Square Root information Filter)

5. *Smapper* comes after the filtering process, it smoothes and maps the covariance, sensitivity, and parameter estimations

6. *Postfit* computes the post-fit data residuals

7. *Postbreak* searches for missed cycle slips by Ninja, modifies the data and reruns GIPSY

8. *Edtpnt2* removes outliers from the data sets

9. The *stacov module* is the final stage that produces the final solution files, which contain the earth centered, earth-fixed coordinates and associated covariance estimates in text format.

The basic script used to run GIPSY was set up to scale, rotate and transform the position solution from the satellite reference (that is the Free-frame) into (IGS 2005) using X-files from the Jet Propulsion Laboratory. All processing used final, precise non-fiducial orbit, earth-orientation, and GPS clock files from JPL. Two stacov files were produced: one in the satellite reference frame and one in IGS05. A second script was run to produce a time series for each site relative to the stable Caribbean or North American plates. Time series velocity errors were calculated using the formulation of Mao et al. (1999) as modified by James (2008).

The data processing methods were similar to those outlined in Turner (2009) and Jansma and Mattioli (2005). In those previous studies, however, v.4 of GIPSY-OASIS II was used with different processing scripts. Component site velocities were calculated in IGS05 using post-processing software modules, which allow estimation of component offsets along with estimates of velocities in a rapid and internally consistent way that includes the full-covariance of each daily site position in the analysis. After obtaining an IGS05 velocity for the latitude, longitude, and radial (or vertical) component and their associated errors, final velocities and errors in the Caribbean

reference frame were calculated using the current best-fit model for Caribbean motion with respect to the IGS05 (DeMets et al., 2007 and DeMets, per. comm, to Mattioli) In addition, a revised CA-ITRF05 pole was calculated (see below). Caribbean fixed velocities include the full covariance of the individual site velocities and the predicted motion of the Caribbean plate at that location (DeMets et al., 2000; 2007)

2.2.1 Caribbean Reference Frame

The Caribbean reference frame has potential limitations. The best-fit angular velocity for five Caribbean GPS sites yields an average residual velocity of 1.5 mm/yr. DeMets et al (2000) produced a published version of the CAR-ITRF00 Euler pole in which they used GPS-derived velocities from Aves Island (AVES) in the east, San Andres Island (SANA) in the west, St. Croix (CRO1) in the U.S Virgin Islands and Cabo Rojo (ROJO) in the southern Dominican Republic as shown in Fig. 1.1. This thesis used the updated 2007 version which incorporates the CGPS site in Barbados (BARB) and data from Nicaragua and Honduras. (DeMets et al., 2007)

Weber et al. (2001) also published another version of the reference frame, which included Barbados (BARB) as well as Isabela (ISAB); the latter has been proved to be on a different tectonic block than the stable Caribbean (Jansma and Mattioli, 2005), thereby increasing uncertainties in the pole calculation, see Figure 1.1 and Figure 1.3.

2.2.2 North American Reference Frame

This thesis will also produce velocity time series results for the entire PRVI network with respect to the North American plate. The results will be used to produce velocity maps of PRVI sites with respect to North America. Velocity maps with respect to the CA-plate and the other with respect to the NAM-plate will be compared to confirm that PRVI is indeed its own microplate whose movement is slow and related to the Caribbean, but statistically different from the North American plate.

CHAPTER 3

GPS DERIVED VELOCITIES AND DATA ANALYSIS

3.1 Data Analysis

Analysis of data was performed at the University of Texas at Arlington, using the GIPSY-OASIS II (version 5) and processing scripts. The free-network solution was transformed, scaled and rotated into the international reference frame (IGS2005). Errors are not shown for daily site positions. Velocity estimates used a weighted least squares fit to daily site positions. The white and the flicker noise values reflect the uncertainties on the derived velocities (Mao et al., 1999). A total of 32 velocity time series results (which comprises 3 different groups of data) were analyzed, (see Table 3.1, Table 3.2, and Table 3.3). The first table (Table. 3.1) is the 11 newly installed continuous sites obtained from the UNAVCO.org data archive. The RINEX data for each site were downloaded from the first available date up to August 13th 2011 when IGS05 was updated to IGS08. The offsets shown in the AOPR site in 2010 and CRO1 site in 2005 were due to antenna swaps, which has been corrected.

Table 3.1 Location of GPS Continuous Sites obtained from UNAVCO.org data archive

	Name of Continuous Site - Date of first data	Site	Lat (N)	Long(E)
1	Anagada - 2010 Feb	ABVI	18.730	295.668
2	Arecibo observatory - 2008 May	AOPR	18.351	293.246
3	Bayamon science park - 2008 May	BYSP	18.410	293.839
4	ST. CROIX VLBA,V/I - 1995 Oct.	CRO1	17.761	295.416
5	CULEBRA ISLAND,PR - 2008 Oct.	CUPR	18.312	294.717
6	MAYAGUEZ TGPR 2010,PR - 2010 Feb	MAYZ	18.223	292.841
7	MIPR CAJA DE MUERTOS ISD,PR - 2008 May	MIPR	17.890	293.473
8	CERRILLOS_PR2008,PR – 2008 May	P780	18.081	293.421
9	MONA ISLAND,PUERTO RICO	MOPR	18.082	292.069
10	ST. THOMAS, US V/I – 2008 Oct.	STVI	18.340	295.026
11	UPRM GEOL DEPT BLD – 1996 Sept.	GEOL	18.210	292.860

The second group of data comprises data obtained during the 2011 campaign along with data collected previously (Jansma et al., 2000; Jansma and Mattioli, 2005), which I reprocessed with GIPSY OASIS II (v5) in IGS05. Table 3.2 shows the campaign sites that have updated 2011 data in my analysis.

Table 3.2 Location of GPS Campaign Sites on which I acquired Data in 2011

	Name of Campaign – Date of initial occupation	Site	Lat (N)	Long(E)
1	ADJUNTAS AGR STATION (data too short for the 2011)	ADJN	18.175	293.202
2	ARECIBO 1	ARC1	18.346	293.246
3	ARECIBO 2	ARC2	18.345	293.249
4	UPRC SCIENCES BLD	CAYE	18.119	293.838
5	CERRILLOS DAM BM	CCM5	18.079	293.421
6	CENTER FOR IND.RES/DEV	CIDE	18.211	292.863
7	LAJAS VALLEY UNI SAN GERMAN	LAJ1	18.083	292.948
8	SOUTH LAJAS VALLEY- AES.UPRM	LAJ2	18.035	292.932
9	PARGUERA, PR	PARG	17.969	292.956
10	MAYAGUEZ AIRPORT	MAZC	18.255	292.850
11	NAT. WEATHER. SERVICE CAROLINA, PR	ZSUB	18.431	294.008
12	VEGA BAJA, OLD FIRESTATION	VEGB	18.446	293.609

The last group of data, (Table 3.3) are the campaign sites, which I analyzed and updated from past velocity results to IGS05 from the previous ITRF00 analysis (Jansma and Mattioli, 2005).

Table 3.3 Location of GPS Campaign Sites without 2011 Data

	Name of Campaign Site without 2011 data	Site	Lat (N)	Long(E)
1	ANEGADA ISLAND	ANEG	18.730	295.668
2	ADJUNTAS AGR STATION	ADJN	18.175	293.202
3	MONA ISLAND, PR	MONA	18.110	292.092
4	SALINA, ALBERGUE OLIMPICO	SALN	18.029	293.766
5	VIEQUES BASE, ISLAND, PR	VIEN	18.121	294.560
6	VIEQUES ISLAND, PR	VIEQ	18.131	294.488
7	ISABELA – 1994 May	ISAB	18.468	292.954
8	DESECHEO ISLAND	DSCH	18.384	292.521
9	FAA,SAN JUAN,PR	ZSUA	18.430	294.006
10	NORTH LAJAS VALLEY	LAJ3	17.992	292.893

3.2 GPS Derived Station Velocities

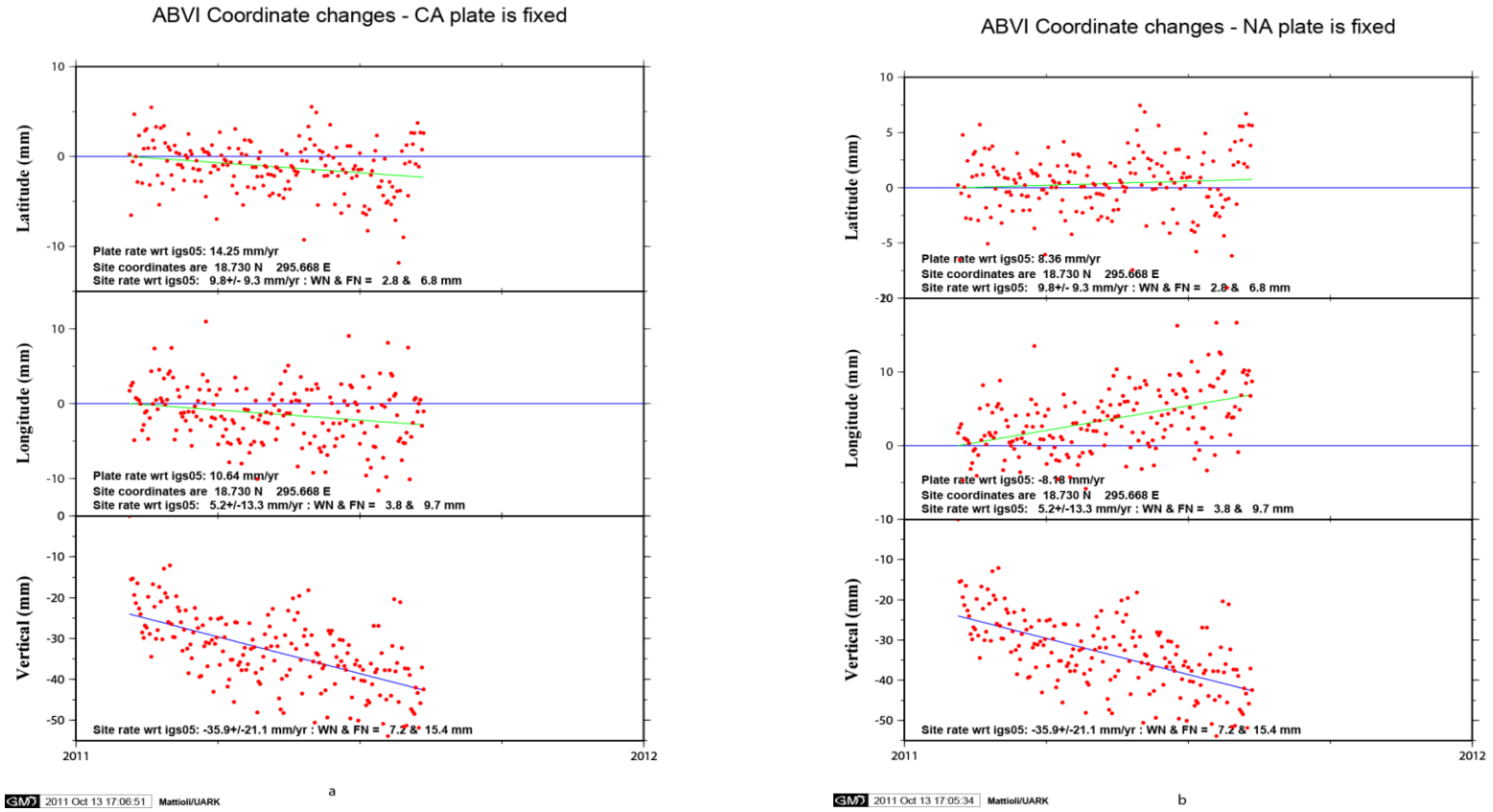

Figure 3.1 Time series for site ABVI. Red dots are the UTC daily position solutions. The blue lines are the predicted plate rates in ITRF05 held fixed (horizontal). The green lines are the least square fit site rates in IGS05 (a) with respect to the Caribbean plate rate-CA and (b) with respect to the North-American plate rate-NA. WN = white noise; FN = flicker noise estimates.

Note: *GPS station coordinate time series for the continuous sites (group 1) are from Figure 3.1 to Figure 3.11.*

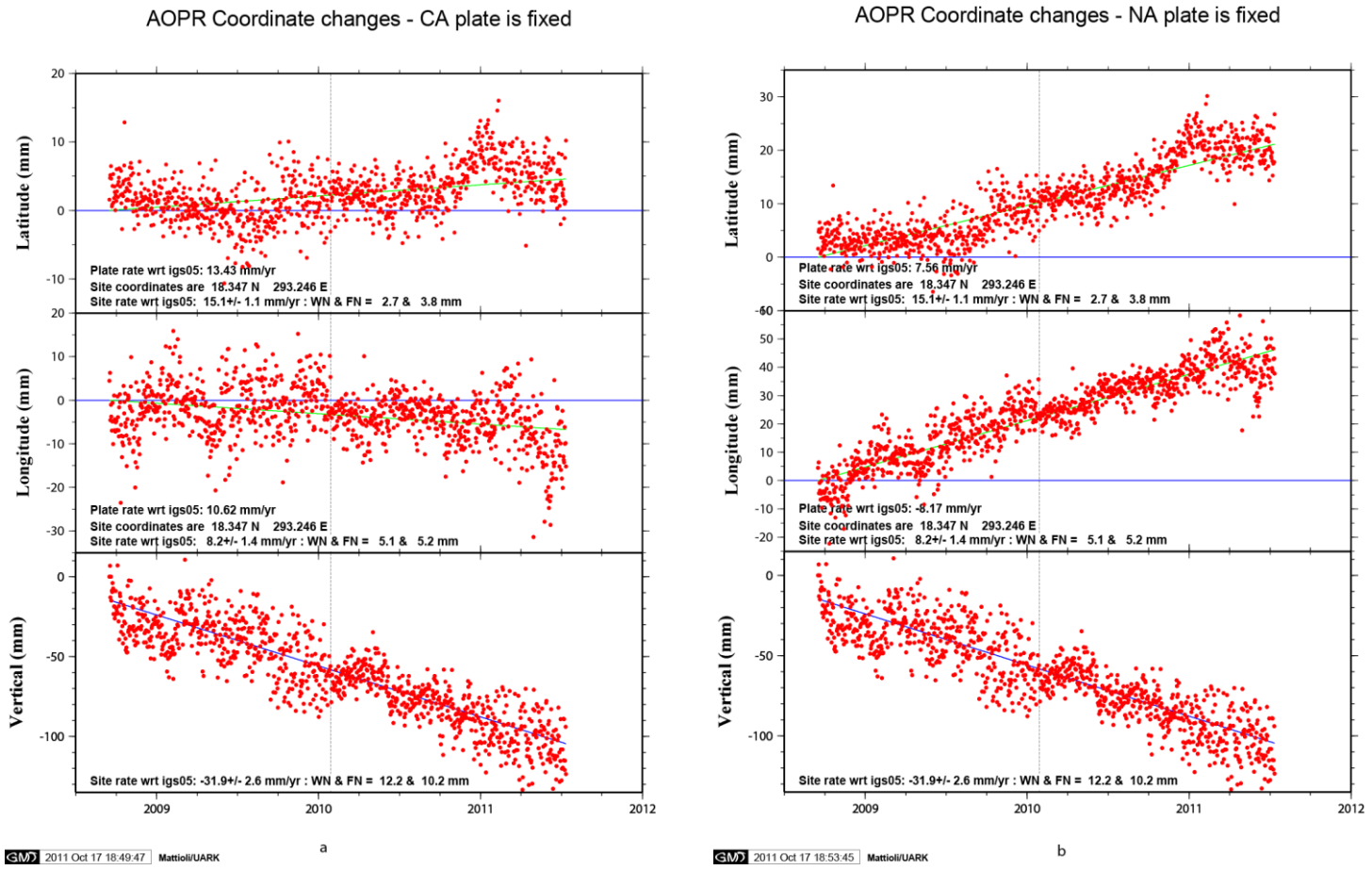

Figure 3.2 Time series for site AOPR. Red dots are the UTC daily position solutions. The blue lines are the predicted plate rates in ITRF05 held fixed (horizontal). The green lines are the least square fit site rates in IGS05 (a) with respect to the Caribbean plate rate-CA and (b) with respect to the North-American plate rate-NA. WN = white noise; FN = flicker noise estimates.

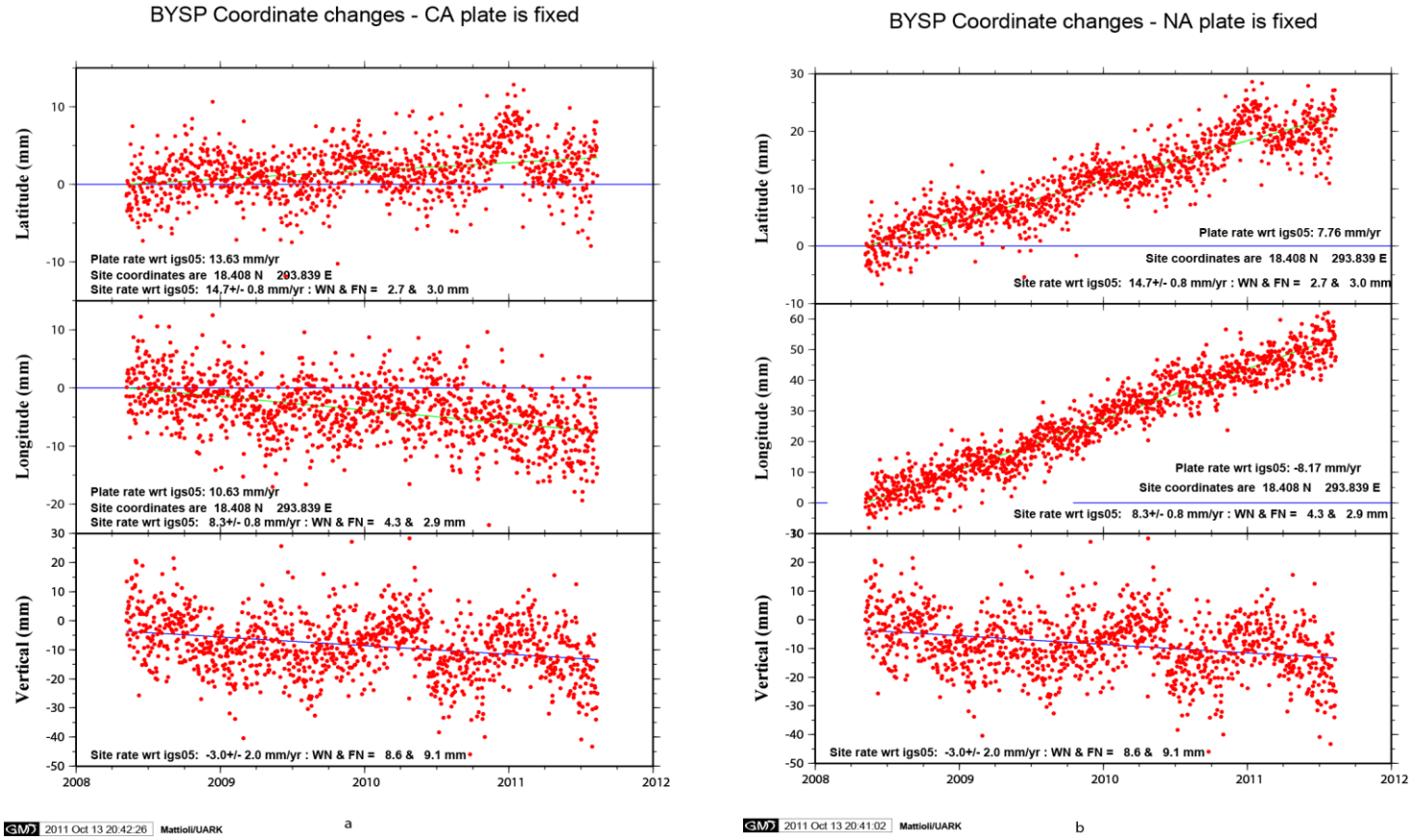

Figure 3.3 Time series for site BYSP. Red dots are the UTC daily position solutions. The blue lines are the predicted plate rates in ITRF05 held fixed (horizontal). The green lines are the least square fit site rates in IGS05 (a) with respect to the Caribbean plate rate-CA and (b) with respect to the North-American plate rate-NA. WN = white noise; FN = flicker noise estimates.

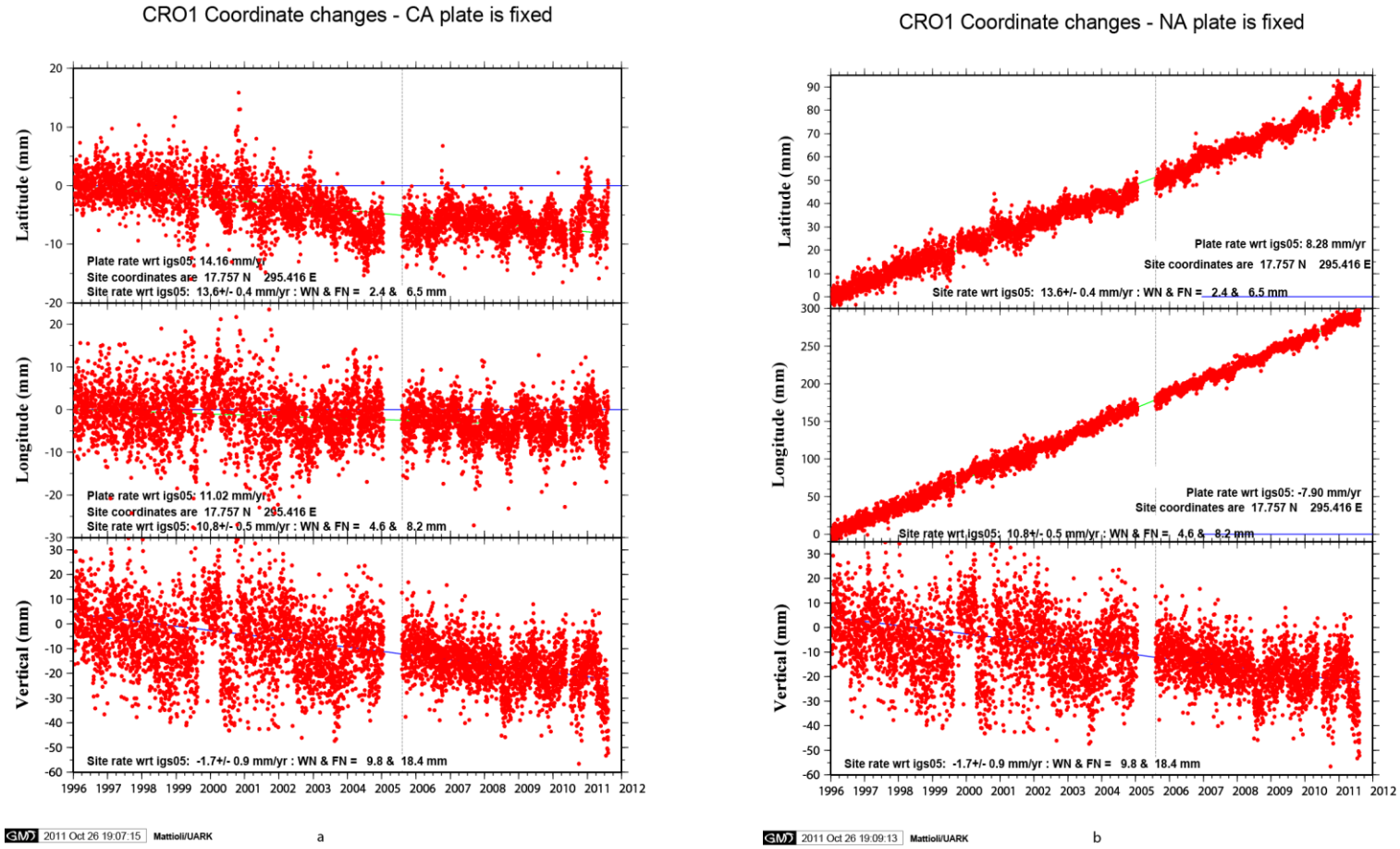

Figure 3.4 Time series for site CRO1. Red dots are the UTC daily position solutions. The blue lines are the predicted plate rates in ITRF05 held fixed (horizontal). The green lines are the least square fit site rates in IGS05 (a) with respect to the Caribbean plate rate-CA and (b) with respect to the North-American plate rate-NA. WN = white noise; FN = flicker noise estimates.

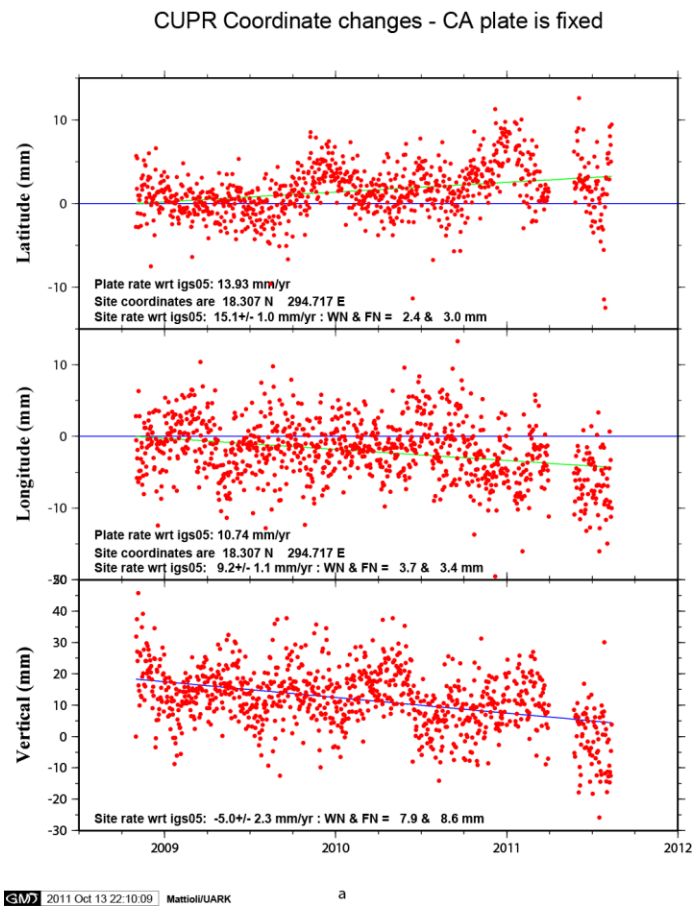

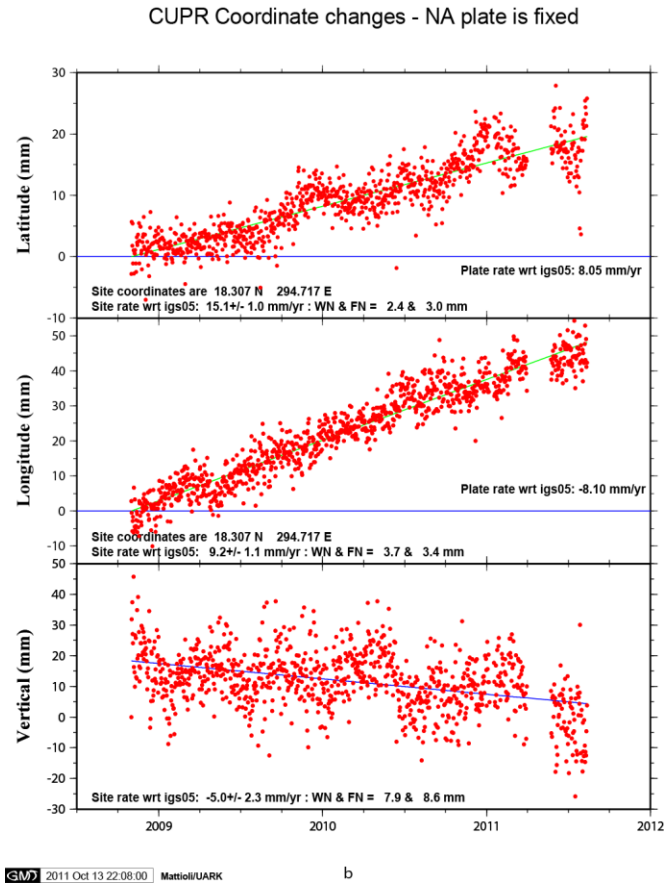

Figure 3.5 Time series for site CUPR. Red dots are the UTC daily position solutions. The blue lines are the predicted plate rates in ITRF05 held fixed (horizontal). The green lines are the least square fit site rates in IGS05 (a) with respect to the Caribbean plate rate-CA and (b) with respect to the North-American plate rate-NA. WN = white noise; FN = flicker noise estimates.

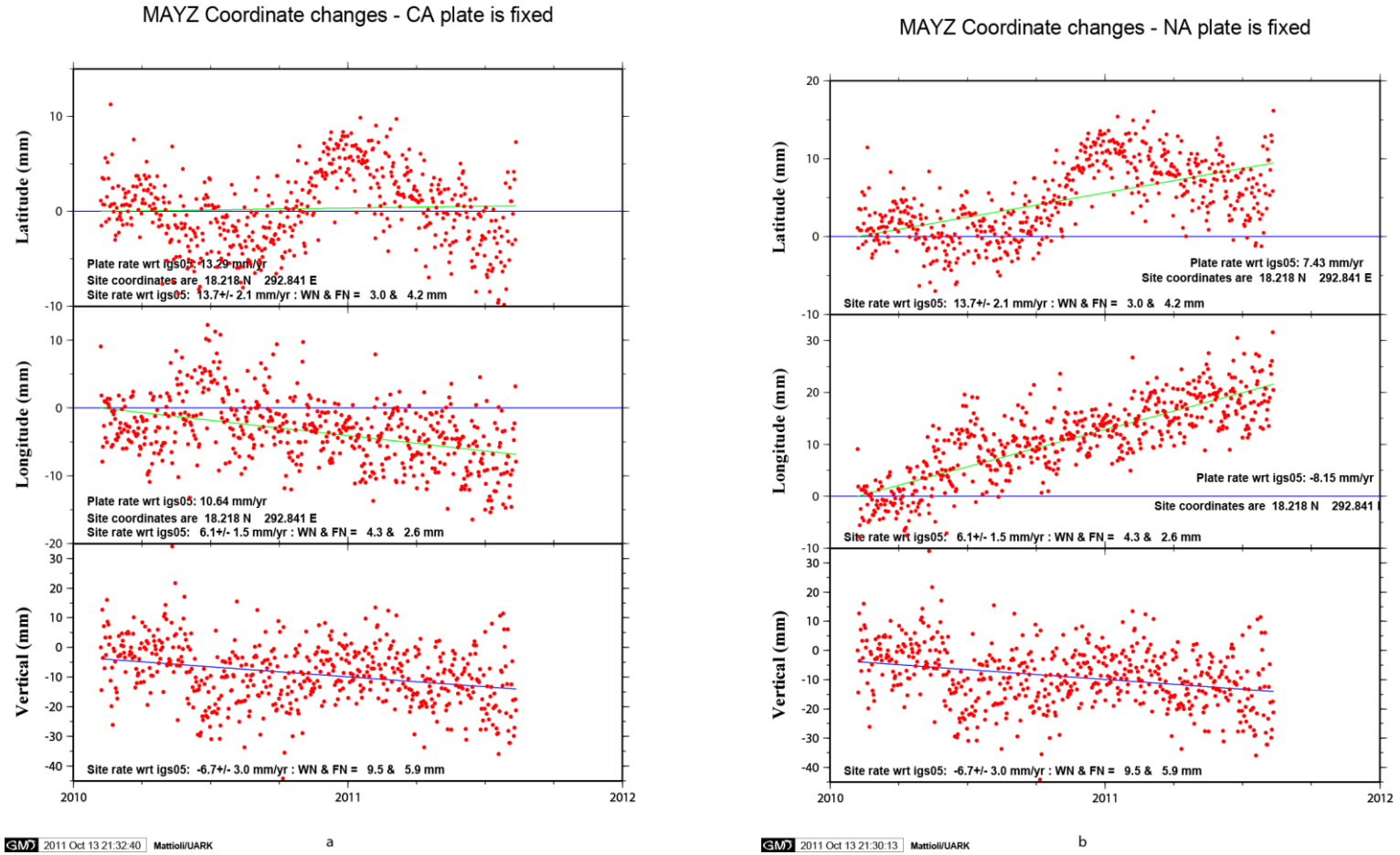

Figure 3.6 Time series for site MAYZ. Red dots are the UTC daily position solutions. The blue lines are the predicted plate rates in ITRF05 held fixed (horizontal). The green lines are the least square fit site rates in IGS05 (a) with respect to the Caribbean plate rate-CA and (b) with respect to the North-American plate rate-NA. WN = white noise; FN = flicker noise estimates.

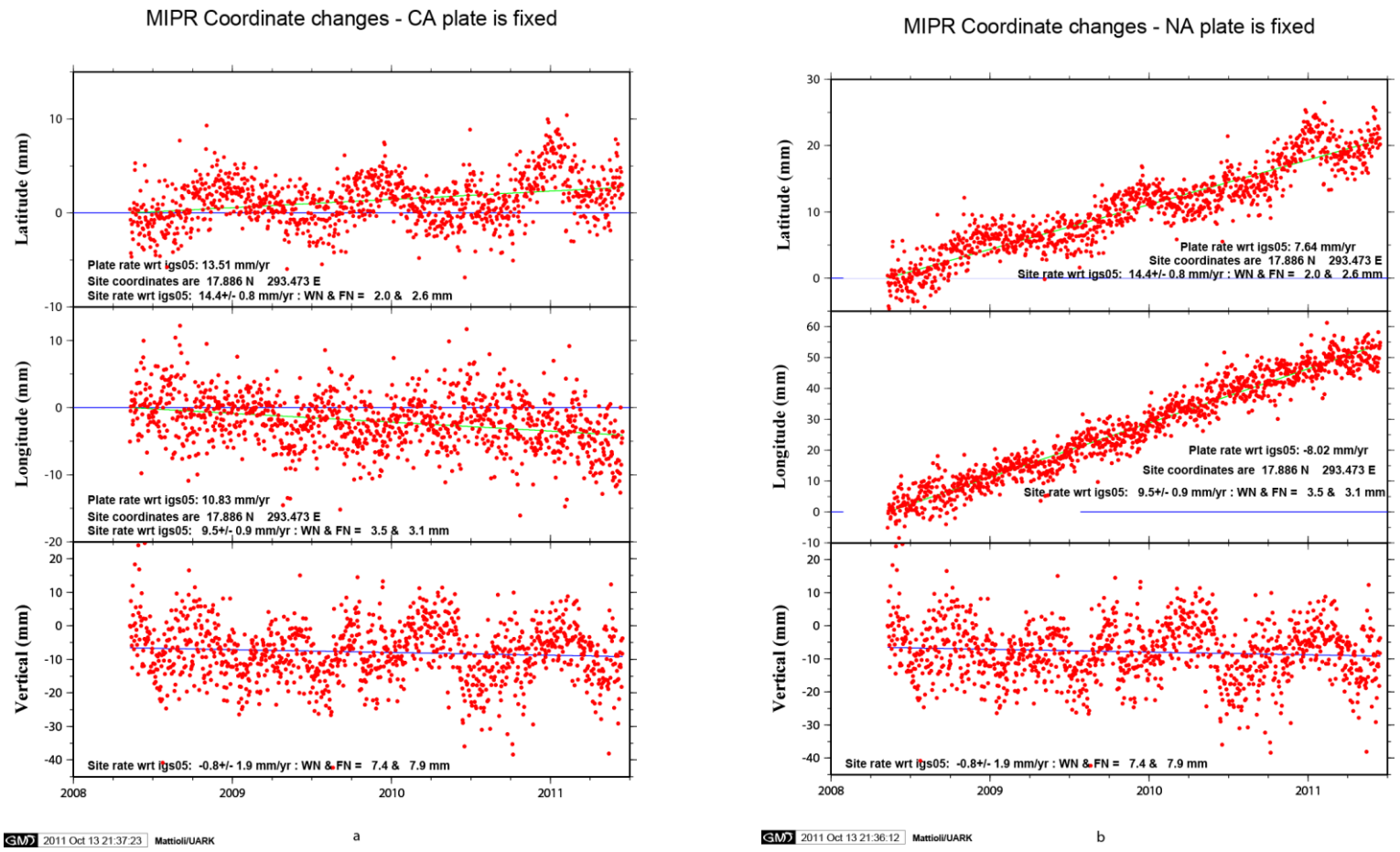

Figure 3.7 Time series for site MIPR. Red dots are the UTC daily position solutions. The blue lines are the predicted plate rates in ITRF05 held fixed (horizontal). The green lines are the least square fit site rates in IGS05 (a) with respect to the Caribbean plate rate-CA and (b) with respect to the North-American plate rate-NA. WN = white noise; FN = flicker noise estimates.

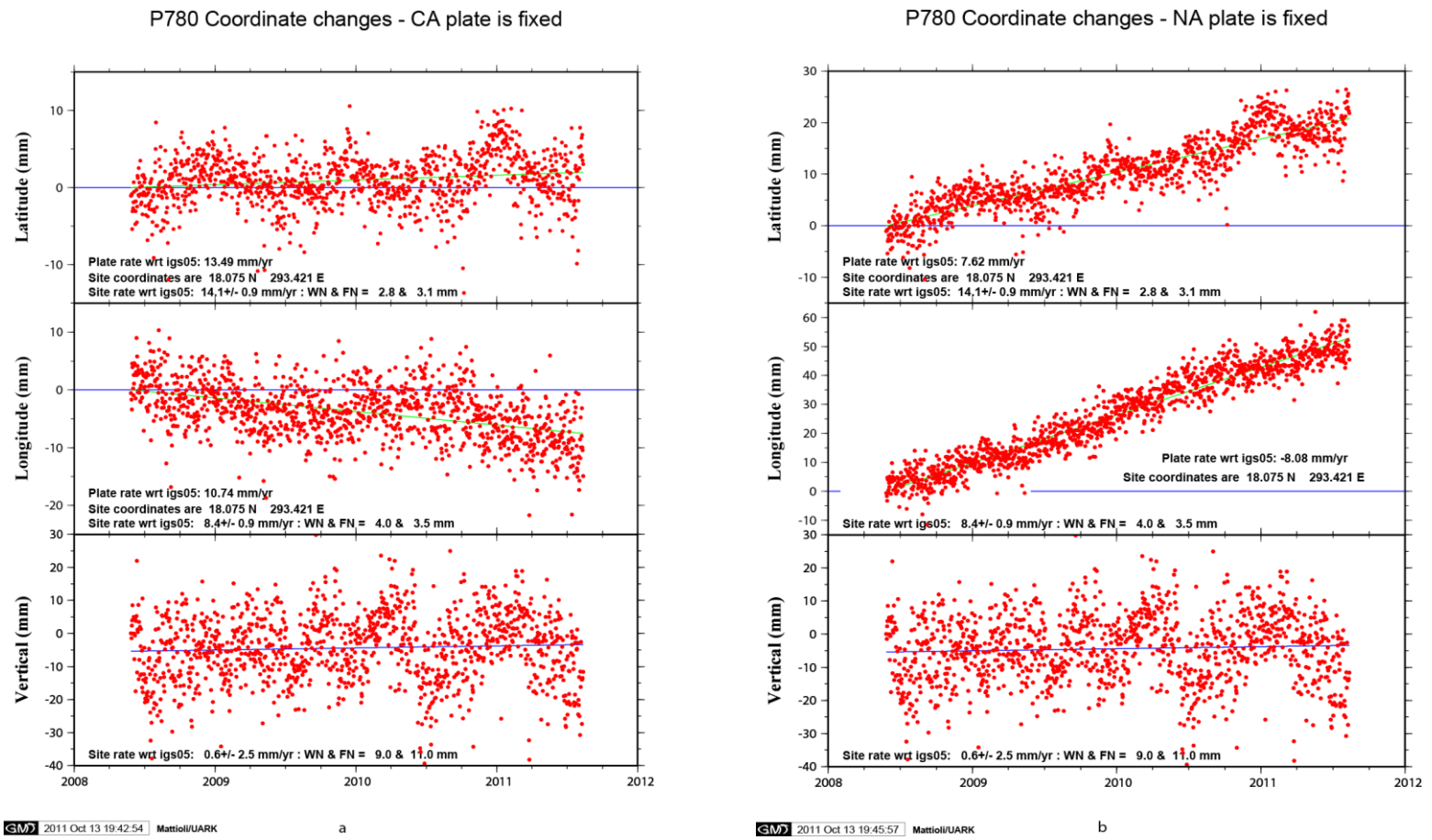

Figure 3.8 Time series for site P780. Red dots are the UTC daily position solutions. The blue lines are the predicted plate rates in ITRF05 held fixed (horizontal). The green lines are the least square fit site rates in IGS05 (a) with respect to the Caribbean plate rate-CA and (b) with respect to the North-American plate rate-NA. WN = white noise; FN = flicker noise estimates.

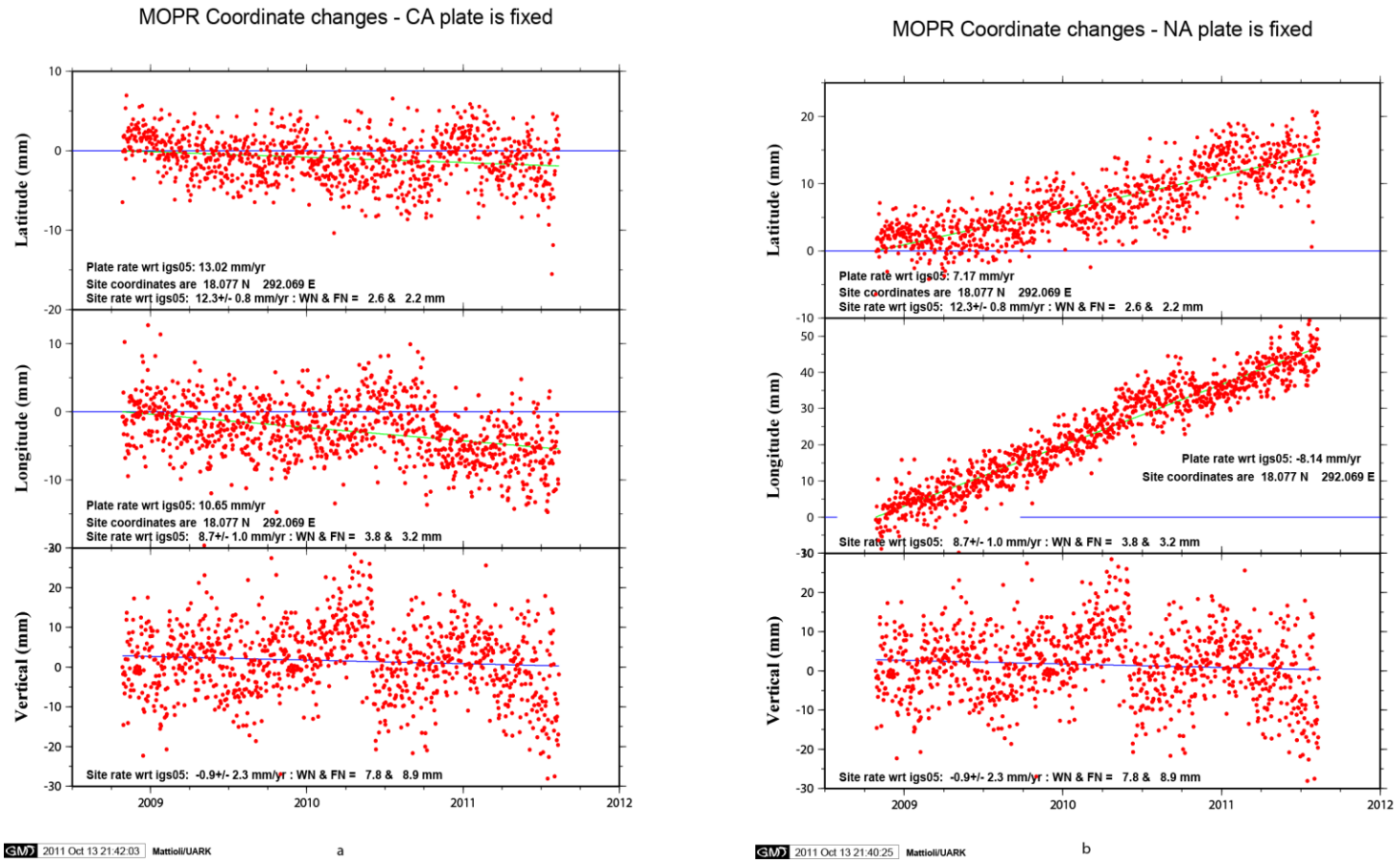

Figure 3.9 Time series for site MOPR. Red dots are the UTC daily position solutions. The blue lines are the predicted plate rates in ITRF05 held fixed (horizontal). The green lines are the least square fit site rates in IGS05 (a) with respect to the Caribbean plate rate-CA and (b) with respect to the North-American plate rate-NA. WN = white noise; FN = flicker noise estimates.

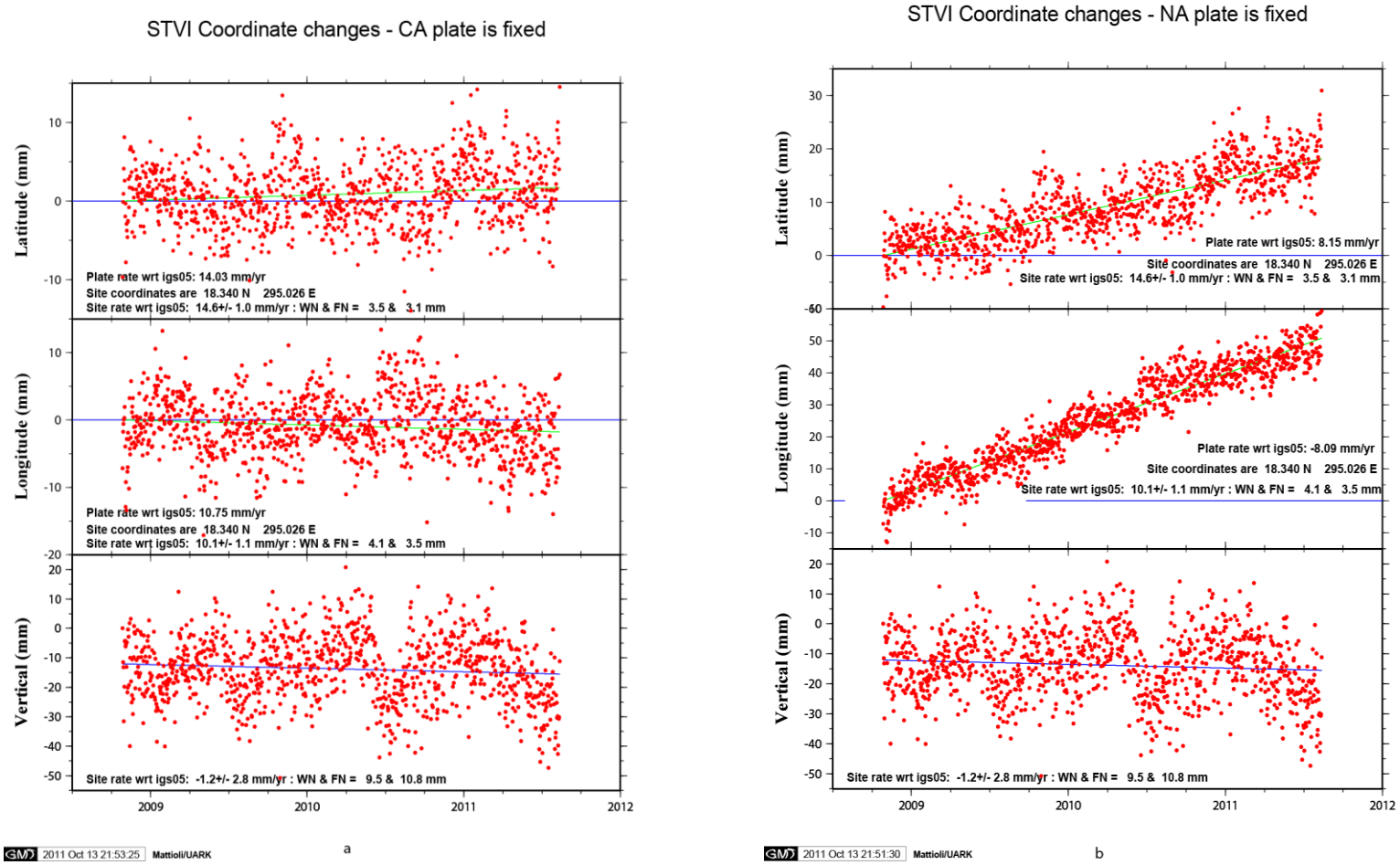

Figure 3.10 Time series for site STVI. Red dots are the UTC daily position solutions. The blue lines are the predicted plate rates in ITRF05 held fixed (horizontal). The green lines are the least square fit site rates in IGS05 (a) with respect to the Caribbean plate rate-CA and (b) with respect to the North-American plate rate-NA. WN = white noise; FN = flicker noise estimates.

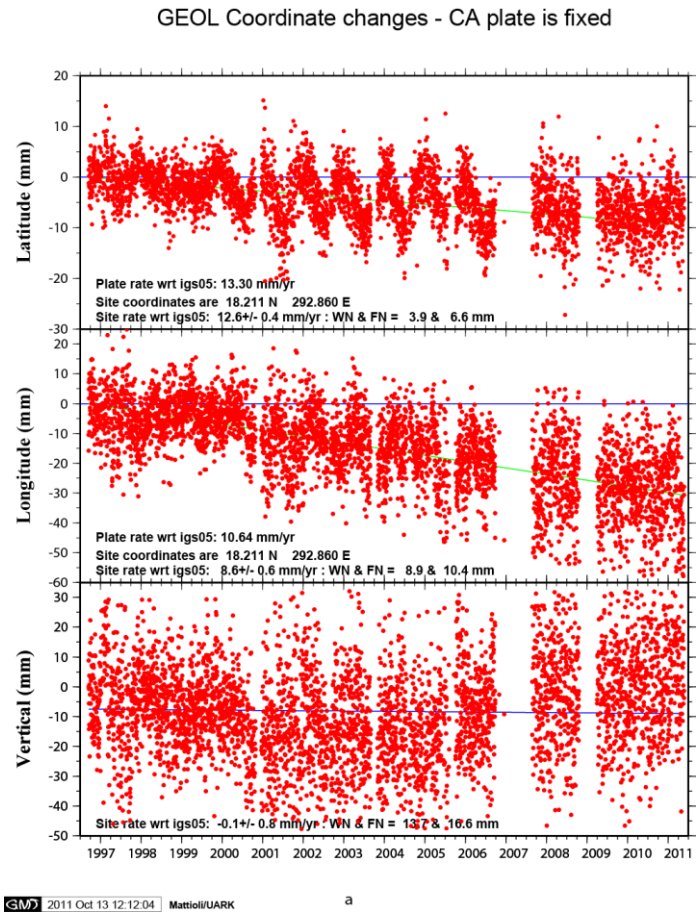

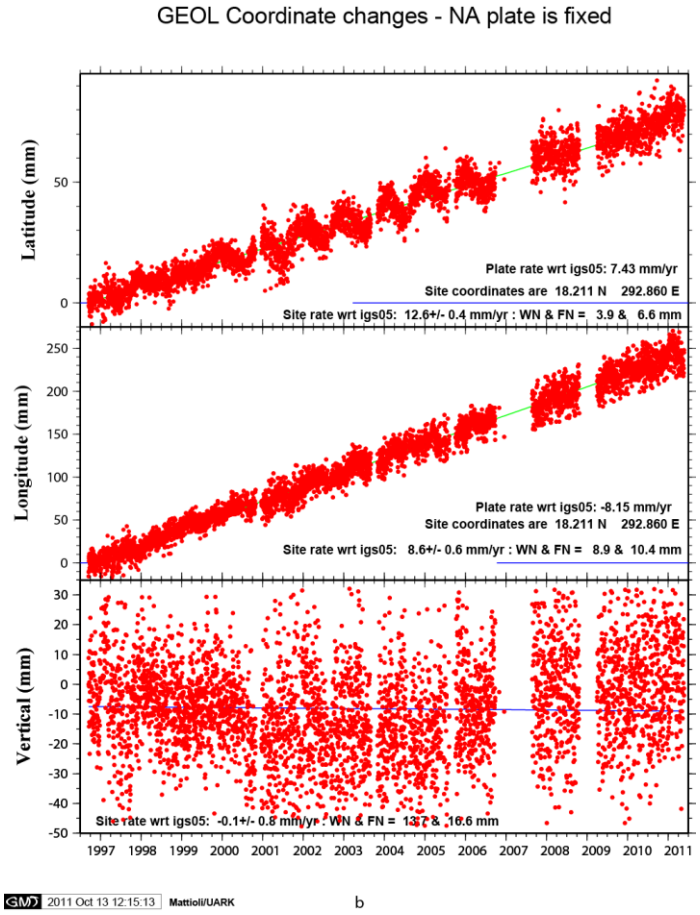

Figure 3.11 Time series for site GEOL. Red dots are the UTC daily position solutions. The blue lines are the predicted plate rates in ITRF05 held fixed (horizontal). The green lines are the least square fit site rates in IGS05 (a) with respect to the Caribbean plate rate-CA and (b) with respect to the North-American plate rate-NA. WN = white noise; FN = flicker noise estimates.

3.2.1 GPS Station Coordinate time Series for the May/June Campaign sites (group 2) Figure 3.12 to Figure 3.23

The table below provides information on the receiver and the antenna combinations, which I used during the May/June 2011 campaign in Puerto Rico; 4 receivers S/N (3833A23922, 3833A23929, 3606A14444, 3725A19501) and 4 Trimble choke ring antennas S/N (090666, 131869, 131871, 131868) were used throughout the campaign. The table also shows which antenna or receiver was moved from one location to the other, looking at the color code a particular antenna was designated to a particular receiver. Figure 3.12 to Figure 3.23 provides the updated time velocities, respectively, for each of the sites provided on this table.

Table 3.4 GPS Antenna and Receiver Information used during May/June 2011 campaign

Site	Antenna Type	Receiver	Ant.Serial Num	Mount Type	Ant. Height	Remarks
ADJN	Trimble choke ring	3833A23922	090666	spike mount	0.50m	time series too short
ARC1	Trimble choke ring	3833A23929	131869	tetrapod stand (yellow)	1.40m	
ARC2	Trimble choke ring	3833A23922	090666	spike mount	0.50m	
CAYE	Trimble choke ring	3606A14444	131871	tetrapod stand(green)	1.24m	antenna adjusted to 1.24m
CCM5	Trimble choke ring	3833A23929	131869	concrete vertical slap	1.14m	antenna on concrete slab
CIDE	Trimble choke ring	3833A23929	090666	half a meter spike mount	0.50m	
LAJ1	Trimble choke ring	3725A19501	131868	spike mount	0.50m	
LAJ2	Trimble choke ring	3606A14444	131871	tetrapod stand (green)	1.50m	
PARG	Trimble choke ring	3725A19501	131868	spike mount	0.50m	
MAZC	Trimble choke ring	3833A23922	131869	spike mouth but 3 adj legs	0.50m	spike mount has 3 adjustable legs
ZSUB	Trimble choke ring	3725A19501	131868	tetrapod stand (yellow)	1.41m	
VEGB	Trimble choke ring	3833A23929	131869	spike mount	0.50m	

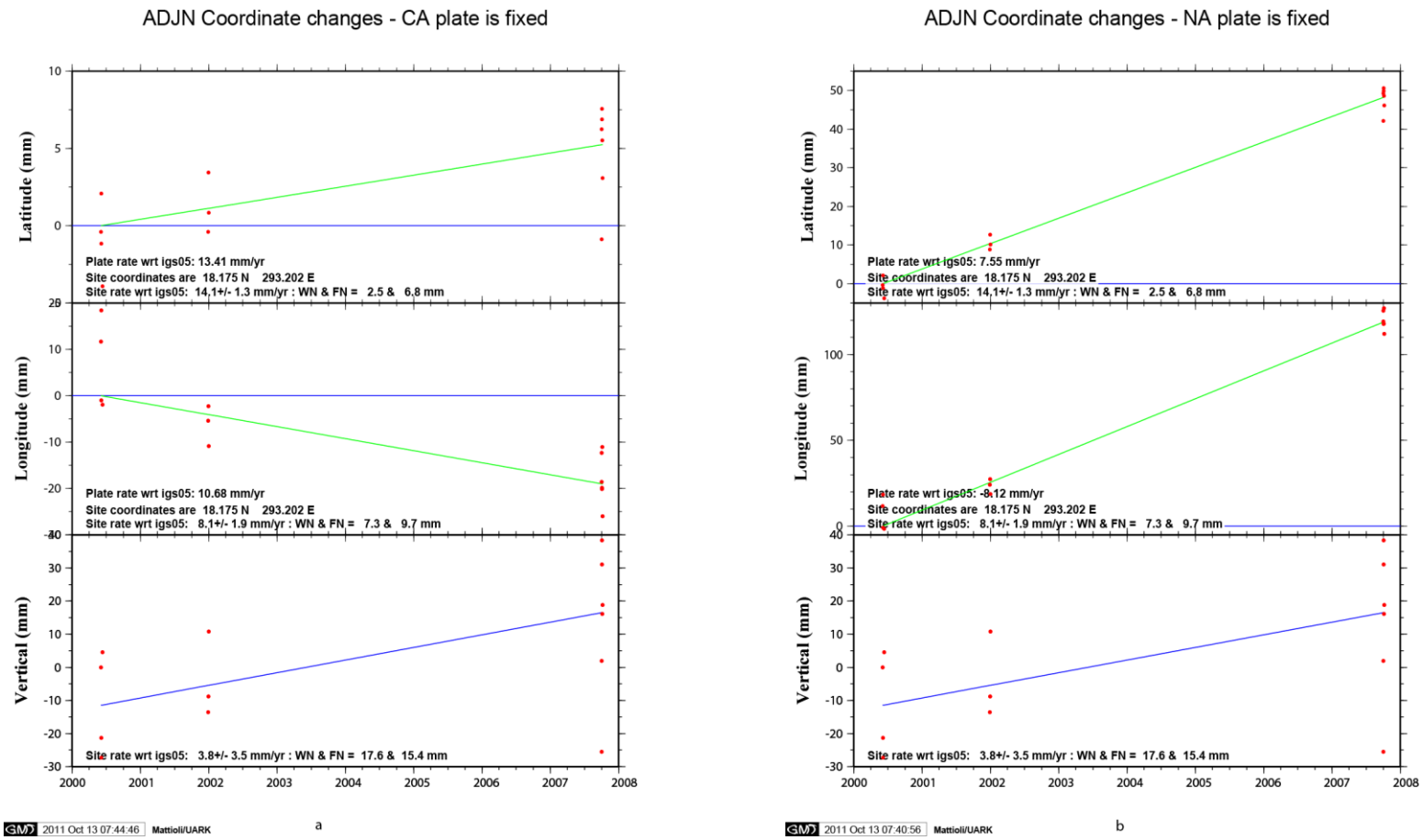

Figure 3.12 Time series for site ADJN. Red dots are the UTC daily position solutions. The blue lines are the predicted plate rates in ITRF05 held fixed (horizontal). The green lines are the least square fit site rates in IGS05 (a) with respect to the Caribbean plate rate-CA and (b) with respect to the North-American plate rate-NA. WN = white noise; FN = flicker noise estimates. Note: *The observed time series for the 2011 campaign was not used in this analysis because it was too short to be included.*

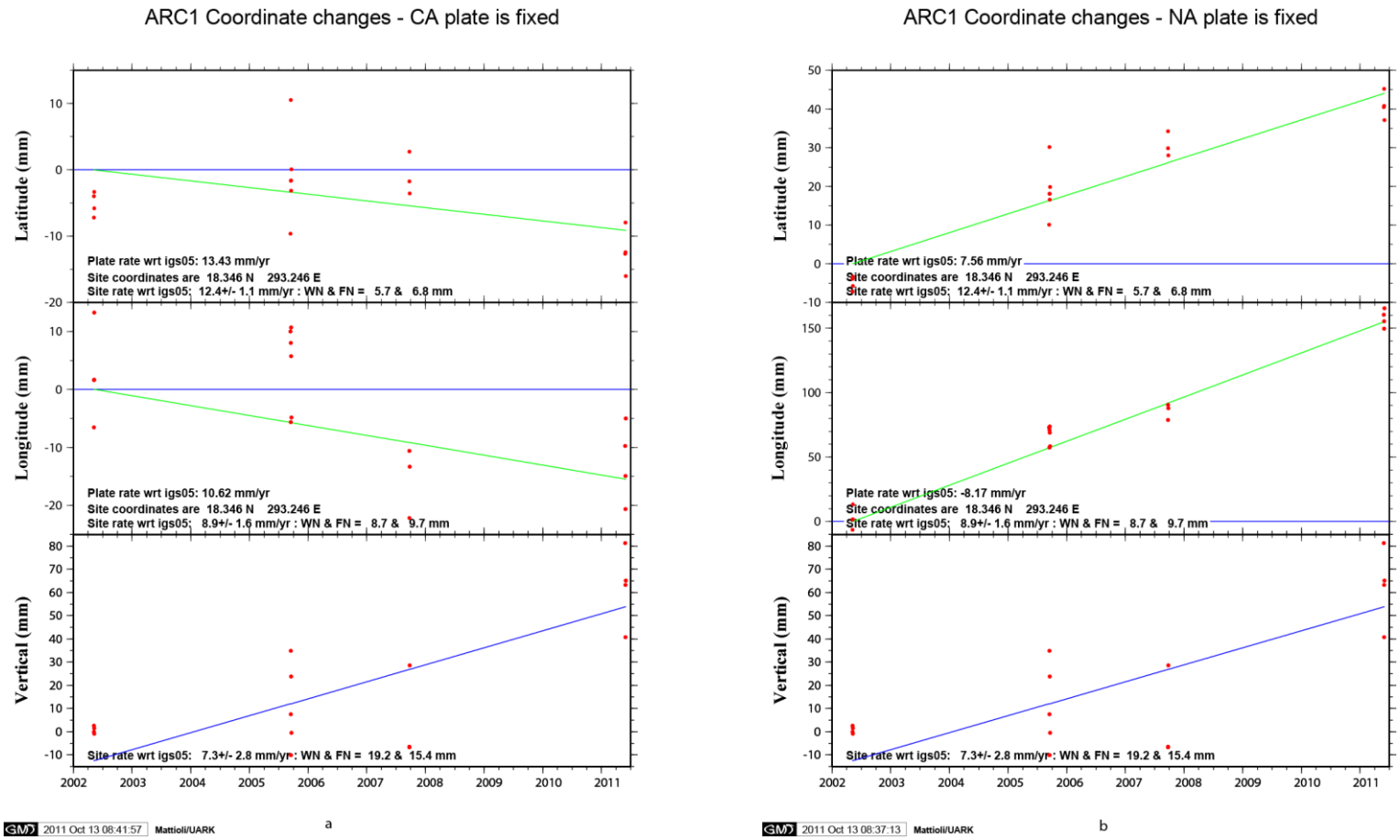

Figure 3.13 Time series for site ARC1. Red dots are the UTC daily position solutions. The blue lines are the predicted plate rates in ITRF05 held fixed (horizontal). The green lines are the least square fit site rates in IGS05 (a) with respect to the Caribbean plate rate-CA and (b) with respect to the North-American plate rate-NA. WN = white noise; FN = flicker noise estimates.

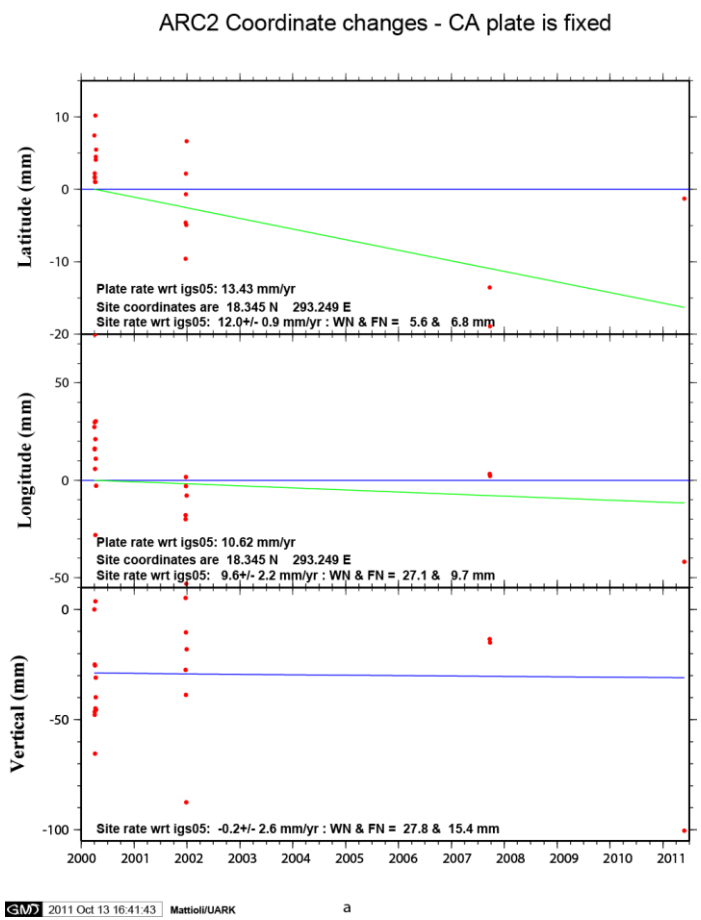

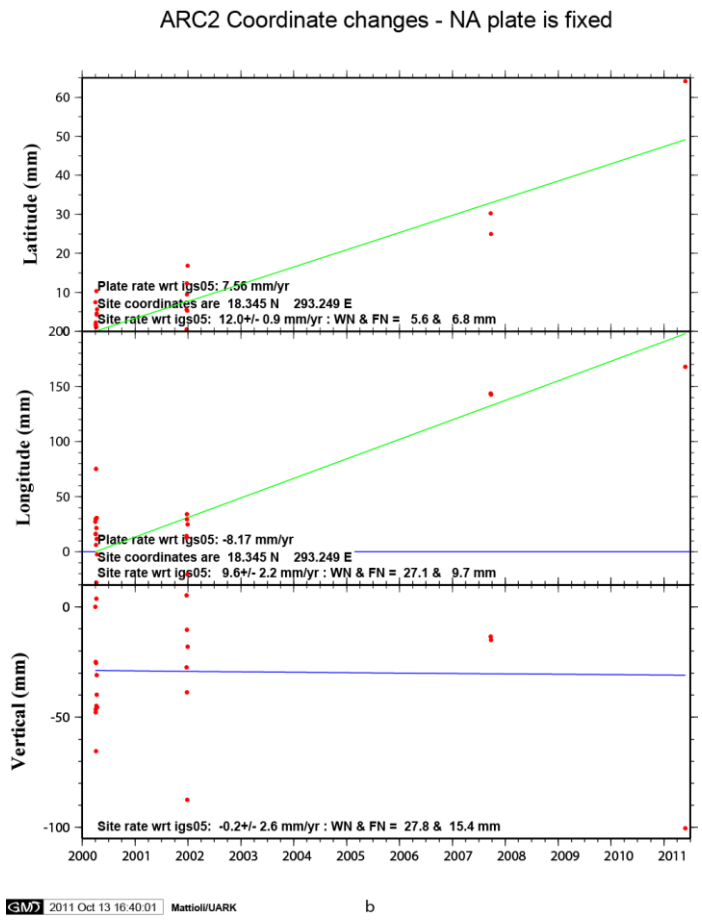

Figure 3.14 Time series for site ARC2. Red dots are the UTC daily position solutions. The blue lines are the predicted plate rates in ITRF05 held fixed (horizontal). The green lines are the least square fit site rates in IGS05 (a) with respect to the Caribbean plate rate-CA and (b) with respect to the North-American plate rate-NA. WN = white noise; FN = flicker noise estimates.

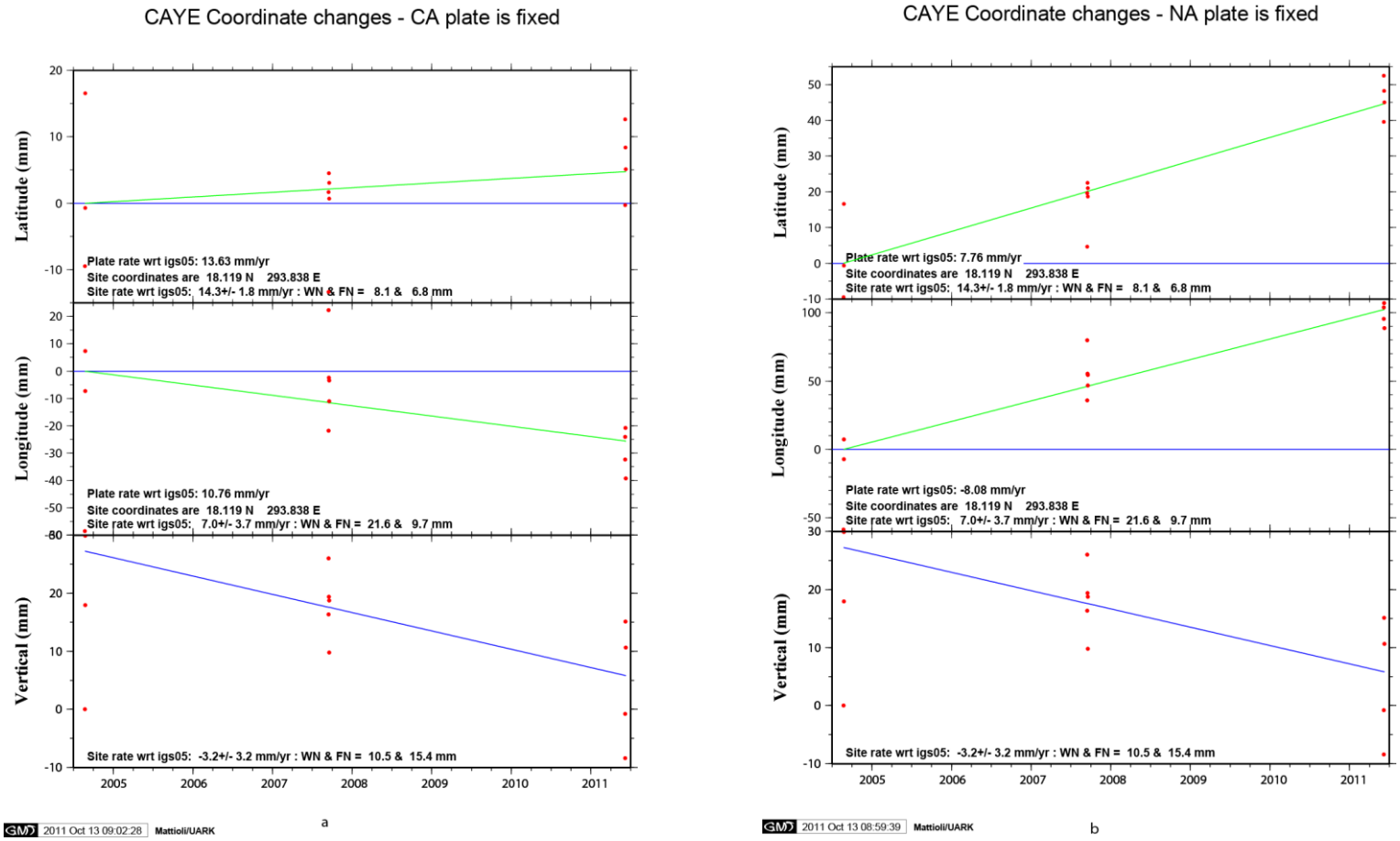

Figure 3.15 Time series for site CAYE. Red dots are the UTC daily position solutions. The blue lines are the predicted plate rates in ITRF05 held fixed (horizontal). The green lines are the least square fit site rates in IGS05 (a) with respect to the Caribbean plate rate-CA and (b) with respect to the North-American plate rate-NA. WN = white noise; FN = flicker noise estimates.

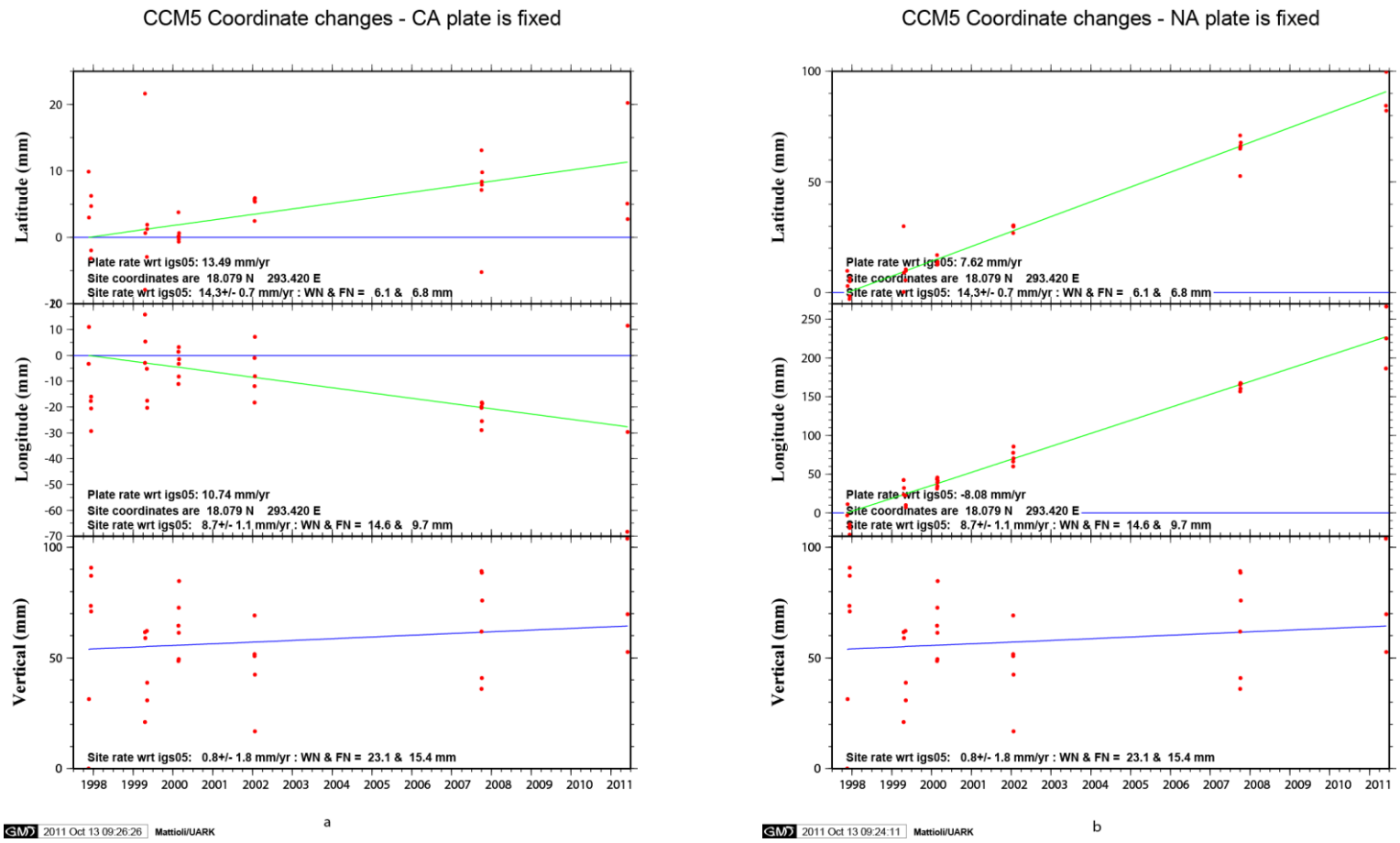

Figure 3.16 Time series for site CCM5. Red dots are the UTC daily position solutions. The blue lines are the predicted plate rates in ITRF05 held fixed (horizontal). The green lines are the least square fit site rates in IGS05 (a) with respect to the Caribbean plate rate-CA and (b) with respect to the North-American plate rate-NA. WN = white noise; FN = flicker noise estimates.

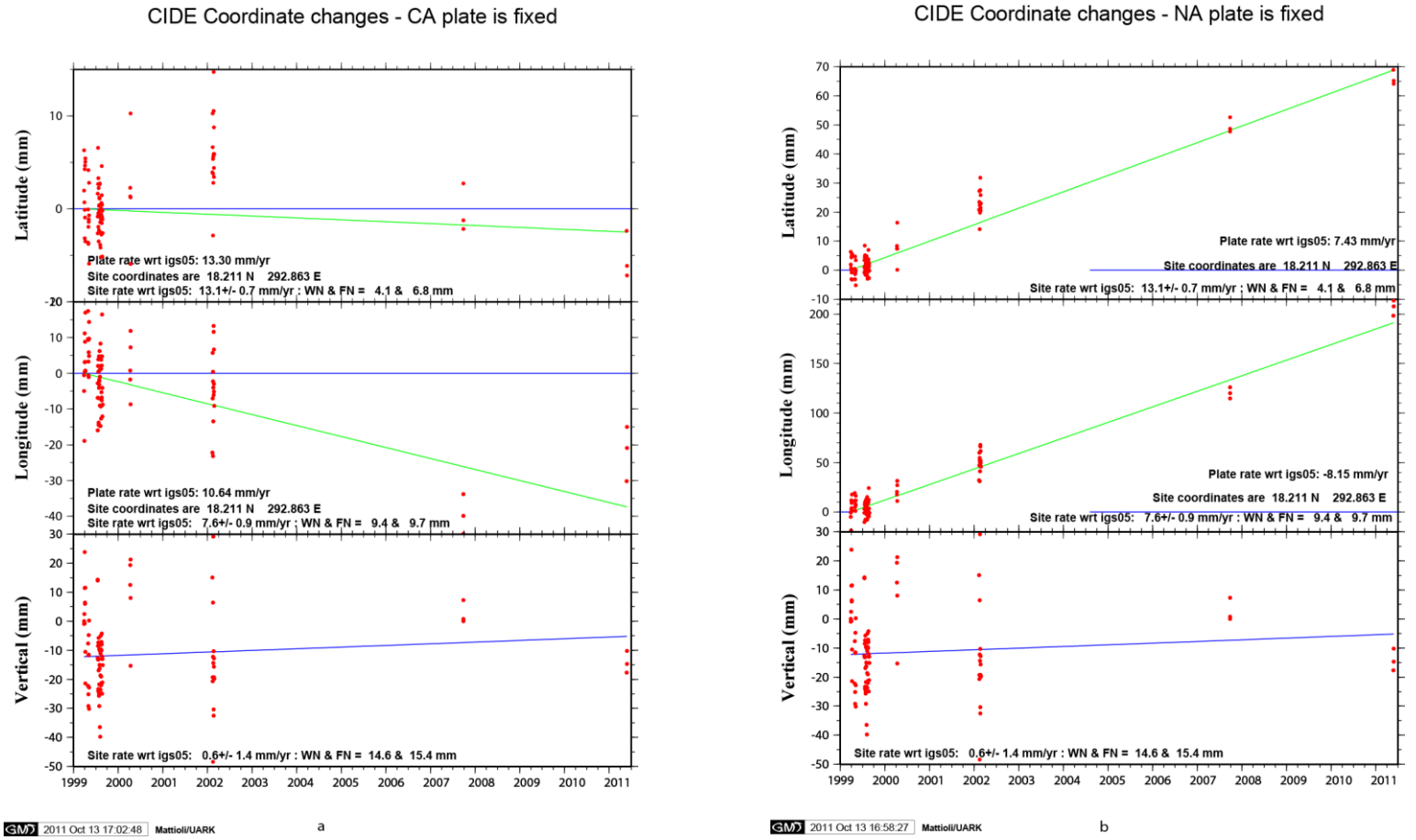

Figure 3.17 Time series for site CIDE. Red dots are the UTC daily position solutions. The blue lines are the predicted plate rates in ITRF05 held fixed (horizontal). The green lines are the least square fit site rates in IGS05 (a) with respect to the Caribbean plate rate-CA and (b) with respect to the North-American plate rate-NA. WN = white noise; FN = flicker noise estimates.

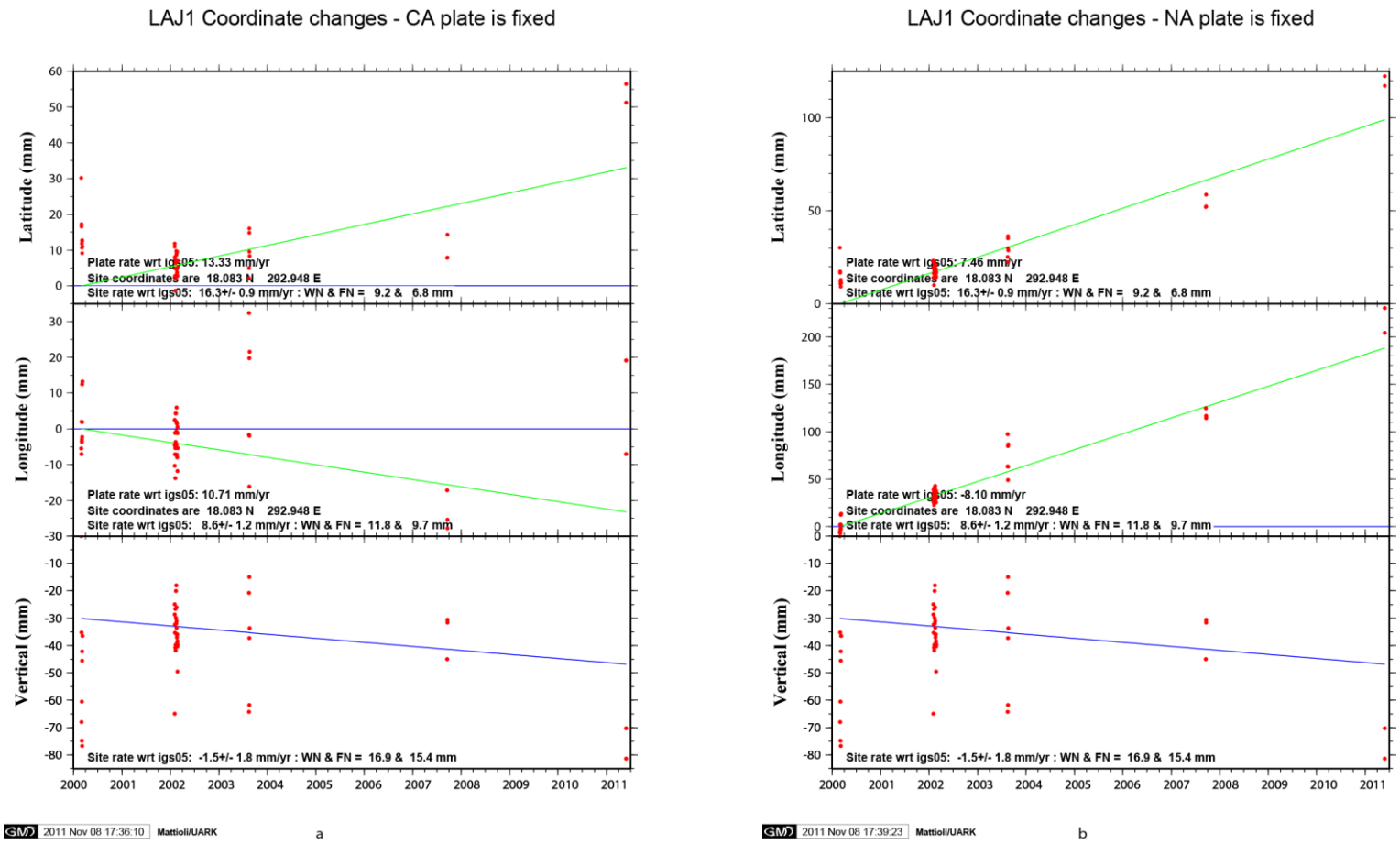

Figure 3.18 Time series for site LAJ1. Red dots are the UTC daily position solutions. The blue lines are the predicted plate rates in ITRF05 held fixed (horizontal). The green lines are the least square fit site rates in IGS05 (a) with respect to the Caribbean plate rate-CA and (b) with respect to the North-American plate rate-NA. WN = white noise; FN = flicker noise estimates.

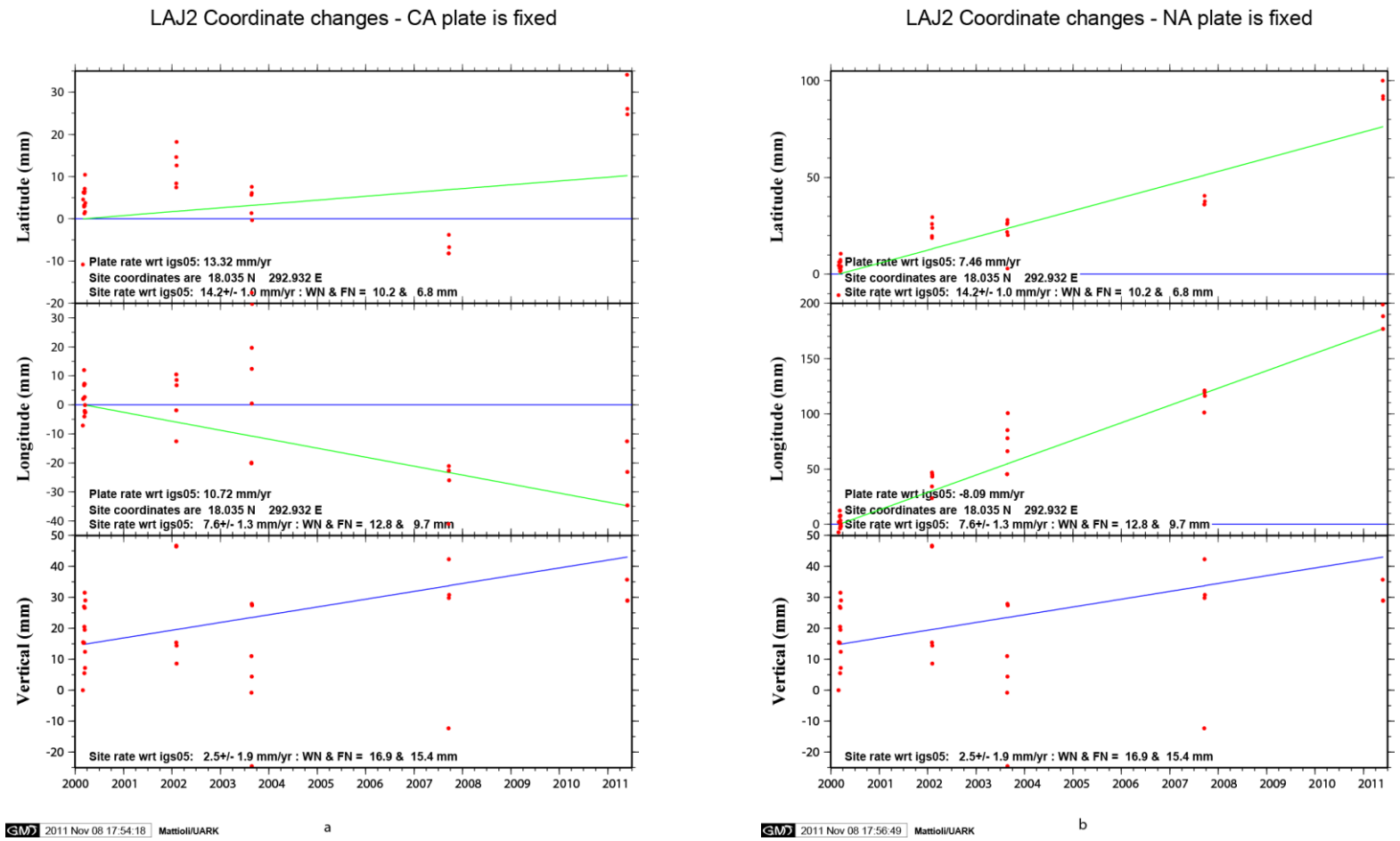

Figure 3.19 Time series for site LAJ2. Red dots are the UTC daily position solutions. The blue lines are the predicted plate rates in ITRF05 held fixed (horizontal). The green lines are the least square fit site rates in IGS05 (a) with respect to the Caribbean plate rate-CA and (b) with respect to the North-American plate rate-NA. WN = white noise; FN = flicker noise estimates.

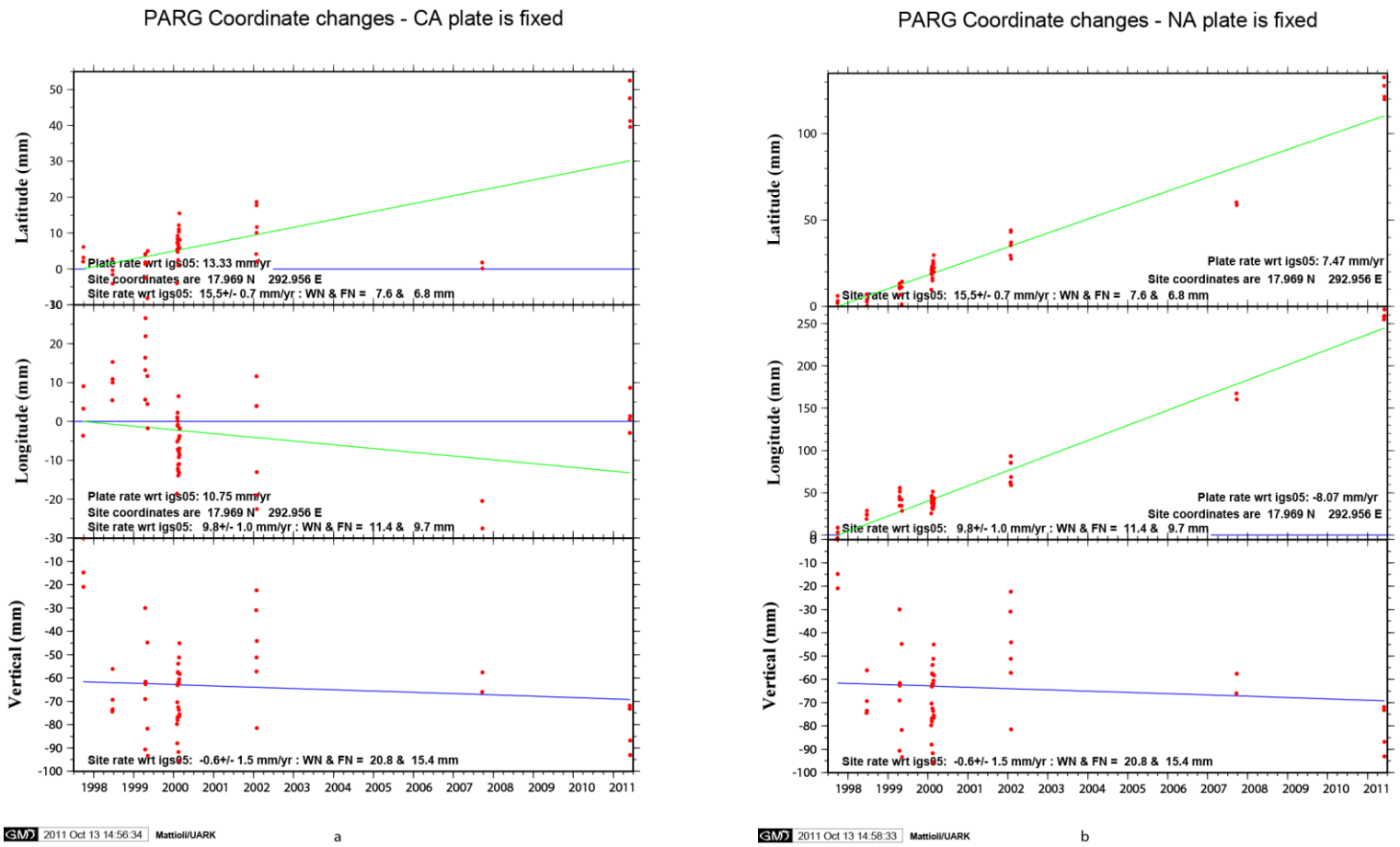

Figure 3.20 Time series for site PARG. Red dots are the UTC daily position solutions. The blue lines are the predicted plate rates in ITRF05 held fixed (horizontal). The green lines are the least square fit site rates in IGS05 (a) with respect to the Caribbean plate rate-CA and (b) with respect to the North-American plate rate-NA. WN = white noise; FN = flicker noise estimates.

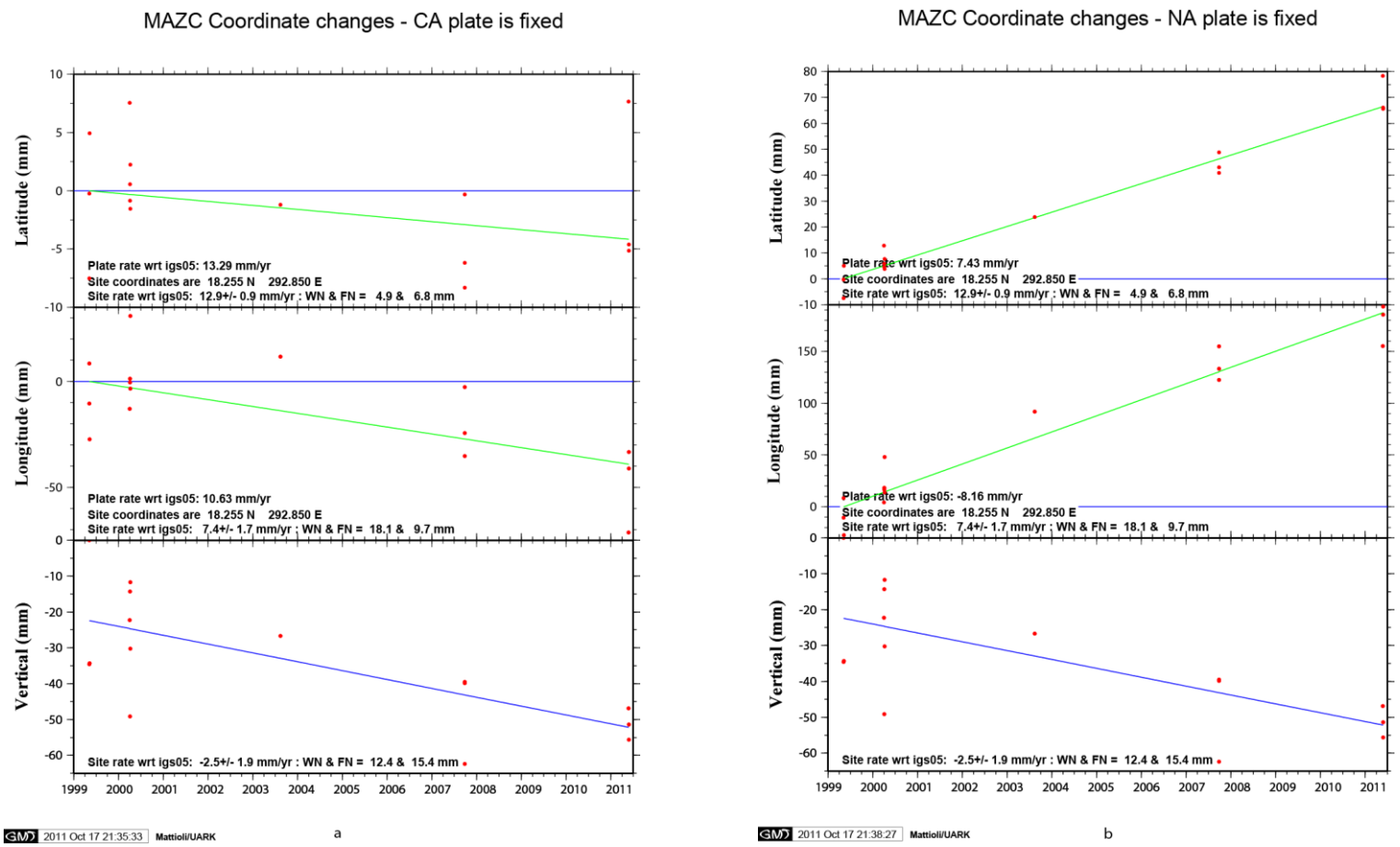

Figure 3.21 Time series for site MAZC. Red dots are the UTC daily position solutions. The blue lines are the predicted plate rates in ITRF05 held fixed (horizontal). The green lines are the least square fit site rates in IGS05 (a) with respect to the Caribbean plate rate-CA and (b) with respect to the North-American plate rate-NA. WN = white noise; FN = flicker noise estimates.

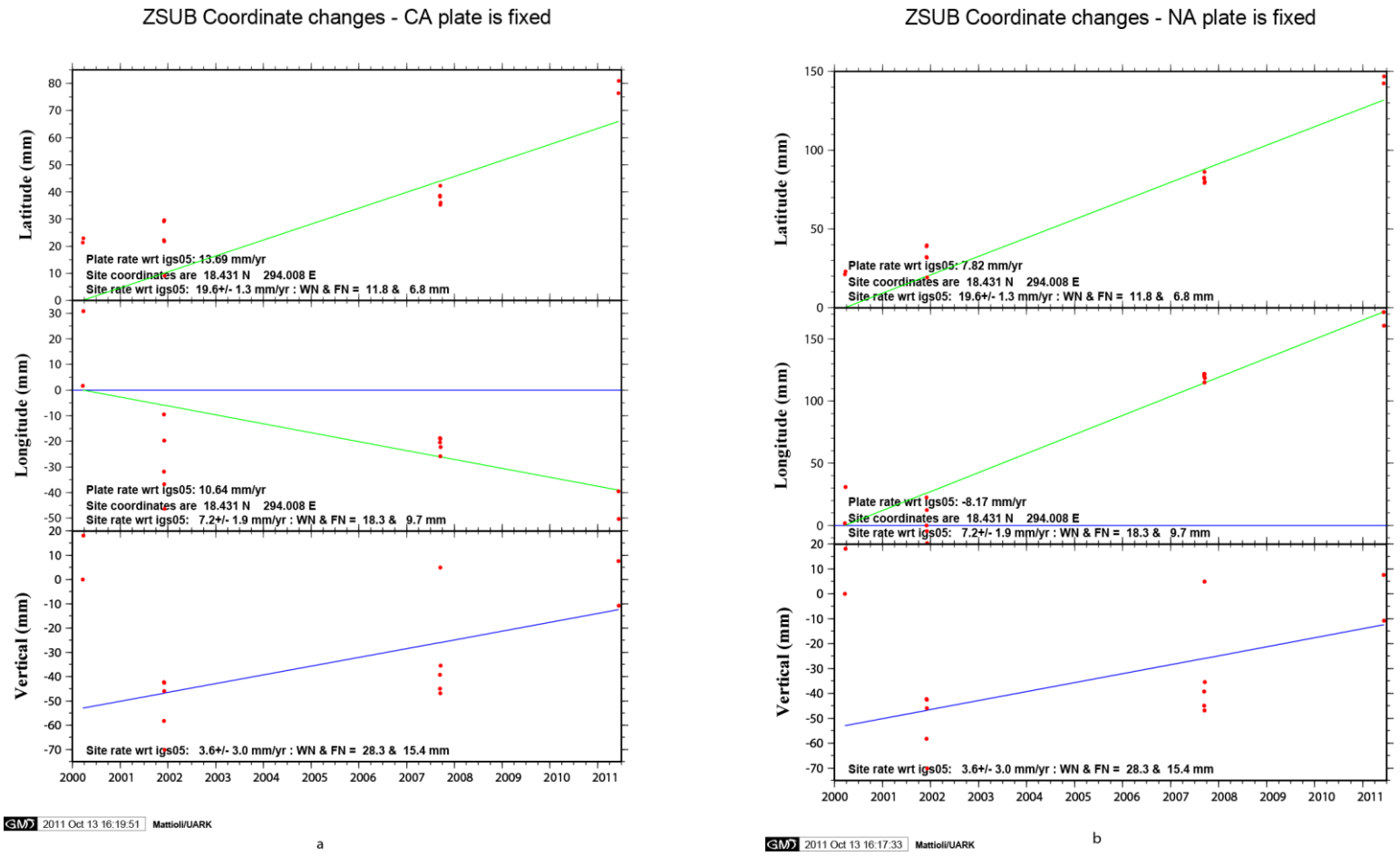

Figure 3.22 Time series for site ZSUB. Red dots are the UTC daily position solutions. The blue lines are the predicted plate rates in ITRF05 held fixed (horizontal). The green lines are the least square fit site rates in IGS05 (a) with respect to the Caribbean plate rate-CA and (b) with respect to the North-American plate rate-NA. WN = white noise; FN = flicker noise estimates

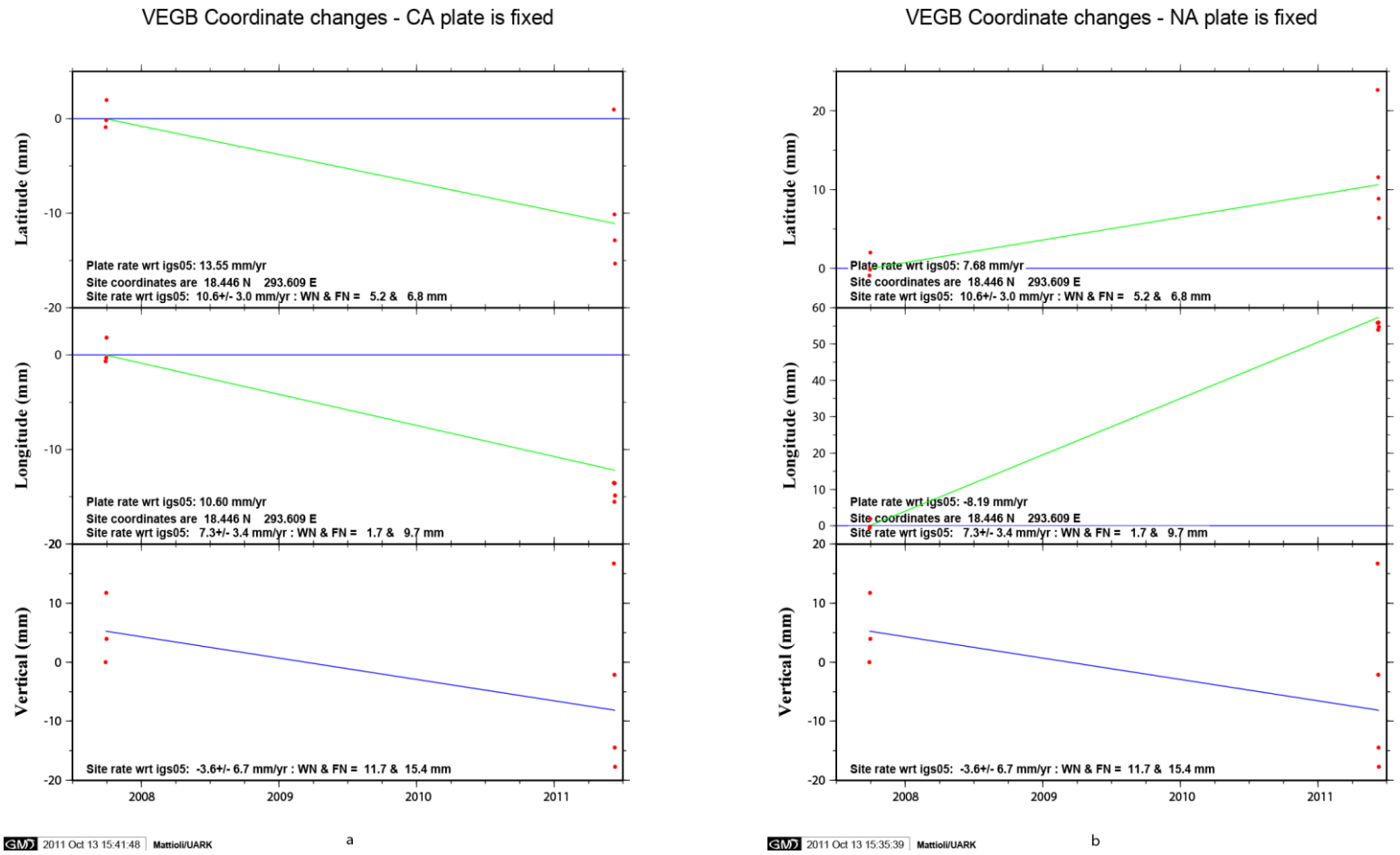

Figure 3.23 Time series for site VEGB. Red dots are the UTC daily position solutions. The blue lines are the predicted plate rates in ITRF05 held fixed (horizontal). The green lines are the least square fit site rates in IGS05 (a) with respect to the Caribbean plate rate-CA and (b) with respect to the North-American plate rate-NA. WN = white noise; FN = flicker noise estimates.

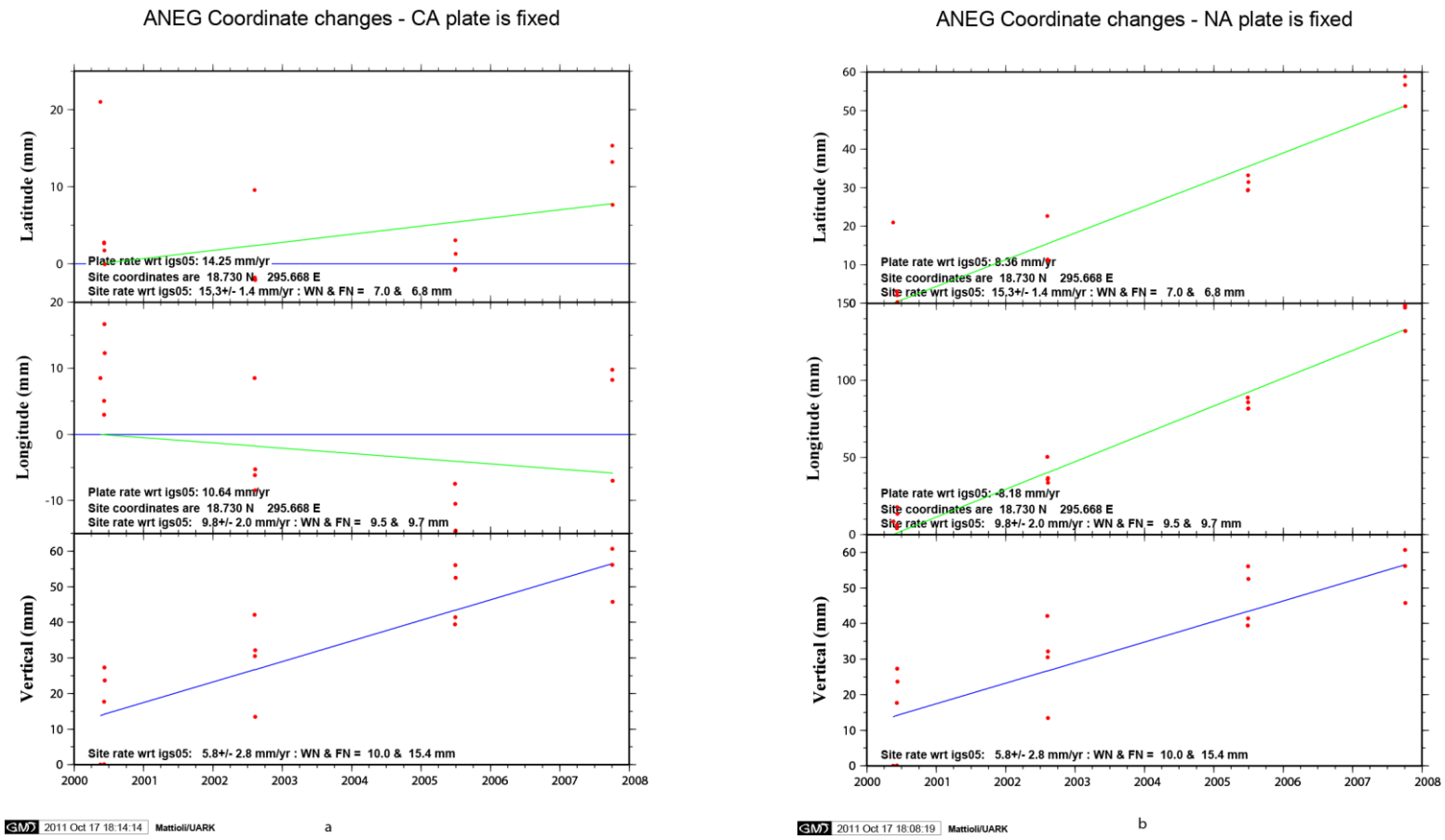

Figure 3.24 Time series for site ANEG. Red dots are the UTC daily position solutions. The blue lines are the predicted plate rates in ITRF05 held fixed (horizontal). The green lines are the least square fit site rates in IGS05 (a) with respect to the Caribbean plate rate-CA and (b) with respect to the North-American plate rate-NA. WN = white noise; FN = flicker noise estimates.

Note: *GPS station coordinate time series for other updated campaign sites (group 3) are from figures 3.24 to 3.32*

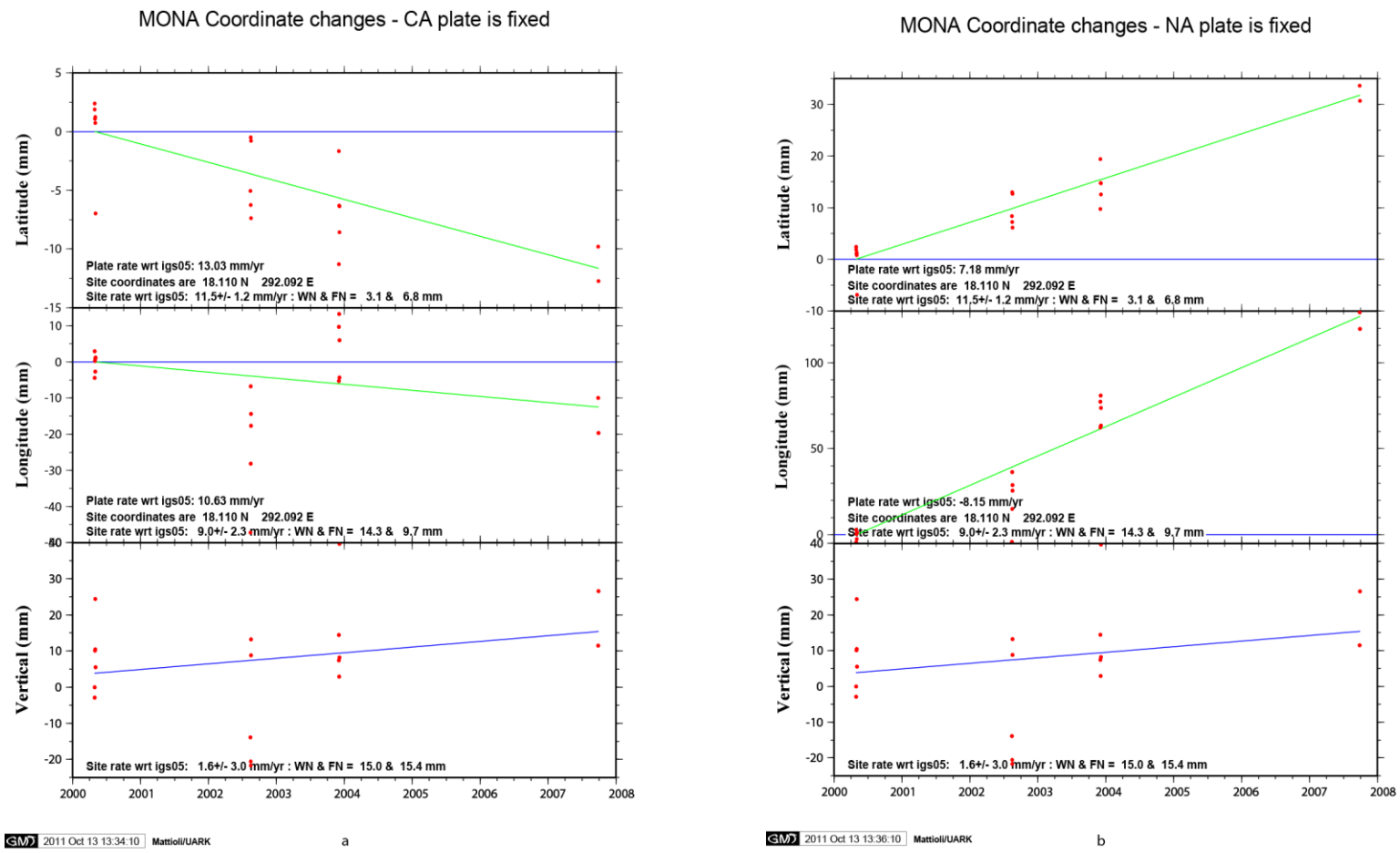

Figure 3.25 Time series for site MONA. Red dots are the UTC daily position solutions. The blue lines are the predicted plate rates in ITRF05 held fixed (horizontal). The green lines are the least square fit site rates in IGS05 (a) with respect to the Caribbean plate rate-CA and (b) with respect to the North-American plate rate-NA. WN = white noise; FN = flicker noise estimates.

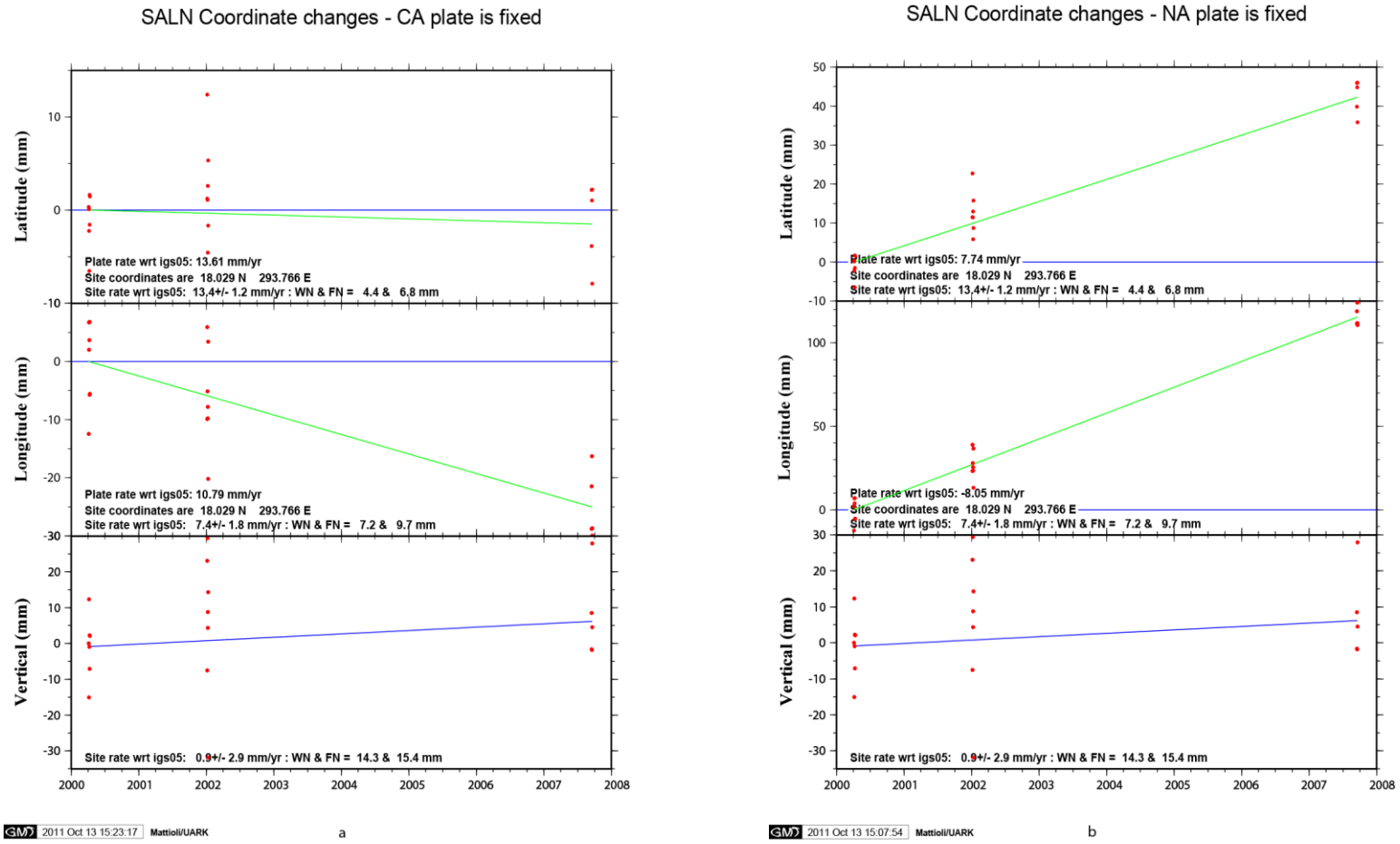

Figure 3.26 Time series for site SALN. Red dots are the UTC daily position solutions. The blue lines are the predicted plate rates in ITRF05 held fixed (horizontal). The green lines are the least square fit site rates in IGS05 (a) with respect to the Caribbean plate rate-CA and (b) with respect to the North-American plate rate-NA. WN = white noise; FN = flicker noise estimates.

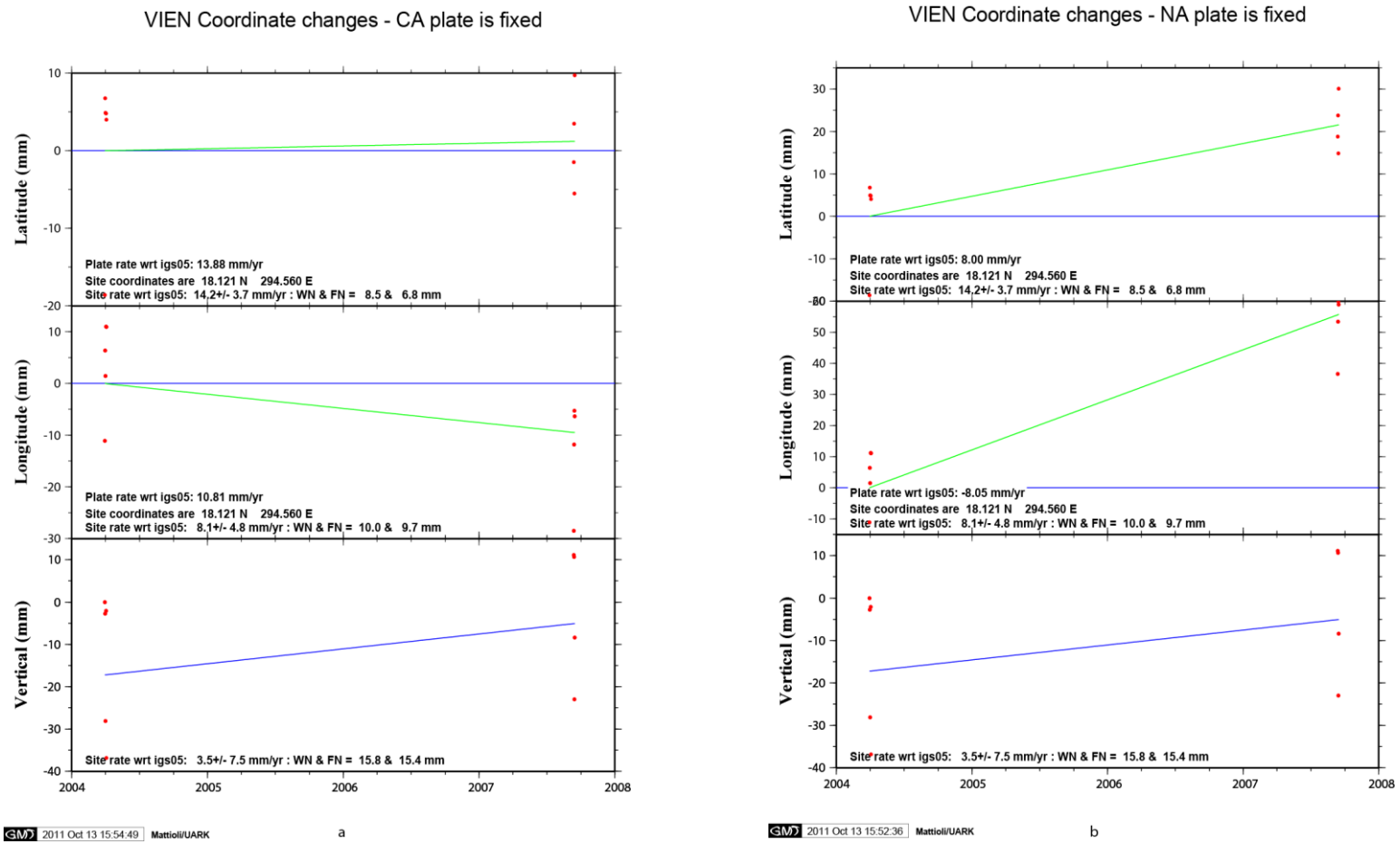

Figure 3.27 Time series for site VIEN. Red dots are the UTC daily position solutions. The blue lines are the predicted plate rates in ITRF05 held fixed (horizontal). The green lines are the least square fit site rates in IGS05 (a) with respect to the Caribbean plate rate-CA and (b) with respect to the North-American plate rate-NA. WN = white noise; FN = flicker noise estimates.

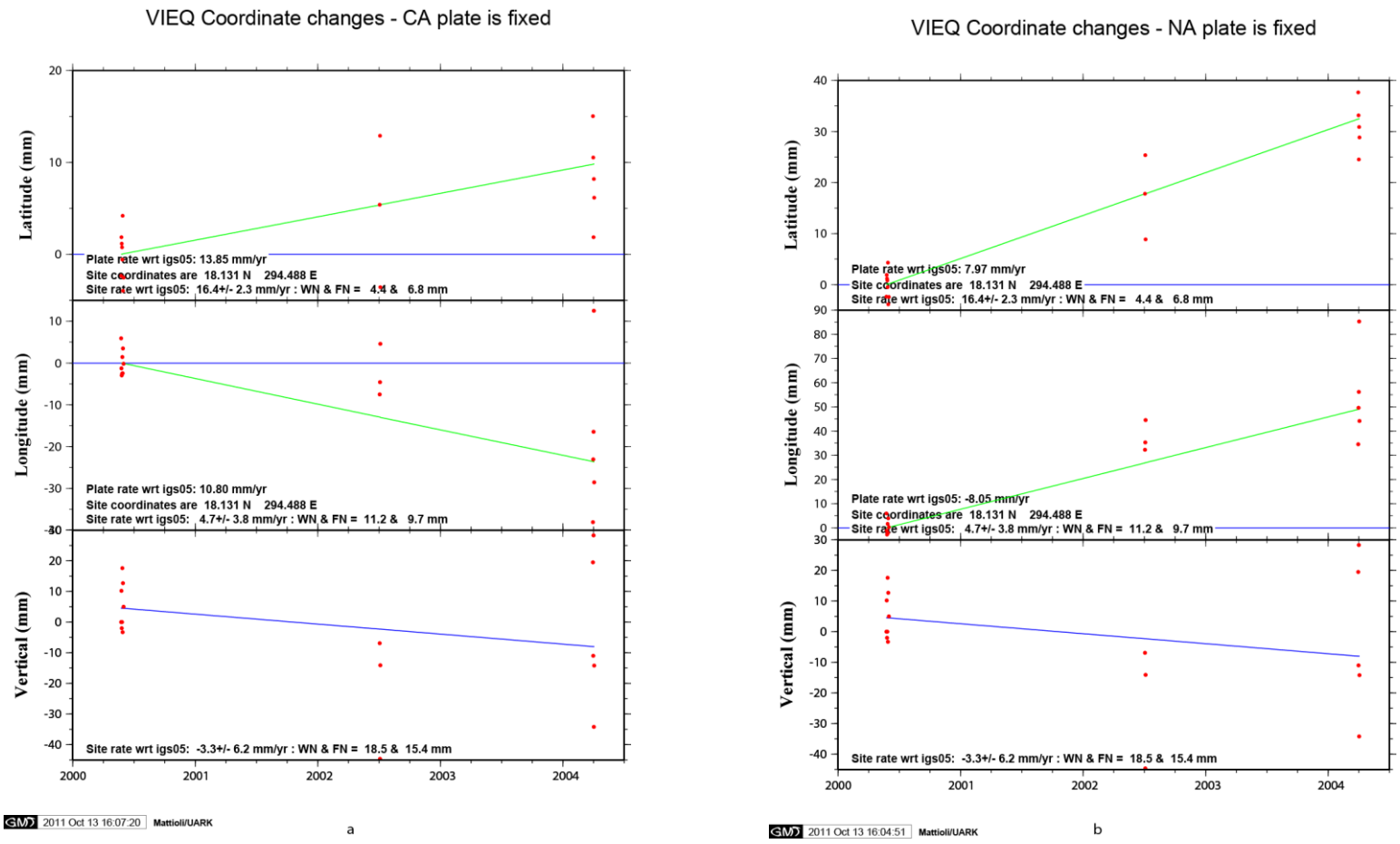

Figure 3.28 Time series for site VIEQ. Red dots are the UTC daily position solutions. The blue lines are the predicted plate rates in ITRF05 held fixed (horizontal). The green lines are the least square fit site rates in IGS05 (a) with respect to the Caribbean plate rate-CA and (b) with respect to the North-American plate rate-NA. WN = white noise; FN = flicker noise estimates.

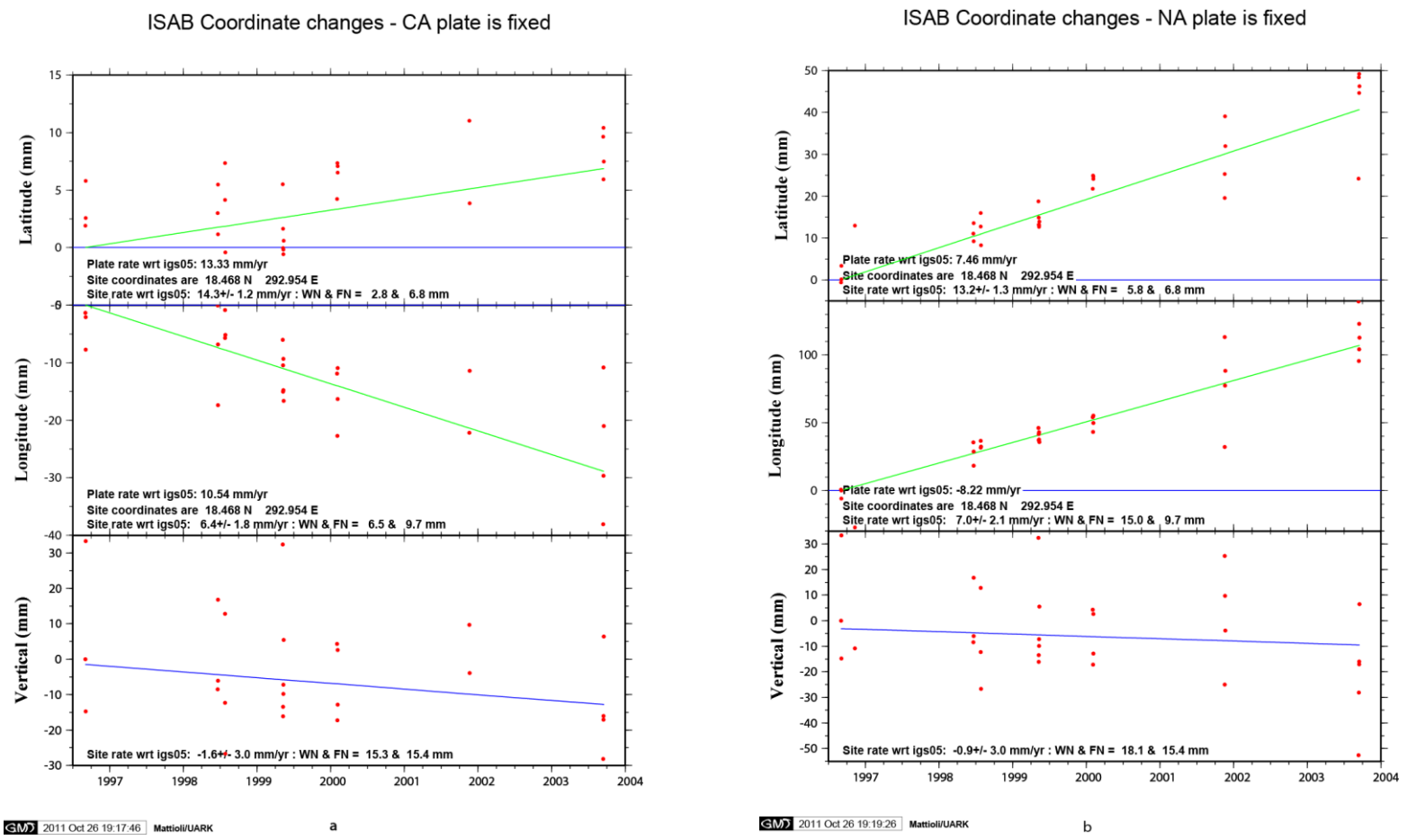

Figure 3.29 Time series for site ISAB. Red dots are the UTC daily position solutions. The blue lines are the predicted plate rates in ITRF05 held fixed (horizontal). The green lines are the least square fit site rates in IGS05 (a) with respect to the Caribbean plate rate-CA and (b) with respect to the North-American plate rate-NA. WN = white noise; FN = flicker noise estimates.

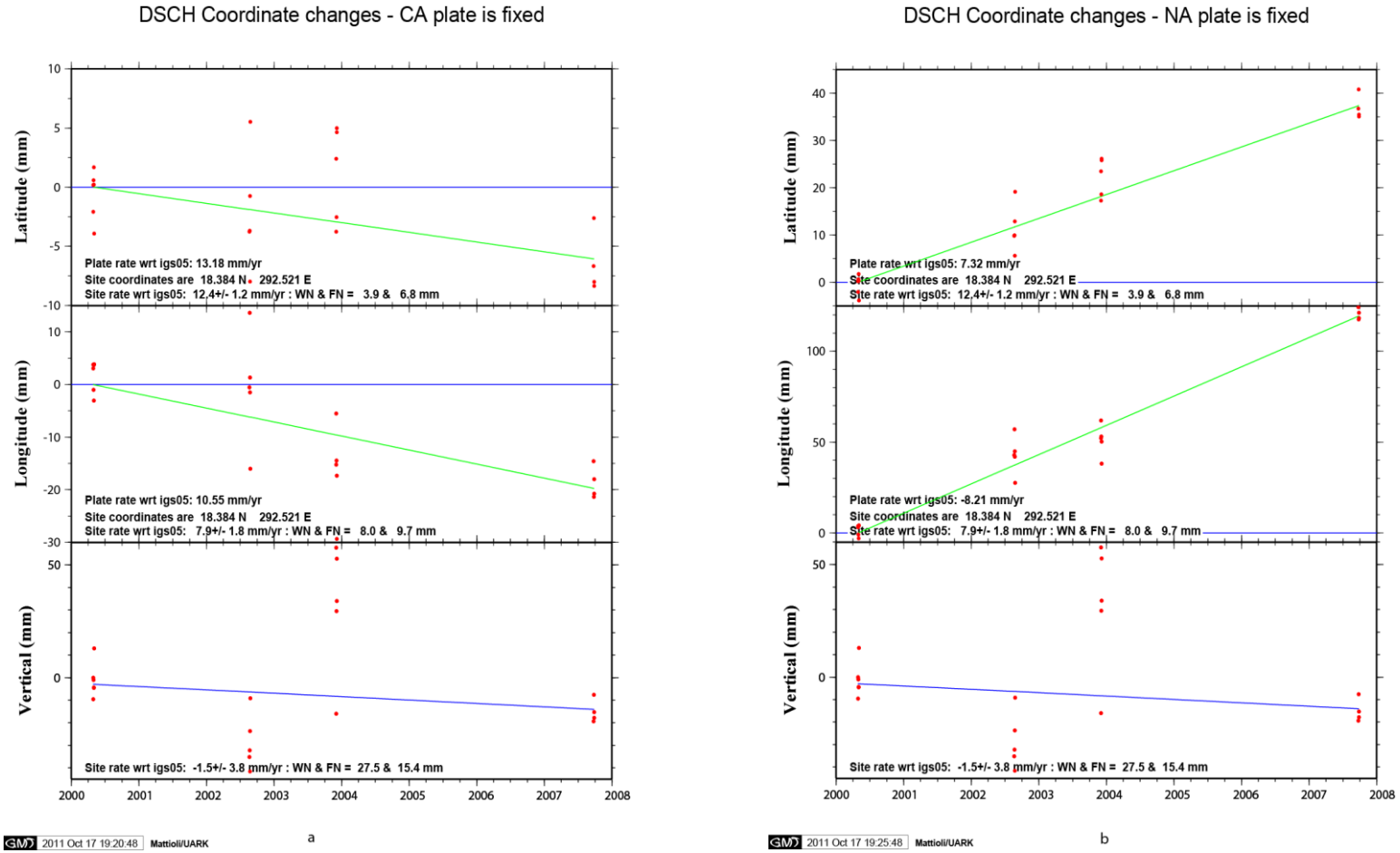

Figure 3.30 Time series for site DSCH. Red dots are the UTC daily position solutions. The blue lines are the predicted plate rates in ITRF05 held fixed (horizontal). The green lines are the least square fit site rates in IGS05 (a) with respect to the Caribbean plate rate-CA and (b) with respect to the North-American plate rate-NA. WN = white noise; FN = flicker noise estimates.

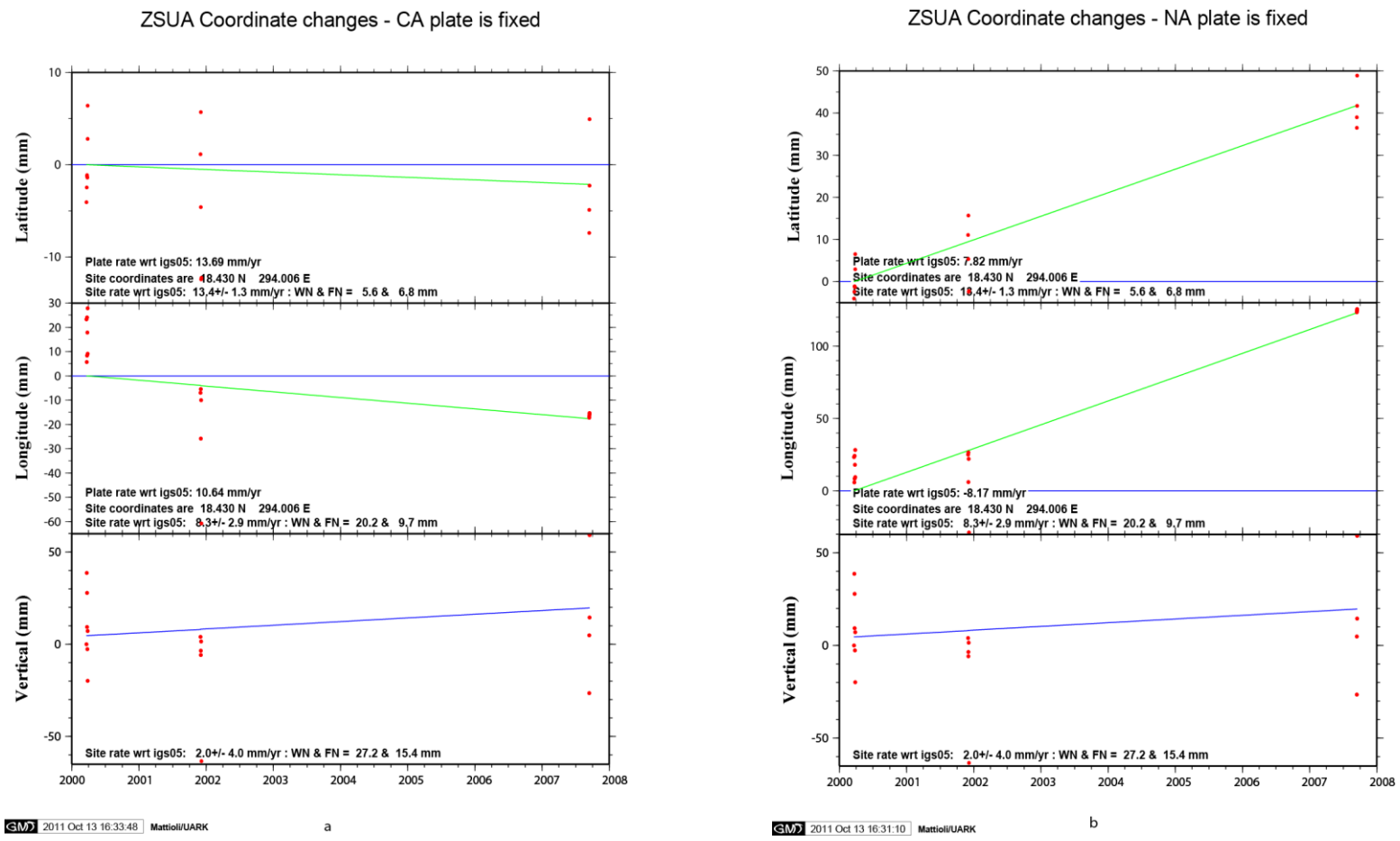

Figure 3.31 Time series for site ZSUA. Red dots are the UTC daily position solutions. The blue lines are the predicted plate rates in ITRF05 held fixed (horizontal). The green lines are the least square fit site rates in IGS05 (a) with respect to the Caribbean plate rate-CA and (b) with respect to the North-American plate rate-NA. WN = white noise; FN = flicker noise estimates.

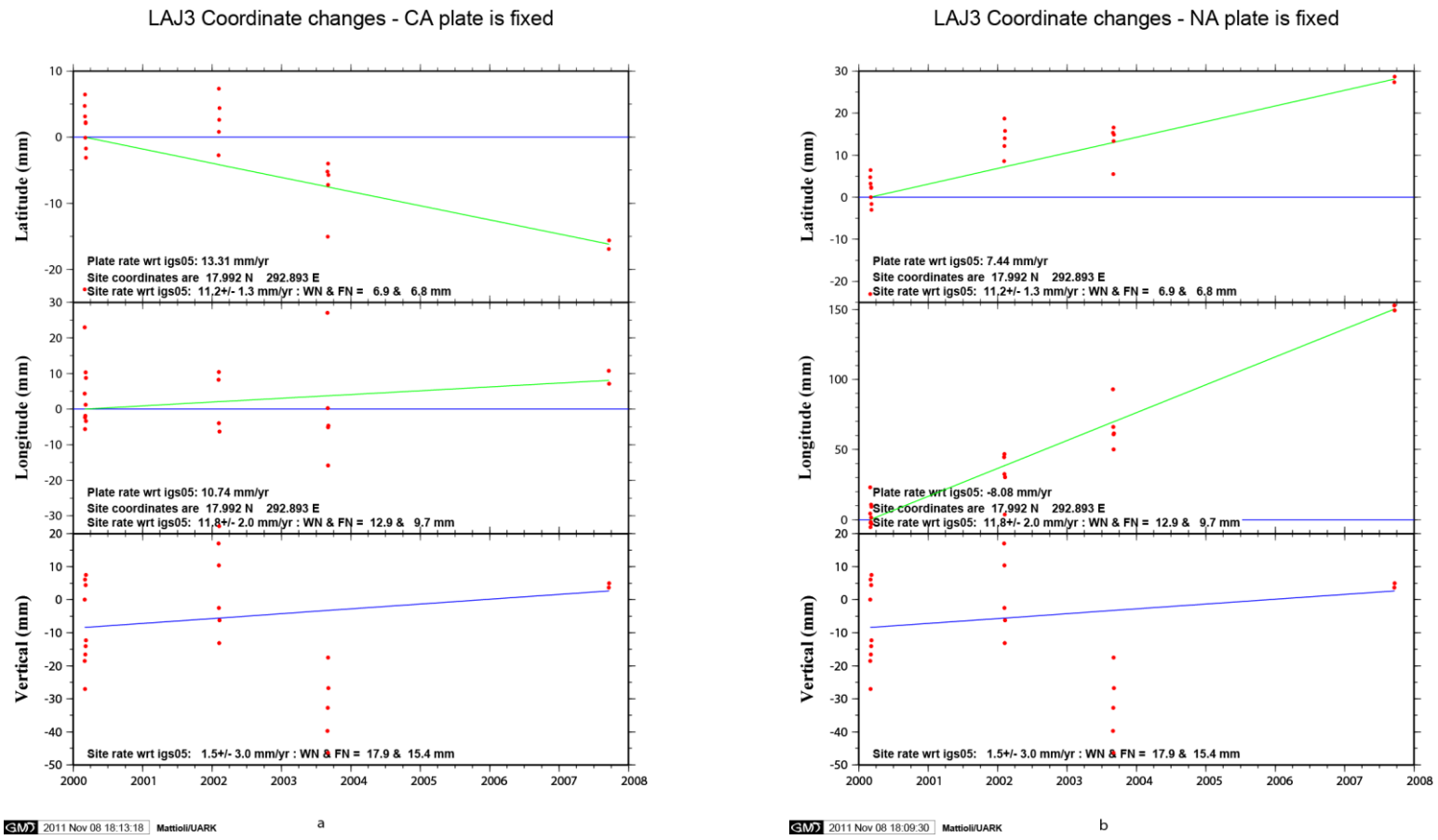

Figure 3.32 Time series for site LAJ3. Red dots are the UTC daily position solutions. The blue lines are the predicted plate rates in ITRF05 held fixed (horizontal). The green lines are the least square fit site rates in IGS05 (a) with respect to the Caribbean plate rate-CA and (b) with respect to the North-American plate rate-NA. WN = white noise; FN = flicker noise estimates.

Table 3.5 Velocities of GPS sites in Puerto Rico and the Virgin Islands in IGS2005 with respect to stable Caribbean Plate

Site name	Site ID	Latitude (N)	Longitude (E)	HAE (m)	IGS2005 (mm/yr) - No Common Mode Correction													CAR rate (mm/yr)		CAR Fixed Velocity (mm/yr)							Span	No. Obs
					Vn	Error	WN	FN	Ve	Error	WN	FN	Vv	Error	WN	FN	RWN	Vn	Ve	Vn	Error	Ve	Error	Vv	Error	Epoch	Years	
Anagada	ABVI	18.730	295.668	678.6	9.8	9.3	2.8	6.8	5.2	13.3	3.8	9.7	-35.9	21.1	7.2	15.4	1.0	14.25	10.64	-4.45	9.30	-5.44	13.30	-35.90	21.10	2011.0945-2011.6123	0.5178	190
Arecibo observatory	AOPR	18.347	293.246	350.7	15.1	1.1	2.7	3.8	8.2	1.4	5.1	5.2	-31.9	2.6	12.2	10.2	1.0	13.43	10.62	1.67	1.10	-2.42	1.40	-31.90	2.60	2008.7090-2011.5274	2.8184	1014
Bayamon science park	BYSP	18.408	293.839	86.6	14.7	0.8	2.7	3.0	8.3	0.8	4.3	2.9	-3.0	2.0	8.6	9.1	1.0	13.63	10.63	1.07	0.80	-2.33	0.80	-3.00	2.00	2008.3484-2011.6123	3.2640	1176
ST. CROIX VLBA, V/I	CRO1	17.757	295.416	-31.8	13.6	0.4	2.4	6.6	10.8	0.5	4.6	8.2	-1.7	1.0	10.2	21.3	1.0	14.16	11.02	-0.56	0.40	-0.22	0.50	-1.70	1.00	1996.0178-2011.6123	15.5946	5245
CULEBRA ISLAND,PR	CUPR	18.307	294.717	-34.6	15.1	1.0	2.4	3.0	9.2	1.1	3.7	3.4	-5.0	2.3	7.9	8.6	1.0	13.93	10.74	1.17	1.00	-1.54	1.10	-5.00	2.30	2008.8320-2011.6123	2.7804	949
MAYAGUEZ TGPR 2010,PR	MAYZ	18.218	292.841	1.0	13.7	2.1	3.0	4.2	6.1	1.5	4.3	2.6	-6.7	3.0	9.5	5.9	1.0	13.29	10.64	0.41	2.10	-4.54	1.50	-6.70	3.00	2010.1000-2011.6123	1.5123	549
MIPR CAJA DE MUERTOS ISD,PR	MIPR	17.886	293.473	7.8	14.4	0.8	2.0	2.6	9.5	0.9	3.5	3.1	-0.8	1.9	7.4	7.9	1.0	13.51	10.83	0.89	0.80	-1.33	0.90	-0.80	1.90	2008.3566-2011.4534	3.0969	1126
CERRILLOS_PR2008,PR	P780	18.075	293.421	154.1	14.1	0.9	2.8	3.1	8.4	0.9	4.0	3.5	0.6	2.5	9.0	11.0	1.0	13.49	10.74	0.61	0.90	-2.34	0.90	0.60	2.50	2008.4030-2011.6123	3.2093	1172
MONA ISLAND,PUERTO RICO	MOPR	18.077	292.069	-38.3	12.3	0.8	2.6	2.2	8.7	1.0	3.8	3.2	-0.9	2.3	7.8	8.9	1.0	13.02	10.65	-0.72	0.80	-1.95	1.00	-0.90	2.30	2008.8210-2011.6123	2.7913	1017
ST. THOMAS, US V/I	STVI	18.340	295.026	-21.6	14.6	1.0	3.5	3.1	10.1	1.1	4.1	3.5	-1.2	2.8	9.5	10.8	1.0	14.03	10.75	0.57	1.00	-0.65	1.10	-1.20	2.80	2008.8210-2011.6123	2.7913	1011
UPRM GEOL DEPT BLD	GEOL	18.211	292.860	-9.9	12.6	0.4	3.9	6.6	8.6	0.6	8.9	10.4	-0.1	0.8	13.7	16.6	1.0	13.30	10.64	-0.70	0.40	-2.04	0.60	-0.10	0.80	1996.7090-2011.3932	14.6841	3709
ADJUNTAS AGR STATION	ADJN	18.175	293.202	519.3	14.1	1.3	2.5	6.8	8.1	1.9	7.3	9.7	3.8	3.5	17.6	15.4	1.0	13.41	10.68	0.69	1.30	-2.58	1.90	3.80	3.50	2000.4221-2007.7630	7.3409	13
ANEGADA ISD	ANEG	18.730	295.668	321.9	15.3	1.4	7.0	6.8	9.8	2.0	9.5	9.7	5.8	2.8	10.0	15.4	1.0	14.25	10.64	1.05	1.40	-0.84	2.00	5.80	2.80	2000.3757-2007.7603	7.3846	16
ARECIBO 1	ARC1	18.346	293.246	323.6	12.4	1.1	5.7	6.8	8.9	1.6	8.7	9.7	7.3	2.8	19.2	15.4	1.0	13.43	10.62	-1.03	1.10	-1.72	1.60	7.30	2.80	2002.3466-2011.4151	9.0685	17
ARECIBO 2	ARC2	18.345	293.249	-36.9	12.0	0.9	5.6	6.8	9.6	2.2	27.1	9.7	-0.2	2.6	27.8	15.4	1.0	13.43	10.62	-1.43	0.90	-1.02	2.20	-0.20	2.60	2000.2500-2007.7274	7.4774	19
UPRC SCIENCES BLD	CAYE	18.119	293.838	370.6	14.3	1.8	8.1	6.8	7.0	3.7	21.6	9.7	-3.2	3.2	10.5	15.4	1.0	13.63	10.76	0.67	1.80	-3.76	3.70	-3.20	3.20	2004.6462-2011.4370	6.7908	11
CERRILLOS_DAM BM	CCM5	18.079	293.421	161.1	14.3	0.7	6.1	6.8	8.7	1.1	14.6	9.7	0.8	1.8	23.1	15.4	1.0	13.49	10.74	0.81	0.70	-2.04	1.10	0.80	1.80	2000.1352-2011.4233	11.2880	20
CENTER FOR IND.RES/DEV	CIDE	18.211	292.863	1.3	13.1	0.7	4.1	6.8	7.6	0.9	9.4	9.7	0.6	1.4	14.6	15.4	1.0	13.30	10.64	-0.20	0.70	-3.04	0.90	0.60	1.40	1999.2342-2011.4041	12.1699	93
DESECHEO ISLAND	DSCH	18.384	292.521	151.6	12.4	1.2	3.9	6.8	7.9	1.8	8.0	9.7	-1.5	3.8	27.5	15.4	1.0	13.18	10.55	-0.78	1.20	-2.65	1.80	-1.50	3.80	2000.3238-2007.7384	7.4146	20
ISABELA	ISAB	18.468	292.954	82.9	13.4	1.3	5.9	6.8	6.8	2.5	21.7	9.7	-0.5	3.1	20.0	15.4	1.0	13.33	10.54	0.07	1.30	-3.74	2.50	-0.50	3.10	1996.6708-2001.8890	5.2183	18
LAJAS VALLEY UNI SAN GERMAN	LAJ1	18.083	292.948	28.7	16.3	0.9	9.2	6.8	8.6	1.2	11.8	9.7	-1.5	1.8	16.9	15.4	1.0	13.33	10.71	2.97	0.90	-2.11	1.20	-1.50	1.80	2000.1626-2011.4041	11.2415	31
SOUTH LAJAS VALLEY-AES.UPRM	LAJ2	18.035	292.932	-3.4	14.2	1.0	10.2	6.8	7.6	1.3	12.8	9.7	2.5	1.9	16.9	15.4	1.0	13.32	10.72	0.88	1.00	-3.12	1.30	2.50	1.90	2000.1626-2011.4041	11.2415	23
NORTH LAJAS VALLEY	LAJ3	17.992	292.893	179.4	11.2	1.3	6.9	6.8	11.8	2.0	12.9	9.7	1.5	3.0	17.9	15.4	1.0	13.31	10.74	-2.11	1.30	1.06	2.00	1.50	3.00	2000.1653-2007.7192	7.5539	19
MAYAGUEZ AIRPORT	MAZC	18.255	292.850	-34.7	12.9	0.9	4.9	6.8	7.4	1.7	18.1	9.7	-2.5	1.9	12.4	15.4	1.0	13.29	10.63	-0.39	0.90	-3.23	1.70	-2.50	1.90	2000.2500-2011.4041	11.1541	12
MONA ISLAND, PR	MONA	18.110	292.092	41.5	11.5	1.2	3.1	6.8	9.0	2.3	14.3	9.7	1.6	3.0	15.0	15.4	1.0	13.03	10.63	-1.53	1.20	-1.63	2.30	1.60	3.00	2000.3238-2007.7411	7.4173	18
PARGUERA, PR	PARG	17.969	292.956	-8.1	15.5	0.7	7.6	6.8	9.8	1.0	11.4	9.7	-0.6	1.5	20.8	15.4	1.0	13.33	10.75	2.17	0.70	-0.95	1.00	-0.60	1.50	2000.0861-2011.4233	11.3372	34
SALINA, ALBERGUE OLIMPICO	SALN	18.029	293.766	128.4	13.4	1.2	4.4	6.8	7.4	1.8	7.2	9.7	0.9	2.9	14.3	15.4	1.0	13.61	10.79	-0.21	1.20	-3.39	1.80	0.90	2.90	2000.2582-2007.7164	7.4582	19
VEGA BAJA, OLD FIRSTATION	VEGB	18.446	293.609	-30.8	10.6	3.0	5.2	6.8	7.3	3.4	1.7	9.7	-3.6	6.7	11.7	15.4	1.0	13.55	10.60	-2.95	3.00	-3.30	3.40	-3.60	6.70	2007.7411-2011.4425	3.7014	7
VIEQUES BASE, ISLAND, PR	VIEN	18.121	294.560	-5.8	14.2	3.7	8.5	6.8	8.1	4.8	10.0	9.7	3.5	7.5	15.8	15.4	1.0	13.88	10.81	0.32	3.70	-2.71	4.80	3.50	7.50	2004.2445-2007.7055	3.4609	9
VIEQUES ISLAND, PR	VIEQ	18.131	294.488	-38.8	16.4	2.3	4.4	6.8	4.7	3.8	11.2	9.7	-3.3	6.2	18.5	15.4	1.0	13.85	10.80	2.55	2.30	-6.10	3.80	-3.30	6.20	2000.3948-2004.2555	3.8607	16
FAA,SAN JUAN,PR	ZSUA	18.430	294.006	-34.1	13.4	1.3	5.6	6.8	8.3	2.9	20.2	9.7	2.0	4.0	27.2	15.4	1.0	13.69	10.64	-0.29	1.30	-2.34	2.90	2.00	4.00	2000.2199-2011.4397	11.2198	14
NAT. WEATHER. SERVICE CAROLINA, P	ZSUB	18.431	294.008	-42.7	19.6	1.3	11.8	6.8	7.2	1.9	18.3	9.7	3.6	3.0	28.3	15.4	1.0	13.69	10.64	5.91	1.30	-3.44	1.90	3.60	3.00	2000.2199-2007.7082	7.4883	16

Note: The table above is with respect to STABLE CARIBBEAN PLATE (CAR). The white and the flicker noise values reflect the uncertainties on the derived velocities (Mao et al., 1999). IGS05 means International GPS Service-Reference Frame 2005. ABVI velocity components were not included in the kinematic analysis because of the short time frame and the large errors.

Table 3.6 Velocities of GPS sites in Puerto Rico and the Virgin Islands in IGS2005 with respect to stable NAM Plate

Site ID	Latitude (N)	Longitude (E)	HAE (m)	IGS2005 (mm/yr) - No Common Mode Correction													NAM rate (mm/yr)		NAM Fixed Velocity (mm/yr)							Span	No. Obs
				Vn	Error	WN	FN	Ve	Error	WN	FN	Vv	Error	WN	FN	RWN	Vn	Ve	Vn	Error	Ve	Error	Vv	Error	Epoch	Years	
ABVI	18.730	295.668	678.6	9.8	9.3	2.8	6.8	5.2	13.3	3.8	9.7	-35.9	21.1	7.2	15.4	1.0	8.36	-8.18	1.44	9.30	13.38	13.30	-35.90	21.10	2011.0945-2011.6123	0.5178	190
AOPR	18.347	293.246	350.7	15.1	1.1	2.7	3.8	8.2	1.4	5.1	5.2	-31.9	2.6	12.2	10.2	1.0	7.56	-8.17	7.54	1.10	16.37	1.40	-31.90	2.60	2008.7090-2011.5274	2.8184	1014
BYSP	18.408	293.839	86.6	14.7	0.8	2.7	3.0	8.3	0.8	4.3	2.9	-3.0	2.0	8.6	9.1	1.0	7.76	-8.17	6.94	0.80	16.47	0.80	-3.00	2.00	2008.3484-2011.6123	3.2640	1176
CRO1	17.757	295.416	-31.8	13.6	0.4	2.4	6.5	10.8	0.5	4.6	8.2	-1.7	0.9	9.8	18.4	1.0	8.28	-7.90	5.32	0.40	18.70	0.50	-1.70	0.90	1996.0178-2011.6123	15.5946	5245
CUPR	18.307	294.717	-34.6	15.1	1.0	2.4	3.0	9.2	1.1	3.7	3.4	-5.0	2.3	7.9	8.6	1.0	8.05	-8.10	7.05	1.00	17.30	1.10	-5.00	2.30	2008.8320-2011.6123	2.7804	949
MAYZ	18.218	292.841	1.0	13.7	2.1	3.0	4.2	6.1	1.5	4.3	2.6	-6.7	3.0	9.5	5.9	1.0	7.43	-8.15	6.27	2.10	14.25	1.50	-6.70	3.00	2010.1000-2011.6123	1.5123	549
MIPR	17.886	293.473	7.8	14.4	0.8	2.0	2.6	9.5	0.9	3.5	3.1	-0.8	1.9	7.4	7.9	1.0	7.64	-8.02	6.76	0.80	17.52	0.90	-0.80	1.90	2008.3566-2011.4534	3.0969	1126
P780	18.075	293.421	154.1	14.1	0.9	2.8	3.1	8.4	0.9	4.0	3.5	0.6	2.5	9.0	11.0	1.0	7.62	-8.08	6.48	0.90	16.48	0.90	0.60	2.50	2008.4030-2011.6123	3.2093	1172
MOPR	18.077	292.069	-38.3	12.3	0.8	2.6	2.2	8.7	1.0	3.8	3.2	-0.9	2.3	7.8	8.9	1.0	7.17	-8.14	5.13	0.80	16.84	1.00	-0.90	2.30	2008.8210-2011.6123	2.7913	1017
STVI	18.340	295.026	-21.6	14.6	1.0	3.5	3.1	10.1	1.1	4.1	3.5	-1.2	2.8	9.5	10.8	1.0	8.15	-8.09	6.45	1.00	18.19	1.10	-1.20	2.80	2008.8210-2011.6123	2.7913	1011
GEOL	18.211	292.860	-9.9	12.6	0.4	3.9	6.6	8.6	0.6	8.9	10.4	-0.1	0.8	13.7	16.6	1.0	7.43	-8.15	5.17	0.40	16.75	0.60	-0.10	0.80	1996.7090-2011.3932	14.6841	3709
ADJN	18.175	293.202	519.3	14.1	1.3	2.5	6.8	8.1	1.9	7.3	9.7	3.8	3.5	17.6	15.4	1.0	7.55	-8.12	6.55	1.30	16.22	1.90	3.80	3.50	2000.4221-2007.7630	7.3409	13
ANEG	18.730	295.668	321.9	15.3	1.4	7.0	6.8	9.8	2.0	9.5	9.7	5.8	2.8	10.0	15.4	1.0	8.36	-8.18	6.94	1.40	17.98	2.00	5.80	2.80	2000.3757-2007.7603	7.3846	16
ARC1	18.346	293.246	323.6	12.4	1.1	5.7	6.8	8.9	1.6	8.7	9.7	7.3	2.8	19.2	15.4	1.0	7.56	-8.17	4.84	1.10	17.07	1.60	7.30	2.80	2002.3466-2011.4151	9.0685	17
ARC2	18.345	293.249	-36.9	12.0	0.9	5.6	6.8	9.6	2.2	27.1	9.7	-0.2	2.6	27.8	15.4	1.0	7.56	-8.17	4.44	0.90	17.77	2.20	-0.20	2.60	2000.2500-2007.7274	7.4774	19
CAYE	18.119	293.838	370.6	14.3	1.8	8.1	6.8	7.0	3.7	21.6	9.7	-3.2	3.2	10.5	15.4	1.0	7.76	-8.08	6.54	1.80	15.08	3.70	-3.20	3.20	2004.6462-2011.4370	6.7908	11
CCM5	18.079	293.421	161.1	14.3	0.7	6.1	6.8	8.7	1.1	14.6	9.7	0.8	1.8	23.1	15.4	1.0	7.62	-8.08	6.68	0.70	16.78	1.10	0.80	1.80	2000.1352-2011.4233	11.2880	20
CIDE	18.211	292.863	1.3	13.1	0.7	4.1	6.8	7.6	0.9	9.4	9.7	0.6	1.4	14.6	15.4	1.0	7.43	-8.15	5.67	0.70	15.75	0.90	0.60	1.40	1999.2342-2011.4041	12.1699	93
DSCH	18.384	292.521	151.6	12.4	1.2	3.9	6.8	7.9	1.8	8.0	9.7	-1.5	3.8	27.5	15.4	1.0	7.32	-8.21	5.08	1.20	16.11	1.80	-1.50	3.80	2000.3238-2007.7384	7.4146	20
ISAB	18.468	292.954	82.90	13.4	1.3	5.9	6.8	6.8	2.5	21.7	9.7	-0.5	3.1	20.0	15.4	1.0	7.46	-8.22	5.94	1.30	15.02	2.50	-0.50	3.10	1996.6708-2001.8890	5.2183	18
LAJ1	18.083	292.948	28.70	16.3	0.9	9.2	6.8	8.6	1.2	11.8	9.7	-1.5	1.8	16.9	15.4	1.0	7.46	-8.10	8.84	0.90	16.70	1.20	-1.50	1.80	2000.1626-2011.4041	11.2415	31
LAJ2	18.035	292.932	-3.40	14.2	1.0	10.2	6.8	7.6	1.3	12.8	9.7	2.5	1.9	16.9	15.4	1.0	7.46	-8.09	6.74	1.00	15.69	1.30	2.50	1.90	2000.1626-2011.4041	11.2415	23
LAJ3	17.992	292.893	179.4	11.2	1.3	6.9	6.8	11.8	2.0	12.9	9.7	1.5	3.0	17.9	15.4	1.0	7.44	-8.08	3.76	1.30	19.88	2.00	1.50	3.00	2000.1653-2007.7192	7.5539	19
MAZC	18.255	292.850	-34.70	12.9	0.9	4.9	6.8	7.4	1.7	18.1	9.7	-2.5	1.9	12.4	15.4	1.0	7.43	-8.16	5.47	0.90	15.56	1.70	-2.50	1.90	2000.2500-2011.4041	11.1541	12
MONA	18.110	292.092	41.5	11.5	1.2	3.1	6.8	9.0	2.3	14.3	9.7	1.6	3.0	15.0	15.4	1.0	7.18	-8.15	4.32	1.20	17.15	2.30	1.60	3.00	2000.3238-2007.7411	7.4173	18
PARG	17.969	292.956	-8.10	15.5	0.7	7.6	6.8	9.8	1.0	11.4	9.7	-0.6	1.5	20.8	15.4	1.0	7.47	-8.07	8.03	0.70	17.87	1.00	-0.60	1.50	2000.0861-2011.4233	11.3372	34
SALN	18.029	293.766	128.40	13.4	1.2	4.4	6.8	7.4	1.8	7.2	9.7	0.9	2.9	14.3	15.4	1.0	7.74	-8.05	5.66	1.20	15.45	1.80	0.90	2.90	2000.2582-2007.7164	7.4582	19
VEGB	18.446	293.609	-30.80	10.6	3.0	5.2	6.8	7.3	3.4	1.7	9.7	-3.6	6.7	11.7	15.4	1.0	7.68	-8.19	2.92	3.00	15.49	3.40	-3.60	6.70	2007.7411-2011.4425	3.7014	7
VIEN	18.121	294.560	-5.8	14.2	3.7	8.5	6.8	8.1	4.8	10.0	9.7	3.5	7.5	15.8	15.4	1.0	8.00	-8.05	6.20	3.70	16.15	4.80	3.50	7.50	2004.2445-2007.7055	3.4609	9
VIEQ	18.131	294.488	-38.80	16.4	2.3	4.4	6.8	4.7	3.8	11.2	9.7	-3.3	6.2	18.5	15.4	1.0	7.97	-8.05	8.43	2.30	12.75	3.80	-3.30	6.20	2000.3948-2004.2555	3.8607	16
ZSUA	18.430	294.006	-34.1	13.4	1.3	5.6	6.8	8.3	2.9	20.2	9.7	2.0	4.0	27.2	15.4	1.0	7.82	-8.17	5.58	1.30	16.47	2.90	2.00	4.00	2000.2199-2011.4397	11.2198	14
ZSUB	18.431	294.008	-42.7	19.6	1.3	11.8	6.8	7.2	1.9	18.3	9.7	3.6	3.0	28.3	15.4	1.0	7.82	-8.17	11.78	1.30	15.37	1.90	3.60	3.00	2000.2199-2007.7082	7.4883	16

Note: The table above is with respect to STABLE NORTH AMERICAN PLATE (NAM). The white and the flicker noise values reflect the uncertainties on the derived velocities (Mao et al., 1999). IGS05 means International GPS Service-Reference Frame 2005. ABVI velocity components were not included in the kinematic analysis because of the short time frame and big the large errors.

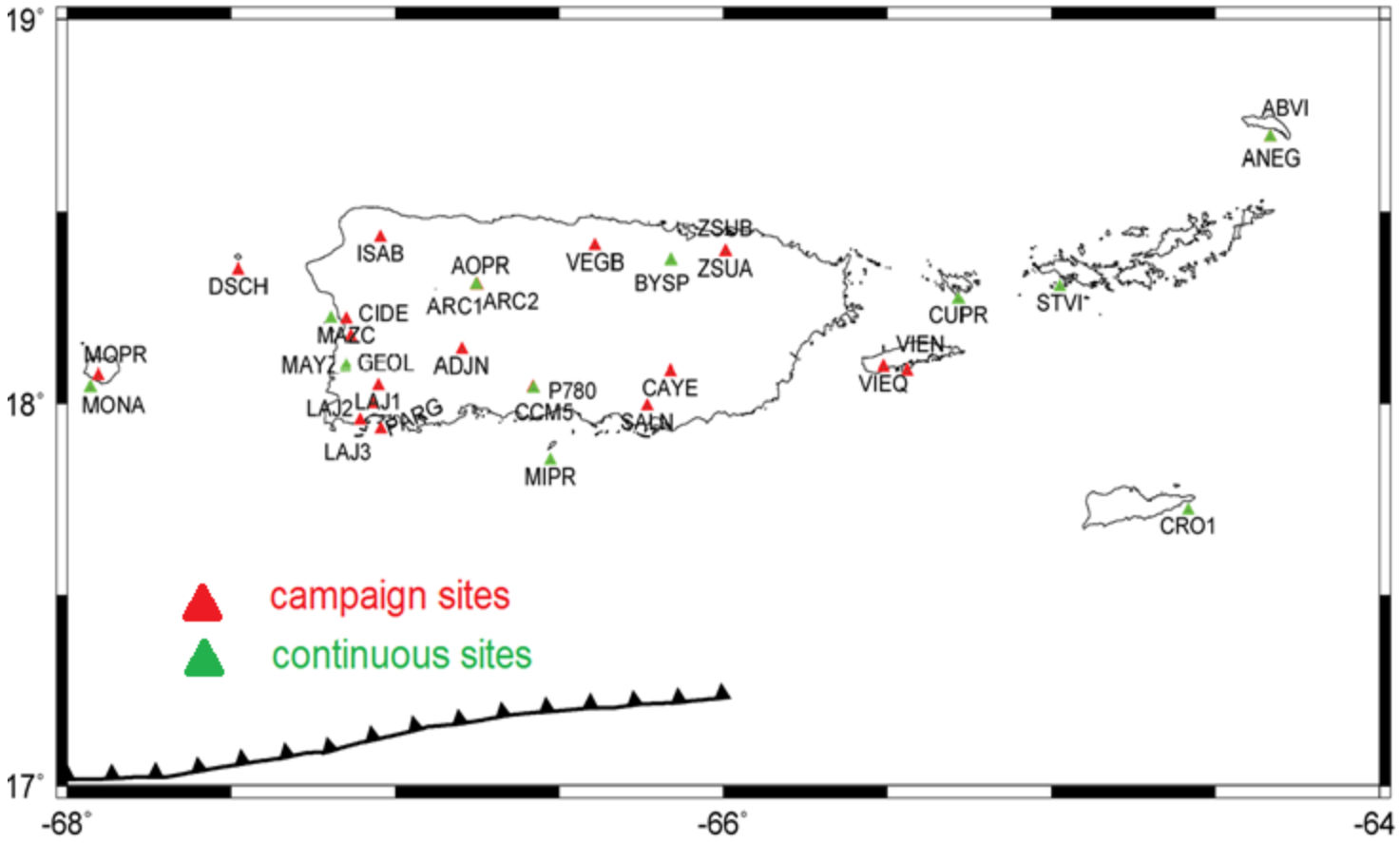

Figure 3.33 Map of Puerto Rico-Virgin Islands GPS continuous and campaign sites.

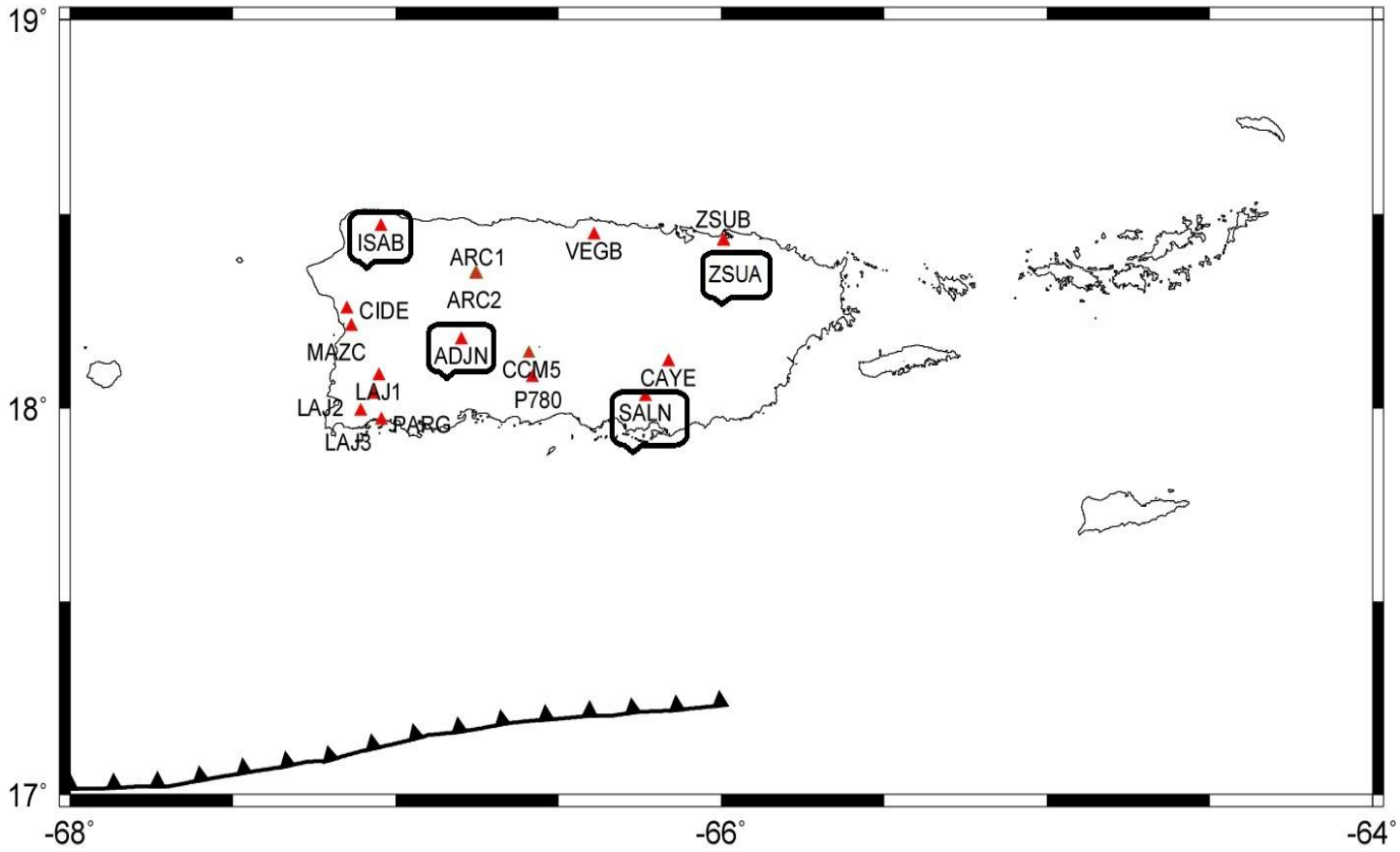

Figure 3.34 Map showing Location of May/June 2011 GPS campaign sites.

Note: The site at ISAB was destroyed and could not be reoccupied, permission was not granted by the authorities in ZSUA and SALN so we could not reoccupy, while the site at ADJN was reoccupied but the time series was too short to be included in this analysis. LAJ3 site-entry was not permitted by the government because of a landslide. All the remaining sites were observed and reoccupied for a minimum of 48 hours.

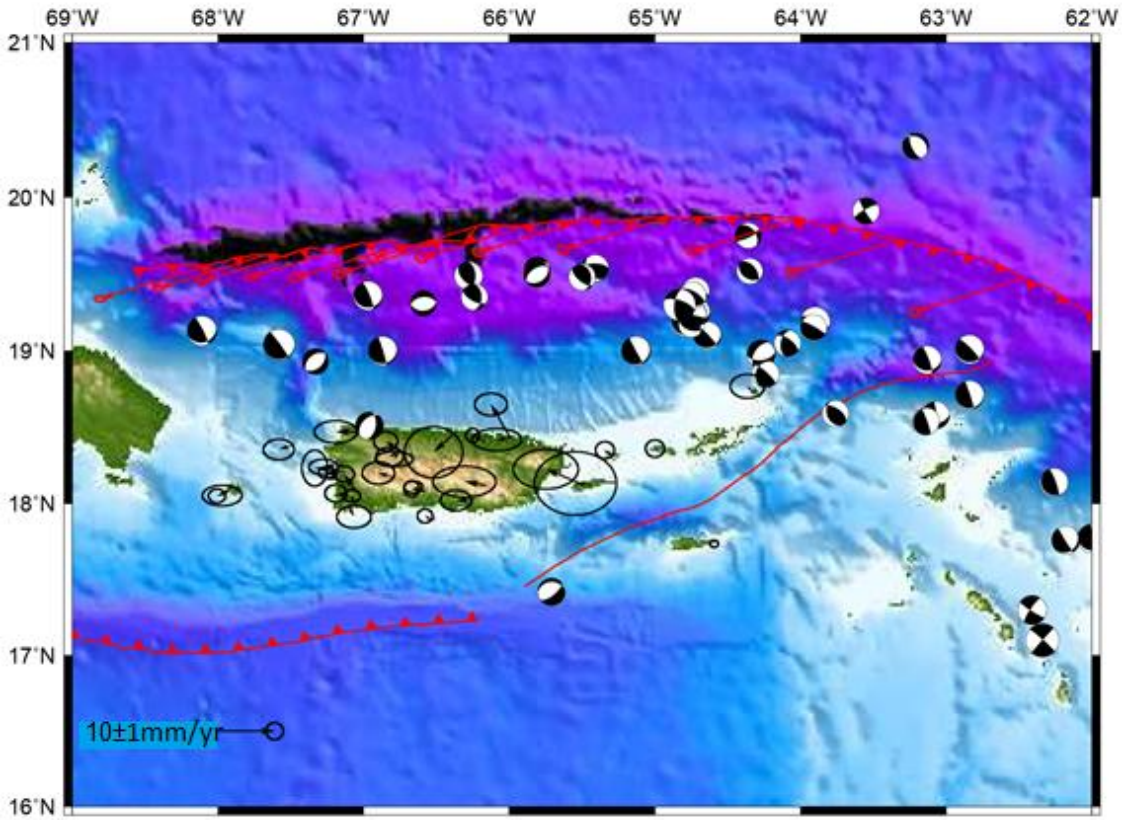

Figure 3.35 Velocity Map of Puerto Rico-Virgin Islands with respect to stable Caribbean Plate

Note: The map also shows the regional faults and focal mechanisms from historic earthquakes for the entire region. Error ellipses for the site positions are scaled to σ/2 error.

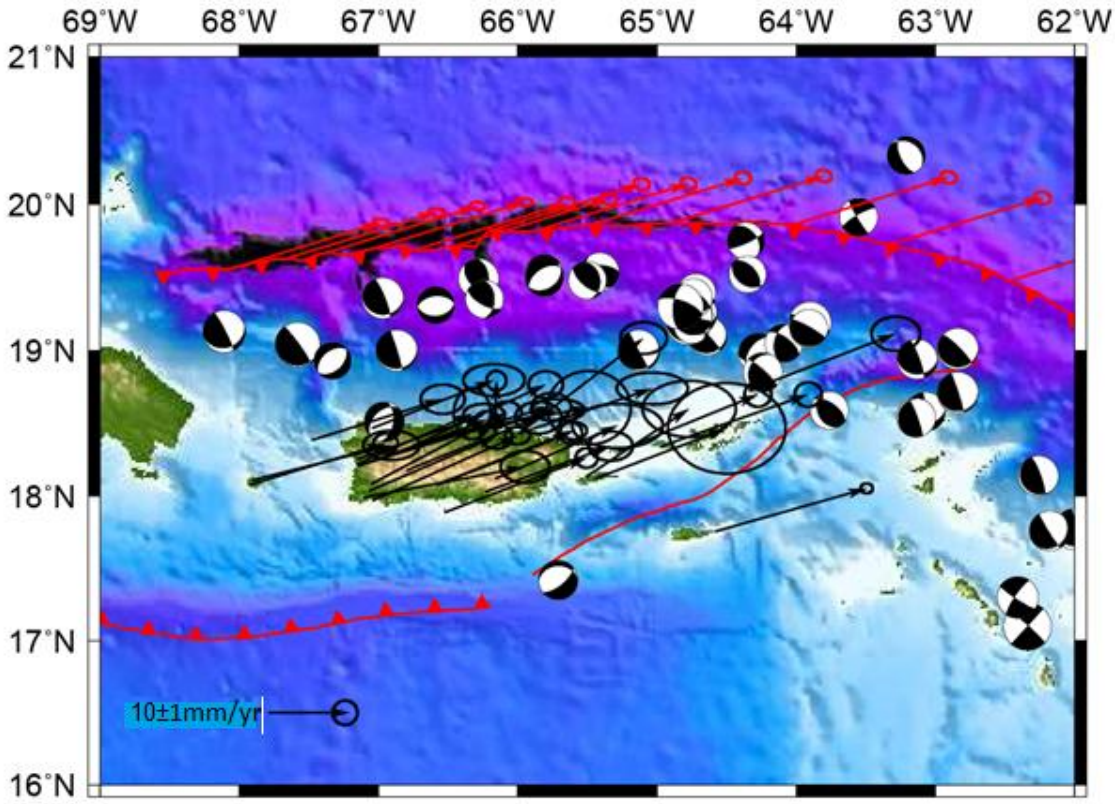

Figure 3.36 Velocity Map of Puerto-Rico Virgin Islands with respect to stable North American Plate

Note: The map also shows the regional faulting activities and focal mechanisms from historic earthquakes for the entire region. Error ellipses for site positions are scaled to σ/2 error.

CHAPTER 4

DISCUSSION OF RESULTS

4.1 GPS-derived velocity for PRVI

The velocity tables, Table 3.5 and Table 3.6 (Chapter 3), which include the site component velocities with respect to ITRF05/IGS05 and the fixed CA and NAM plates can be used to determine: (1) the internal deformation within the PRVI microplate; and (2) the components of motion of the PRVI microplate with respect to the lager CA and NAM plates. First, the determination of internal deformation, or rigidity, will involve sites located proximal to a zone of elastic strain accumulation. Using the method described by Ward (1990), the horizontal velocities of some chosen sites around the zone of active deformation can be inverted and the weighted least squares best fit angular velocity for the chosen sites determined. Average rate misfit for the horizontal velocity components is also calculated. The data and their estimated uncertainties provide an estimation of internal deformation. Second, the GPS site velocities from the PRVI microplate can be used to constrain the components of angular velocity that predicts the rate and direction of rigid body motion in both the western and eastern part of the microplate.

While velocity uncertainties increase from west to east on average, the velocity data presented here not only constrains the motion of western Puerto Rico, but also the eastern part of the PRVI block, where the available data and sites are much younger with the exception of CUPR, STVI, and CRO1. Thus, this thesis provides constraints on the motion of western and eastern Puerto Rico; however, the main focus is to update the PRVI velocity with respect to IGS05 and to produce velocity maps, with respect to CAR-plate and the NAM-plate, which will be compared to confirm the fact that PRVI is indeed its own microplate, whose movement is slow and closely related to the Caribbean, but statistically different from both the larger North-American and Caribbean plates.

4.2 Relative Motion between the Caribbean and the North American Plate

The Northwestern University Velocity Model 1A (NUVEL-1A) (DeMets et al., 1990) predicted relative motion of the Caribbean plate with respect to North America as 11±3 mm/yr to the east (near Puerto Rico) as compared to 37±5 mm/yr to the northeast (near Puerto-Rico) derived from earthquake slip vectors (Sykes et al., 1982; Deng and Sykes, 1995). CANAPE (Caribbean North American Plate Experiment) constrained motion of the Caribbean plate with respect to North America at Cabo Rojo (southern Dominica Republic) and predicted the value as 20.6±1.2 mm/yr towards N89°E±3° (Dixon et al., 1998). This CANAPE prediction was re-examined and additional data was added by Jansma et al., 2000, and the predicted value was modified to 19.4±1.2 mm/yr with a revised azimuth toward N79°E±3°. Another prediction was later made by (DeMets et al., 2000), defining the motion of the Caribbean plate relative to North American and estimating it as 19.2±1.3 mm/yr toward N69E±3. In summary, the relative motion of the Caribbean with respect to North America has been very poorly defined and is in a continuous state of revision due to lack of enough geodetic and other geophysical constraints (e.g. magnetic anomalies and earthquake slip vectors).

4.3 Kinematic Analysis

4.3.1 Velocities Relative to North American Plate

The velocities of sites in PRVI relative to the North American plate are shown in Table 3.6 (Chapter 3) and Figure 4.1 – 4.2. To describe the velocities of GPS sites in PRVI relative to the North American plate, the angular velocity that describes the motion of the North American plate with respect to IGS05 (DeMets pers.comm to G. Mattioli) was used to predict the North American IGS05 velocity at each of the GPS sites; the predicted plate velocity value in IGS05 at each site was subtracted from the site velocity (IGS05) and the covariance that describes the uncertainties in both was summed, giving the NAM fixed velocities (mm/yr) and their respective errors at each site in terms of the horizontal velocities (north and east), which were used to construct the velocity maps in Figure 4.1 and Figure 4.2.

GPS-derived velocities with respect to NAM are similar for all sites in Puerto Rico and the northern Virgin Islands at the 95% confidence level with the error increasing from west to east and decreasing at the eastern edge of the Virgin Islands (probably because sites around the eastern Virgin Islands are older sites). Individual site velocities range from 2.92 (VEGB) to 11.8 mm/yr (ZSUB) for the north component, while the east value ranges from 12.75 (VIEQ) to 19.88 mm/yr (LAJ3). This thesis predicts the velocity for motion of PRVI (IGS05) relative to North America as 17.63 ± 2.17mm/yr toward N69°E±3°. This velocity can be used to describe the motion of PRVI relative to North America. If we compare the velocity of PRVI obtained in this thesis to the predicted value of motion of Caribbean plate relative to North America plate being 19.2 ± 1.3 mm/yr toward N69E±3 (DeMets et al., 2000), the velocities with respect to North America are 1.57 mm/yr slower than that of the Caribbean plate. The velocity obtained in this thesis relative to NAM can also be compared to that of (Jansma and Mattioli, 2005), which predicts the motion of PRVI relative to North America as 16.9 ±1.1 mm/yr toward N68°E±3.

Motion of PRVI relative to North America is slower compared to that between the rigid Caribbean and North American plate. Errors for site positions in Figure 4.1 are scaled to $\sigma/2$ error. Considering the general velocity trend from the (NAM) data, comparison of the GPS velocity for PRVI obtained in this thesis with respect to North America with the total North America-Caribbean relative motion is consistent with the suggestion that up to 85% of North America-Caribbean plate motion is accommodated by the Puerto Rico trench and the offshore faults north of Puerto Rico.

At the 95% confidence level, GPS site velocities in Puerto Rico relative to NAM are similar, with the exception of LAJ3. If NAM plate is fixed, all the 32 available sites move towards the NAM plate in the NE direction except for LAJ3 which deviates slightly south. If we are to ignore the LAJ3 velocity because of the likely active on-going deformation around this area, my results are consistent with Jansma and Mattioli (2005), which predicts northeastward translation

of the PRVI block relative to North America and left lateral transpression across the Puerto Rico trench (North).

4.3.2 Velocities Relative to Caribbean Plate

The velocities of sites in PRVI relative to the Caribbean plate are shown in Figures 4.3 and 4.4 and Table 3.5 (Chapter 3). To describe the velocities of GPS sites in PRVI relative to the Caribbean plate, the angular velocity that describes motion of the Caribbean plate with respect to IGS05 was used to predict the Caribbean IGS05 velocity at each of the GPS sites; the predicted plate velocity value in IGS05 at each site was subtracted from the site velocity (IGS05) and the covariance that describes the uncertainties in both was summed. The methodology for generating the velocity relative to the Caribbean plate is similar to that described above for the velocity relative to the North American plate.

Individual site velocities range from -2.95 (VEGB) to 5.91 mm/yr (ZSUB) for the north components, while the east value ranges from -6.10 (VIEQ) to 1.06 mm/yr (LAJ3). The velocity for motion of PRVI relative to Caribbean obtained in this thesis is 2.42 ± 2.1 mm/yr toward S81°W±35°. This velocity describes the motion of PRVI relative to the Caribbean, and can be compared to that of Jansma and Mattioli, (2005) which predicts the motion of PRVI relative to Caribbean as 2.4 ±1.4 mm/yr toward S79°W±26°.

From velocity Table 3.5 (Chapter 3) and Figures 4.3 and 4.4, the motion of PRVI is indeed slow relative to the Caribbean. Error ellipses for the site positions in Figure 4.4 are scaled to σ/2 error. Generally, the GPS velocity uncertainties obtained here are in many cases as large as the velocities of each site itself (Figure 4.4), If we assume the present estimates of Caribbean plate and PRVI block motion are correct, then the velocity data obtained in this thesis with respect to the Caribbean plate is consistent with 2-3 mm/yr of PRVI block motion relative to the Caribbean.

From the velocity maps in Figure 4.4 (CAR-plate fixed), the motion of the 32 sites from this thesis can be categorized into the following 4 groups with respect to the Caribbean:

(a) the sites that are moving directly or closely WEST: ISAB, SALN, ZSUA, MAYZ, CAYE, VIEN, CIDE, MAZC, LAJ2, CCM5, P780, and ADJN (12)
(b) the sites that are moving SOUTH-WEST: MONA, MOPR, DSCH, ARC1, ARC2, GEOL, and VEGB (7)
(c) the sites that are moving SOUTH: *CRO1* (oldest and probably the most accurate), LAJ3, and ABVI? (3)
(d) the sites that are moving NORTH-WEST: ANEG, STVI, CUPR, ZSUB, VIEQ, BYSP, AOPR, MIPR, AOPR, and LAJ1 (10)

Considering that the available data in this thesis can be *comfortably* categorized into 4 different groups as shown above, these data do not support the theory of Jansma and Mattioli (2005), which predicts shortening across the Puerto Rico trench and left lateral transpression across the Puerto Rico trench (North) and the Muertos trough (South) of Puerto Rico. Instead, it will support the theory of counter-clockwise rotation of a rigid Puerto Rico-Virgin Islands block about a vertical axis located in the southeast of the island of Puerto Rico, which will give rise to extension across the western Puerto Rico trench, and shortening and compression across the Muertos trough south of western Puerto Rico.

To assess whether the present GPS velocities from sites in Puerto Rico are consistent with significant motion of PRVI relative to the Caribbean plate, it is advisable we test for the existence of a separate microplate using the F-ratio test as applied by Stein and Gordon (1984). This method is not sensitive to overestimates or underestimates of velocity uncertainties. The method simply compares the least squares fits of models that use two angular velocities and one angular velocity, respectively, to fit a set of kinematic observations.

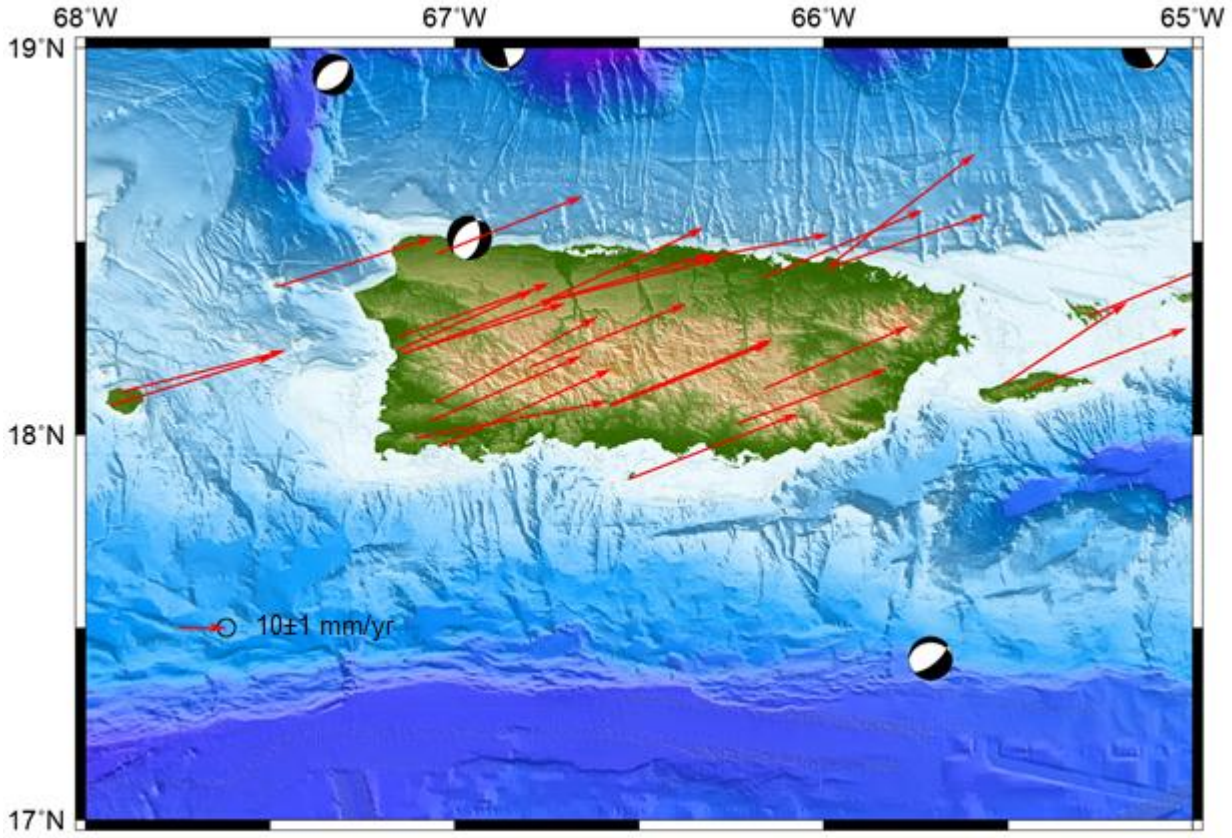

Figure 4.1 High resolution velocity maps of Puerto Rico-Virgin Islands with respect to stable North American Plate.

Note: The high resolution map (bathymetry/topographic data) is without error ellipses, and thus only includes the site velocity vectors.

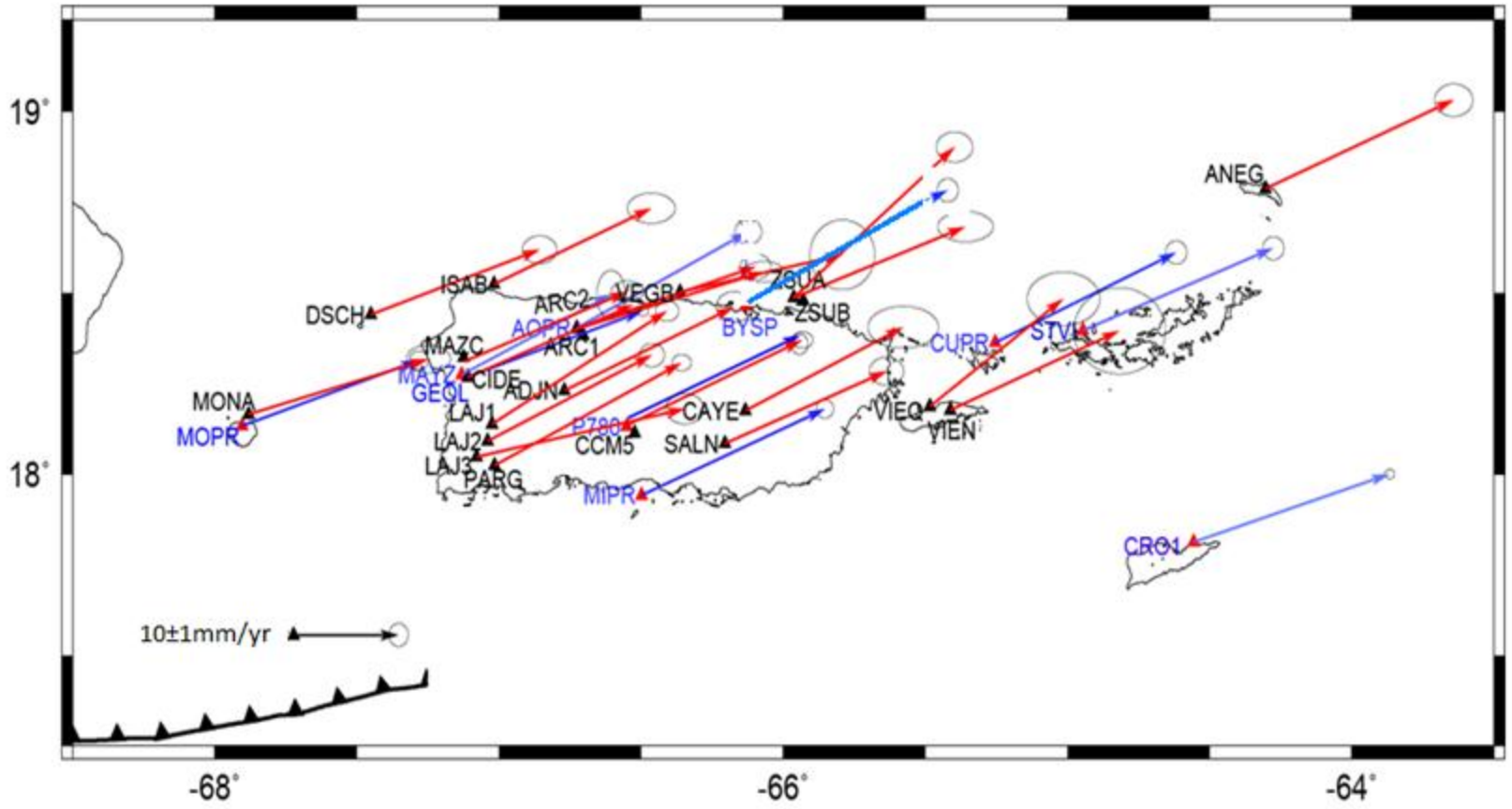

Figure 4.2 Velocities of Puerto Rico-Virgin Islands with respect to stable North American Plate.

Note: This PRVI map shows the velocity directions for each site and its error. Continuous sites are shown as blue arrows and red triangles, while campaign sites are shown as red arrows and black triangles. Error ellipses for site positions are scaled to σ/2 errors.

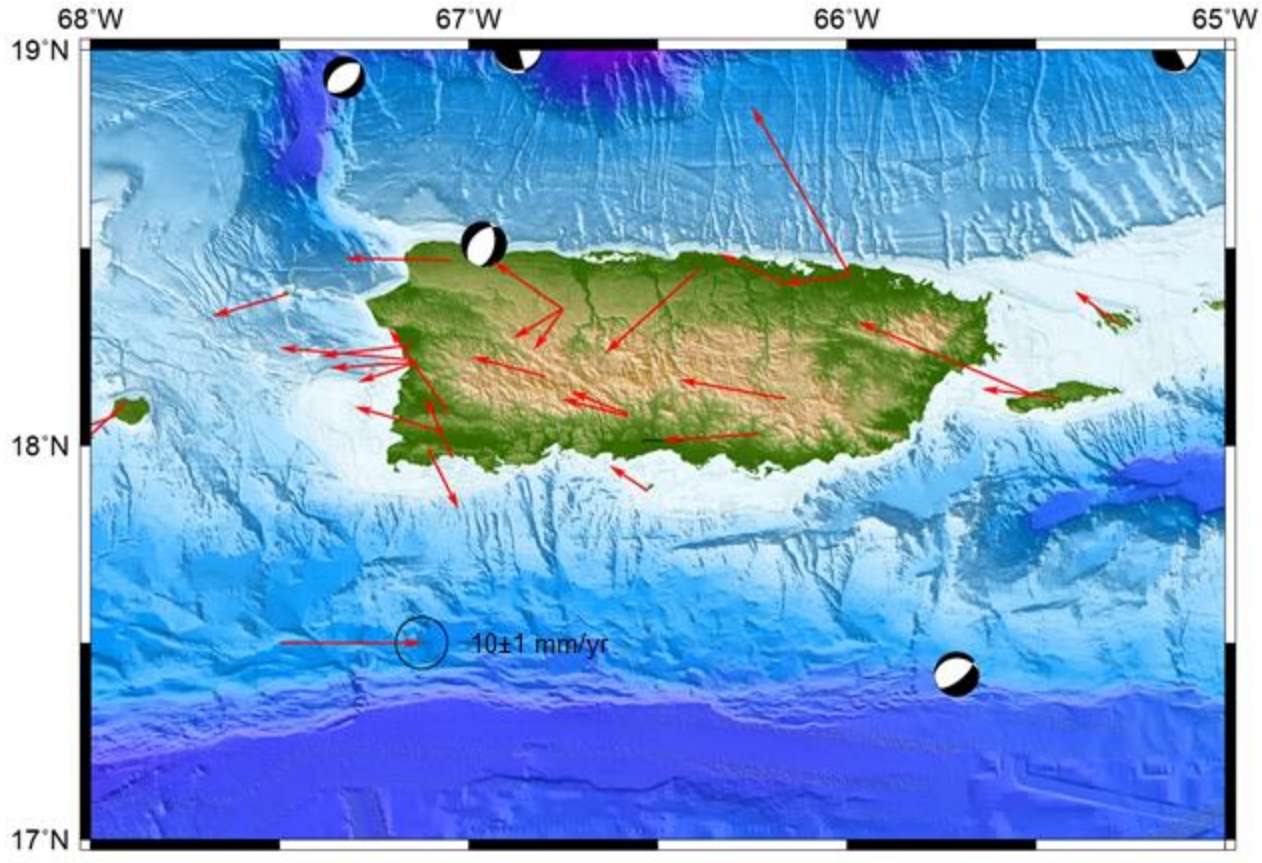

Figure 4.3 High resolution velocity maps of Puerto Rico-Virgin Islands with respect to stable Caribbean Plate.

Note: The high resolution map (bathymetry/topographic data) is without error ellipses, and thus only includes the site velocity vectors.

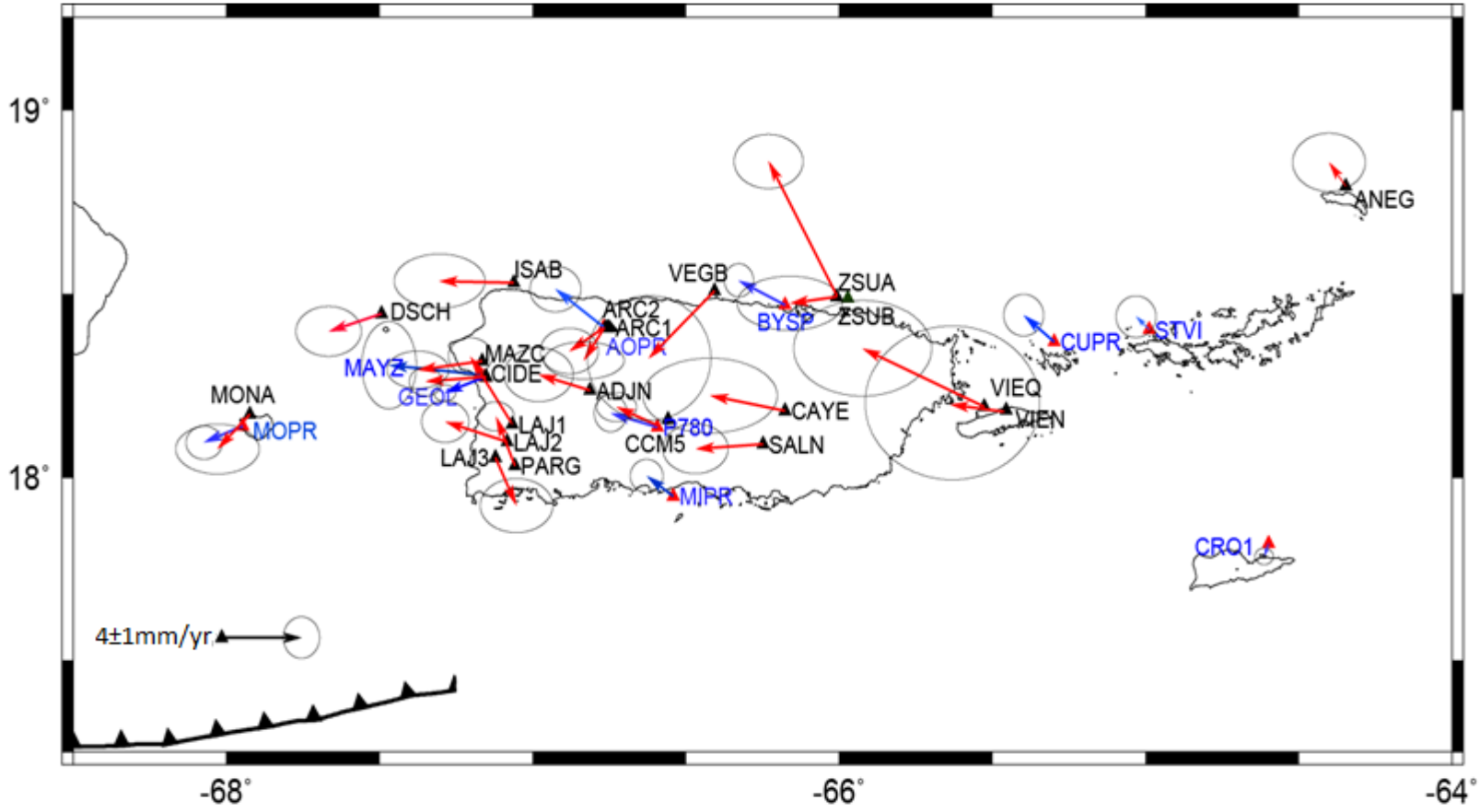

Figure 4.4 Velocities of Puerto Rico-Virgin Islands with respect to stable Caribbean Plate.

Note: This PRVI map shows the velocity directions for each site and its error. Continuous sites are shown as blue arrows and red triangles, while campaign sites are shown as red arrows and black triangles. Error ellipses for the site positions are scaled to σ/2 error.

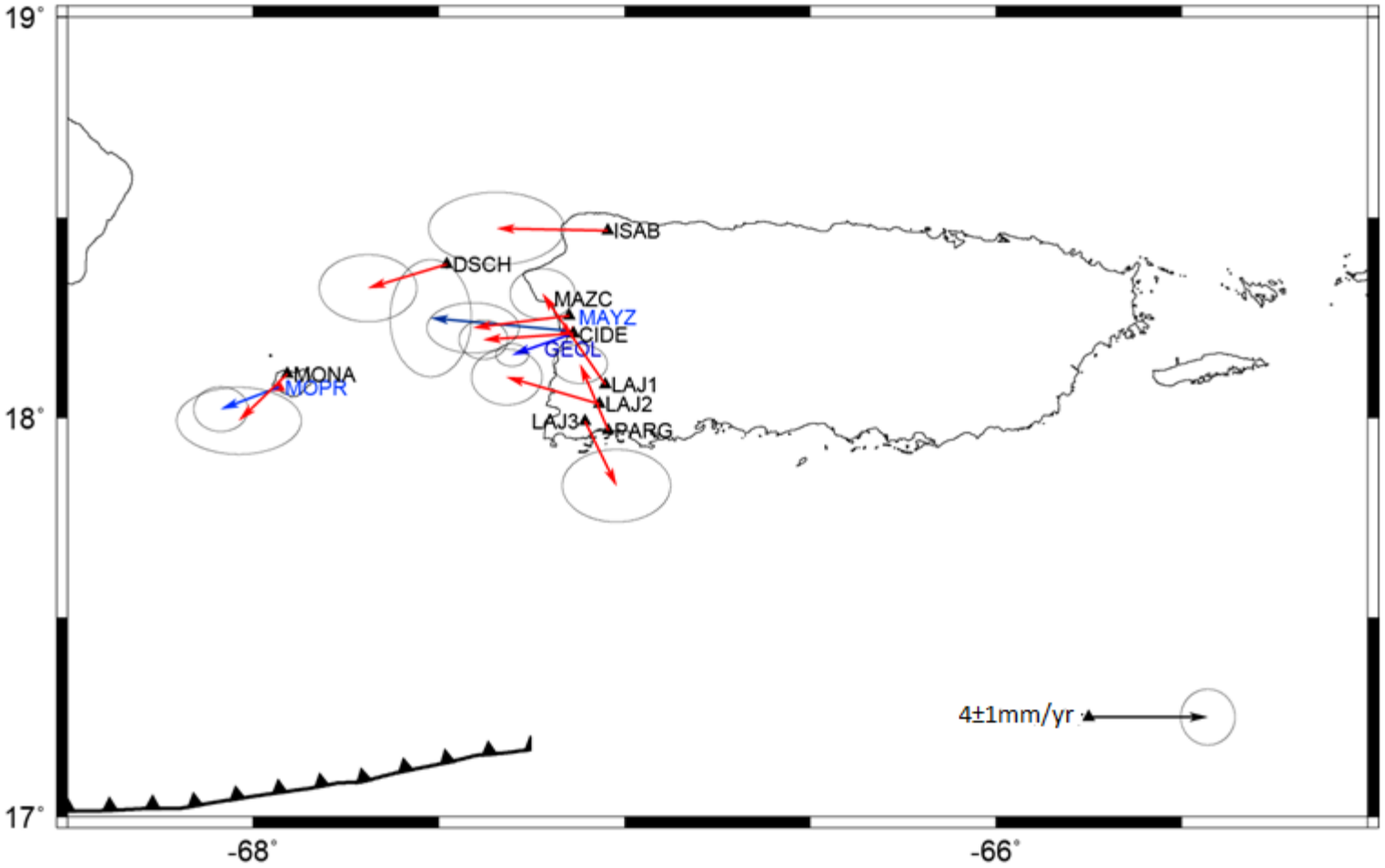

Figure 4.5 Velocities of Western Puerto Rico-Virgin Islands block with respect to stable Caribbean plate.

Note: red color indicates a continuous site, blue color indicates a campaign site.

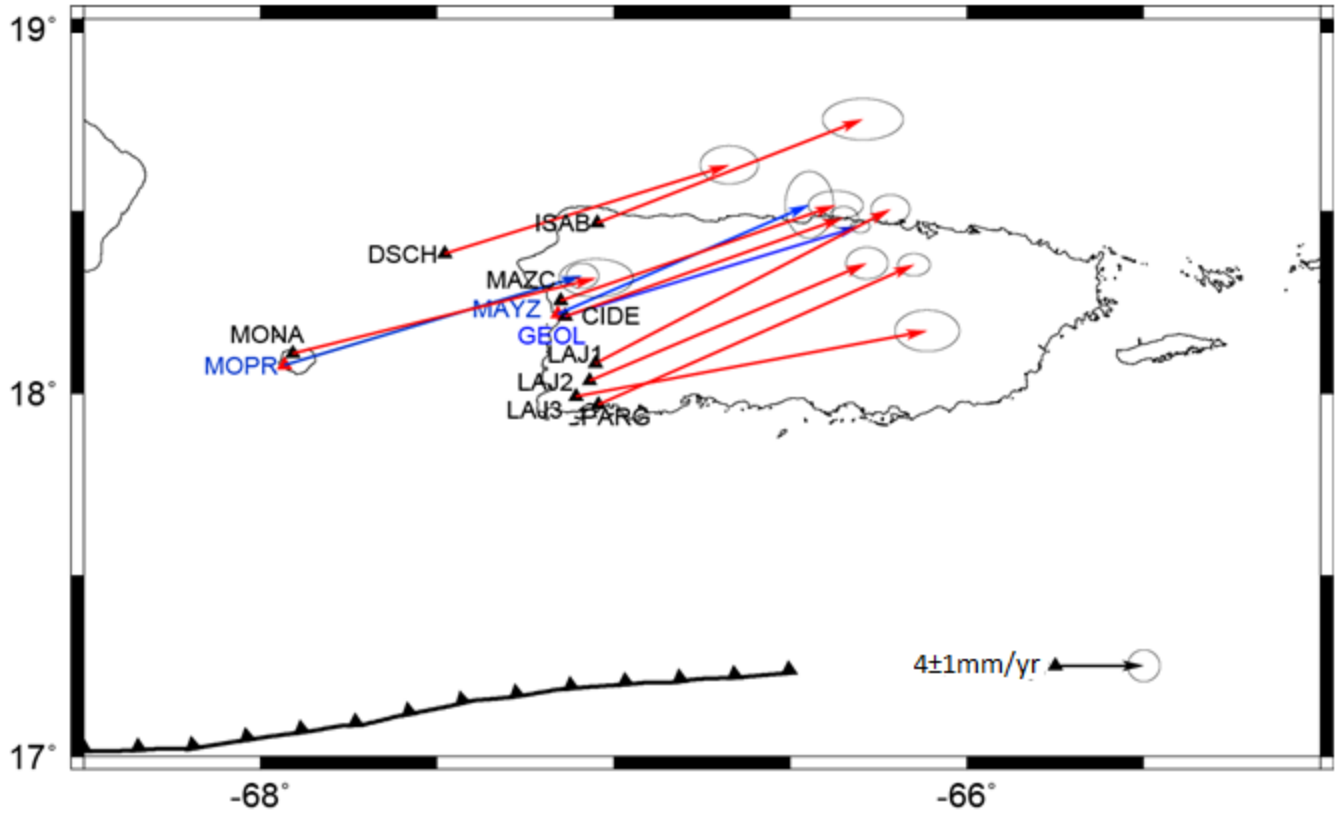

Figure 4.6 Velocities of Western Puerto Rico-Virgin Islands block with respect to stable North American plate.

Note: red color indicates a continuous site, blue color indicates a campaign site.

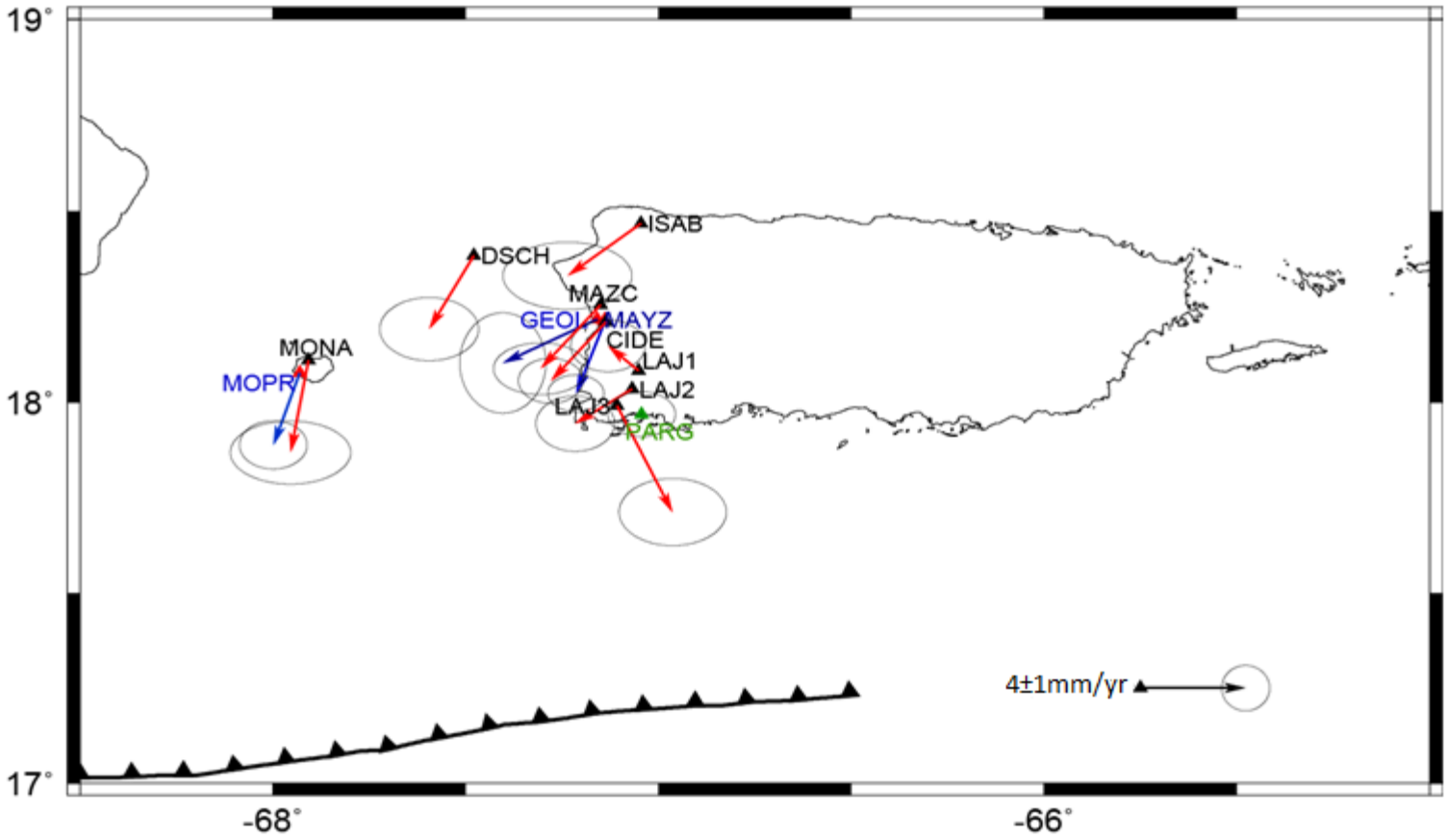

Figure 4.7 Velocities of Western Puerto Rico-Virgin Islands block with respect to stable Pargeura Site (PARG)

Note: red color indicates a continuous site, blue color indicates a campaign site, and green indicates the fixed PARG site.

4.3.3 Plate Inversion output Results

According to the analysis made by (written comm. G. Mattioli) *to prove whether PRVI is an independent plate the following results were obtained:*

F (3 plate) = 9.168

F (99.9%) = 5.78 for (v1=3; v2=122)

F (3 plate) >> F (0.999)

therefore hypothesis proved that PRVI is a separate plate from CA at the 99.9% confidence (4 sigma). The source of the data used to define PR-CA-ITRF05 is from (DeMets et al., 2007 and written comm. of C. DeMets to G. Mattioli) updated to August 2011, see Appendix B for data and details.

4.3.4 Velocities of Western Puerto Rico-Virgin Islands

In this section I attempt to better constrain the tectonic processes in southwestern Puerto Rico, in particular around the Lajas Valley, to understand the proposed deformation in western PRVI (Meltzer et al., 1995; Prentice et al., 2004). 12 sites: MAYZ, MOPR, GEOL, CIDE, DSCH, ISAB, LAJ1, LAJ2, LAJ3, MAZC, MONA, and PARG were used to analyze western and southwestern Puerto Rico. The analyses were done based on three reference frames: (a) with respect to a fixed Caribbean plate; (b) with respect to fixed North American Plate; and (c) with respect to a fixed a La Parguera site (PARG).

4.3.4.1 Western PRVI with Respect to Fixed Caribbean Plate

Table 4.1 was used to generate the velocity map of PRVI in Figure 4.5 above with respect to a fixed Caribbean. Error ellipses on this map are scaled to σ/2 error. Most of the velocities are moving west or slightly southwest with the exception of LAJ1 (moving NW), PARG (moving NW) and LAJ3 (moving southwest) in an opposite direction from LAJ1 and PARG. The average velocity for the 12 sites with respect to the CAR-plate is 2.33±1.8 mm/yr (similar to that of previous workers). Neglecting the Lajas Valley velocity and PARG, Figure 4.5 and Table 4.1

also show the slow and similar velocity between PRVI block and the Caribbean plate.

Table 4.1 Velocities of western PRVI with respect to fixed CAR-plate

Lon(E)	Lat (N)	Ve	Vn	Error East	Error North	SITE
292.841	18.218	-4.54	0.41	1.50	2.10	MAYZ
292.069	18.077	-1.95	-0.72	1.00	0.80	MOPR
292.860	18.211	-2.04	-0.70	0.60	0.40	GEOL
292.863	18.211	-3.04	-0.20	0.90	0.70	CIDE
292.521	18.384	-2.65	-0.78	1.80	1.20	DSCH
292.954	18.468	-3.74	0.07	2.50	1.30	ISAB
292.948	18.083	-2.11	2.97	1.20	0.90	LAJ1
292.932	18.035	-3.12	0.88	1.30	1.00	LAJ2
292.893	17.992	1.06	-2.11	2.00	1.30	LAJ3
292.850	18.255	-3.23	-0.39	1.70	0.90	MAZC
292.092	18.110	-1.63	-1.53	2.30	1.20	MONA
292.956	17.969	-0.95	2.17	1.00	0.70	PARG

4.3.4.2 Western PRVI with respect to fixed North American Plate

Table 4.2 below was used to generate the velocity map of PRVI in Figure 4.6 with respect to a fixed North America plate. Error ellipses on this map are scaled to σ/2. 11 of the 12 sites are moving NE with the exception of LAJ3, which is moving east-northeast. Neglecting the LAJ3 velocity, Figure 4.6 and Table 4.2 below also show that PRVI movement is statistically different from that of NAM. The average velocity for the 12 sites with respect to the NAM plate is 17.47±1.8 mm/yr toward N70°E±35°.

Table 4.2 Velocities of western PRVI with respect to Fixed NAM-plate

Lon(E)	Lat (N)	Ve	Vn	Error east	Error north	SITE
292.841	18.218	14.25	6.27	1.50	2.10	MAYZ
292.069	18.077	16.84	5.13	1.00	0.80	MOPR
292.860	18.211	16.75	5.17	0.60	0.40	GEOL
292.863	18.211	15.75	5.67	0.90	0.70	CIDE
292.521	18.384	16.11	5.08	1.80	1.20	DSCH
292.954	18.468	15.02	5.94	2.50	1.30	ISAB
292.948	18.083	16.70	8.84	1.20	0.90	LAJ1
292.932	18.035	15.69	6.74	1.30	1.00	LAJ2
292.893	17.992	19.88	3.76	2.00	1.30	LAJ3
292.850	18.255	15.56	5.47	1.70	0.90	MAZC
292.092	18.110	17.15	4.32	2.30	1.20	MONA
292.956	17.969	17.87	8.03	1.00	0.70	PARG

4.3.4.3 Western PRVI With Respect to Fixed Parguera Site

Table 4.3 below was used to generate the velocity map of PRVI in Figure 4.7, with respect to fixed Parguera site (PARG). Error ellipses for site positions on this map are scaled to σ/2. All the sites are moving southwest except for LAJ1 and LAJ3, which are moving in the opposite direction. The average velocity for the 12 sites with respect to fixed PARG is 2.55 ± 2.2 mm/yr toward N58°E±35°.

Table 4.3 Velocities of western PRVI with respect to fixed PARG-plate

Lon(E)	Lat (N)	Ve	Vn	Error east	Error north	SITE
292.841	18.218	-3.59	-1.76	1.80	2.21	MAYZ
292.069	18.077	-1.00	-2.89	1.41	1.06	MOPR
292.860	18.211	-1.09	-2.87	1.17	0.81	GEOL
292.863	18.211	-2.09	-2.37	1.35	0.99	CIDE
292.521	18.384	-1.70	-2.95	2.06	1.39	DSCH
292.954	18.468	-2.79	-2.10	2.69	1.48	ISAB
292.948	18.083	-1.16	1.00	1.56	1.14	LAJ1
292.932	18.035	-2.17	-1.39	1.64	1.22	LAJ2
292.893	17.992	2.11	-4.28	2.24	1.48	LAJ3
292.850	18.255	-2.28	-2.56	1.97	1.14	MAZC
292.092	18.110	-0.68	-3.70	2.51	1.39	MONA
292.956	17.969	0.00	0.00	1.41	0.99	PARG

Figures 4.5 and 4.6 depict LAJ1 and LAJ3 as moving in opposite directions. If the kinematics of this is modeled, it will closely resemble a displacement feature lying between LAJ1 and LAJ3. LAJ1 is moving toward the NW while LAJ3 is moving toward the SW. Assuming a simple 2D model, what is happening around this region can be illustrated in Figure 4.8 below. This model suggests that there is a localized structure in the Lajas Valley with possible extensional features and a left-lateral (strike-slip fault).

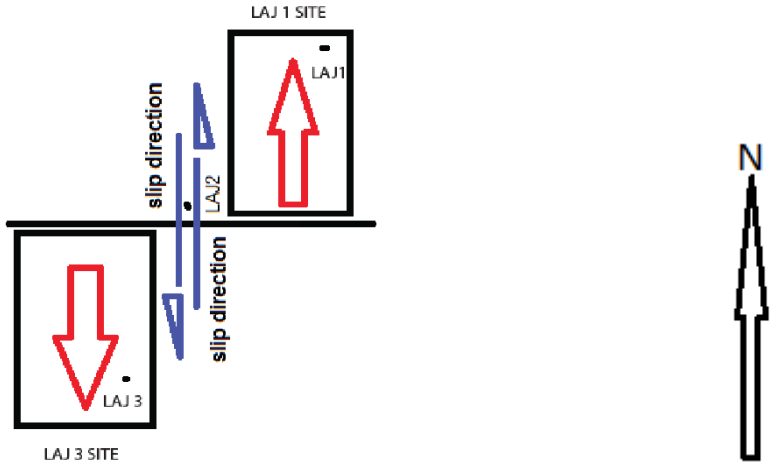

(a)

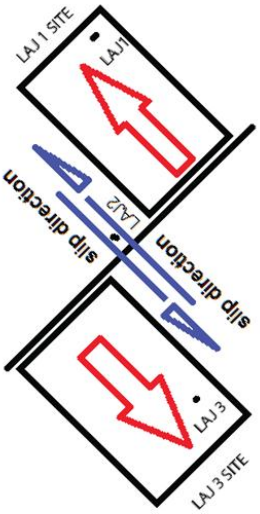

(b)

Figure 4.8 2D Schematic Model of the deformation in Lajas Valley (a) faulting and displacement within the Lajas Valley, (b) localized counterclockwise rotation of Lajas Valley

The 2D model above suggests a possible explanation of the past deformation in the Lajas Valley. LAJ1 was displaced and LAJ3 displaced, along opposites sides of a left- lateral strike slip fault. LAJ2 being at the center of the two sites, between LAJ1 and LAJ3, subsided during faulting and displacement, and occupies the lowest altitude, at the bottom of the valley. There is a high possibility that LAJ2 is within the zone that accommodates the slip between LAJ1 and LAJ3. If this is true, strain accumulation along the fault will influence the velocity and movement of LAJ2, however, the motion recorded by GPS predicts the possible on-going deformation and movements in the Lajas Valley.

After the displacement and faulting, the whole Lajas Valley was probably rotated counter clockwise as part of further deformation processes. This is only possible if the whole Lajas Valley is detached from PRVI. This could explain the opposite velocities between LAJ1 and LAJ3.

My result is in agreement with (Jansma and Mattioli 2005) on the following: that the Lajas Valley in the southwest is a zone where *microseismicity is greatest*, and is the locus of highest permissible on-land deformation. My results also support their prediction of left lateral motion along the southern boundaries of Puerto Rico-Virgin Islands (though this left-lateral motion seems localized to this region according to my data), but there is every possibility that this feature might extend off shore southwest of PRVI. If one considers east-west extension across the Island of Puerto Rico of 5±3mm/yr (Jansma and Mattioli, 2005), the structures in the Lajas Valley are likely oblique slip faults, where LAJ3 is on the higher side vertically, LAJ1 is on the lower side, and LAJ2 is at the center where there is dip-slip and strike-slip motion.

CHAPTER 5

CONCLUSION

Velocity data of 32 PRVI sites were updated with respect to IGS05 up to August 13th 2011. The data were used to produce velocity maps with respect to CAR-plate and the NAM-plate, which confirmed that PRVI is its own microplate, whose movement is slow and closely related to the Caribbean, but statistically different from both the North-American and Caribbean plates themselves. This is supported by plate inversion output results at 99% confidence level

The predicted velocity for motion of PRVI relative to North America is 17.63 ± 2.1 mm/yr toward N69°E±3°. This velocity can be used to describe the motion of PRVI relative to North America, and is very similar to Jansma and Mattioli (2005), which predicts the motion of PRVI relative to North America as 16.9 ±1.1 mm/yr toward N68°E±3. The predicted velocity for motion of PRVI relative to the Caribbean is 2.42 ± 2.1mm/yr toward S81ºW±35°. This velocity can also be used to describe the motion of PRVI relative to the Caribbean, and is similar to that of (Jansma and Mattioli, 2005) which predicts the motion of PRVI relative to Caribbean as 2.4 ±1.4 mm/yr toward S79°W±26°.

After displacement and faulting within the Lajas region, the whole Lajas Valley was possibly rotated counter clockwise as part of further deformation processes, implying that the whole Lajas Valley is somehow detached or is in the process of detaching from the Island of Puerto Rico.

The Lajas Valley in the southwest is a zone where microseismicity is greatest, and is possibly the locus of highest permissible on-land deformation. There is left lateral motion along the southern boundaries of PRVI (though it may be localized to the Lajas region), but there is every possibility that this feature might extend off shore southwest of PRVI.

The influence of extension on Lajas Valley, which is on the Island of Puerto Rico, will closely resemble a localized oblique slip fault, where LAJ3 is on the higher side vertically, LAJ1 is on the lower side and LAJ2 is at the center where there is dip-slip and strike-slip motion.

Data from this thesis does not support the model of tectonic escape (Jany et al, 1987), which suggests that the PRVI experiences tectonic escape to the east, squeezed like a pumpkin seed between converging Caribbean and North America plates, creating a velocity gradient that would change sign along a perpendicular traverse from the North America to Caribbean plate. Instead, the data from this thesis supports that PRVI may be attached to the Caribbean plate at the eastern edge and that motion of PRVI relative to North America is slower than that between the rigid Caribbean and North America plates, precluding eastward tectonic escape of the PRVI block.

While the details are somewhat different from that reported by Jansma and Mattioli (2005), the overall conclusion that PRVI is generally moving west relative to CA remains valid. The new data now show that counter clockwise rotation is beginning to be observed.

.

APPENDIX A

CAMPAIGN SITE DESCRIPTIONS FOR THE MAY/JUNE 2011 CAMPAIGN

ADJN-ADJUNTAS AGRICULTURAL STATION

This site is located in Adjuntas, in the central part of the island. The site is on the property of the Adjuntas Experimental Station, which is owned by UPRM. The pin is located on top of a small concrete building that is in front of the store house which houses two big gas tanks for the experimental station. The pin location makes the site secure, stable, and it also has a good sky view. AC power is available from the adjacent main building. To reach the site simply input the coordinate of this site (Latitude 18.175 and Longitude 293.202) in your car GPS and drive down to the location. Unfortunately the data collected at this site was too short to be included as part of the 2011 analysis. Photographs of the sites are given in Figure A1. Contact Mr. Essau Orengo 787-829-3614 for information and access.

ARC2-ARECIBO

This station is located within the facility of the National Astronomy and Ionosphere Center at the Arecibo Observatory. The pin is located at the helicopter pad and has a good sky view when not covered with tall grasses. A permit must be obtained before you can get access to this area. For information and access, call the observatory at 787-878-2612 or Mike Nolan at 787-878-2612. To drive down to the main gate simply input the coordinates of the sites (Latitude 18.346N and Longitude 293.246E) in your car GPS. Photographs of the site are given in Figure A2.

ARC1- ARECIBO

This station is also located within the facility of the National Astronomy and Ionosphere Center at the Arecibo Observatory. The pin is located in a fairly slippery and rough area. There may not be a good sky view because of the growing trees, which need to be cut down so it is advisable to bring a machete. A permit must be obtained before you can get access to this area. The location of ARC1 is quite close to the Observatory facility and AC power is also available here. For information and access call the observatory at 787-878-2612 or Mike Nolan at 787-878-

2612. To drive down to the main gate simply input the coordinates of the sites (Latitude 18.345N and Longitude 293.249E) on your car GPS. Photographs of the site are shown in Figure A3.

CAYEY- UPRC SCIENCES BUILDING

The site is located within the University of Puerto Rico – Cayey Sciences building. The pin is located on the roof of the Sciences building, and has an excellent sky view. AC power is available, and the location of the site makes it stable and very secure. Driving down to the place is quite easy because of the good road network; insert the coordinates of the site (Latitude 18.119N and Longitude 293.838E) on your car GPS and it will take you to the Sciences building. To get access to the place contact the Dean of Administration. The photographs of the sites are shown in Figure A4.

CCM5-CERRLLOS DAM

This is the Cerillos Control Mark 5 site at the Cerillos Dam in Ponce. CCM5 is on a concrete block 3m wide and 5m long on the western side of the reservoir north of the dam. The site is on a steel filled concrete cylinder 20cm in diameter and 1.16m tall; it has a mount into which one can insert 1'' diameter brass pin which was designed on a mounting screw of the antenna, usually used with a rotating optical plummet. This site has a nice sky view but there is no AC power available. To get to the place, input the coordinates of the site in your car GPS (Latitude 18.119N and Longitude 293.421E) and it will take you to the gate; however, it is necessary to get an appointment before going. Contact the administrative staff at 787- 841-3181. The photograph of the site is shown in Figure A5.

CIDE- CENTER FOR INDUSTRIAL RESEARCH

This site is located within the UPRM campus on top of the Center for Industrial Research and Economic Development building. It has a very nice sky view and the place is accessible. This site has AC power available and the location of the pin makes it secure and very reliable. To get

to the place use your car GPS with coordinates (Latitude 18.211 and Longitude 292.863), however, one will need to contact the CIDE office before you can get to the top of the building. The photographs of the site are shown in Figure A6.

LAJ1-LAJAS VALLEY

The site is part of the Lajas Valley transect and it is located on the campus of Interamerican University in San German, north of the Lajas valley. The pin is on top of the gymnasium building on the campus, opposite the central soccer and athletic field. AC power is available, although difficult to use without a 100' extension cord; the location is very secure with a good sky view; however, care must be taken while mounting the antenna because of the pin's location at the edge of the building. To get to the location use your car GPS (Latitude 18.083N and Longitude 292.948E), to gain access to the roof contact Mrs. Frances Alvarado at 787-892-2315, whose office is on the second floor of the building. The photographs of the site are shown in Figure A7.

LAJ2-SOUTH LAJAS VALLEY

This site is located in the Lajas Agricultural Experimental Station, UPRM. The pin is on top of an outcrop of hydrothermally altered sandstones. To get to the location use a car GPS with Latitude 18.035N and Longitude 292.932E. The terrain is very rugged; there is a cow farm adjacent the location and no AC power is available. Bring a machete and a shovel because grass and trees might need to be cut down. Permission must be granted at the Administrative building. Contact Hector Rodriguez at 787-899-1530. The photographs of the site are shown in Figure A8.

PARG-PARGUERA

This site is on the Parguera Island and one needs to take a ferry to get there. Necessary arrangements must be made with the secretary at the UPRM Geology department and the Marine Sciences department. The site is facing the ocean with a good sky view. A car GPS can only take

one down to the shore of the island, (Latitude 18.035N and Longitude 292.932E) where a ferry must be taken from that point. The pin is glued with epoxy to a hard exposed boulder rock. There is no AC power and the site is secure, but care needs to be taken for heavy ocean breezes. The photographs of the site are shown in Figure A9.

MAZC-MAYAGUEZ AIRPORT

This site was installed by the National Geodetic Survey (NGS) inside the Mayaguez Airport. It is quite close to the runway, and there is no AC power available. The location is secure and the airport no longer has commercial flights. The pin is not a standard (NGS) brass plate; it is located on the upper left corner of a drainage system in the open field. To get to the main gate use your car GPS with (Latitude 18.255N and Longitude 292.850E), however, prior to setting up geodetic equipment access must be granted by the Airport manager to get to the site. Contact Hiram Forestier at 787-833-0148 or 787-265-7065. The photographs of the site are shown in Figure A10.

VEGB-VEGA BAJA

This site is located on top of an abandoned fire station, which is now converted to an office for emergency purposes, and used in conjunction with the Police department located right behind the site. The pin is located right on top of the building at the center. It has excellent sky view, and there is AC power available from inside the building. To get to the location use a car GPS with Latitude 18.446N and Longitude 293.609E. Permission to access the site is required prior to set up. Contact the Vega Baja fire station or the administrative offices at the site at 787-858-2330. The photographs of the site are shown in Figure A11.

ZSUB-NATIONAL WEATHER STATION

This site is in front of the National Weather Service station (NWS), which is an agency under the National Oceanic and Atmospheric Administration (NOAA) at Carolina. Use the

coordinates (Latitude 18.446N and Longitude 294.008E) on a car GPS to get to the location. Permission to access the site is necessary from the manager at the (NWS). Contact the secretary at 787-253-4586 or 787-729-8805. The photographs of the site are shown in Figure A12.

Figure A1. Photographs of site ADJN acquired during June 2011 campaign. (A) Photoview facing the northwest. (B) Photoview facing the south.

Figure A2. Photographs of site ARC1 acquired during May 2011 campaign. (A) Photoview facing west. (B) Geodetic monument at ARC1, the geodetic benchmark is inside a concrete slab cemented into local bedrock.

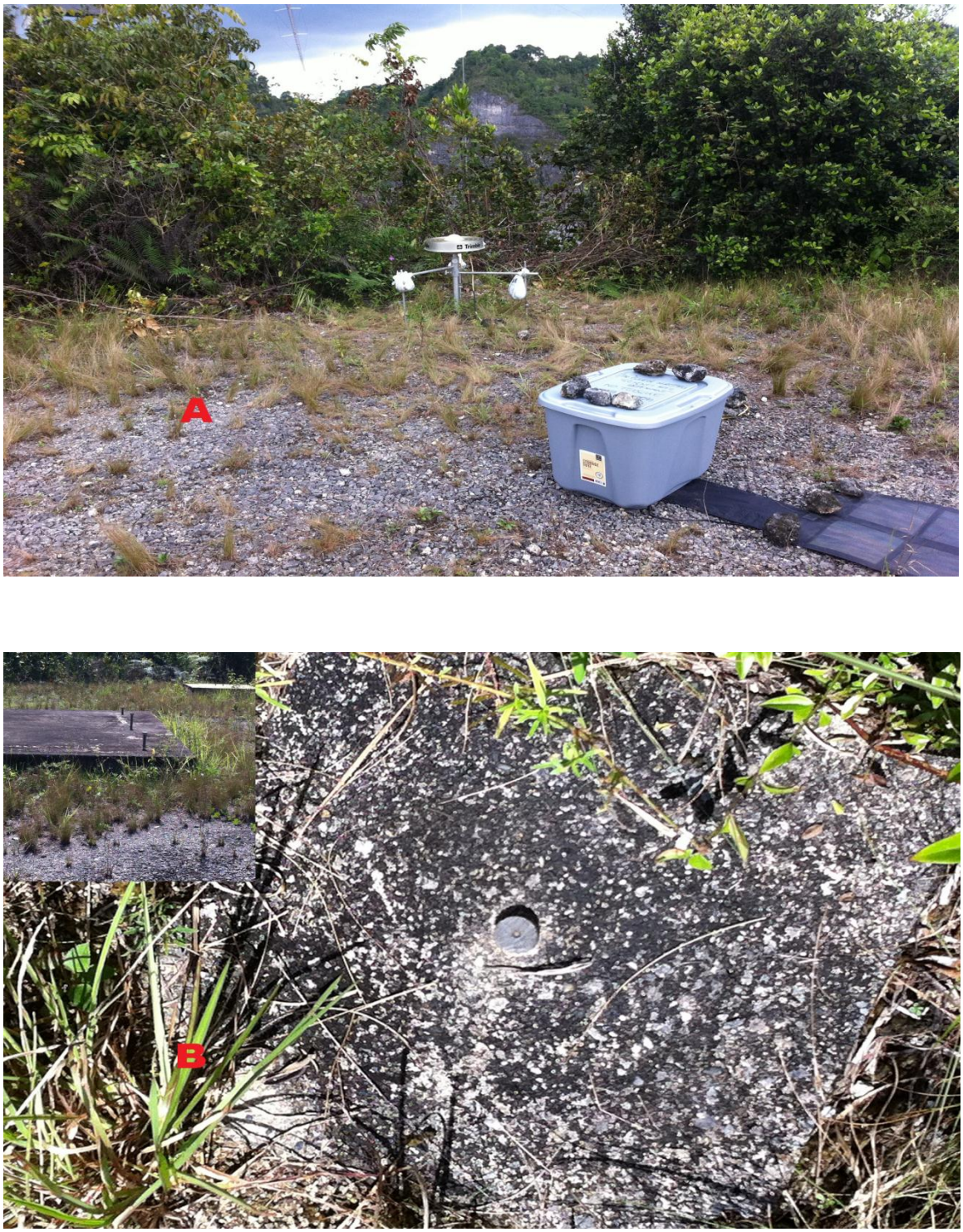

Figure A3. Photographs of site ARC2 acquired during May 2011 campaign. (A) Photoview facing south. (B) Geodetic monument at ARC2. The pin is epoxied into concrete adjacent to the helipad.

Figure A4. Photographs of site CAYE acquired during June 2011 campaign. (A) Photoview of the antenna facing north. (B) Photoview facing northwest while the inset photo is the view facing east.

Figure A5. Photographs of site CCM5-PONCE acquired during June 2011. (A) Photoview of the site with solar power backup connected to the receiver facing northwest. (B) Photoview facing west while the inset photo shows the hole without an antenna. Note: This pipe will allow you to insert a 1'' diameter brass antenna mount.

Figure A6. Photographs of site CIDE acquired during May 2011 campaign. (A) Photoview facing the east. (B) Photoview facing the west.

Figure A7. Photographs of site LAJ1 acquired during May 2011 campaign (A) Photoview of the antenna facing north. (B) Photoview facing east of the gymnasium building with the antenna right on top. Inset photo shows close up of antenna setup (must use a 0.5m spike mount at this site).

Figure A8. Photographs of site LAJ2 acquired during May 2011 campaign (A) Photoview facing west. (B) Photoview facing southwest.

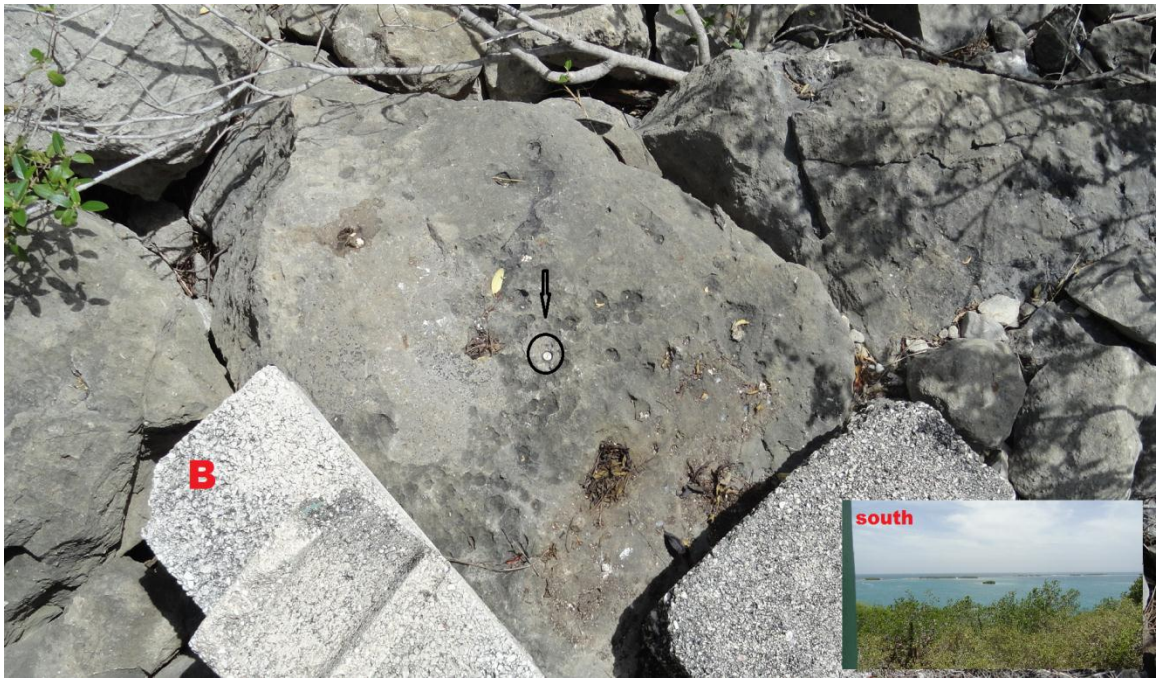

Figure A9. Photographs of site PARG acquired during June 2011 campaign (A) Photoview facing southwest and a mini shade near the site (B) Photoview of the geodetic pin inside the boulder, while the inset photo is the view facing south.

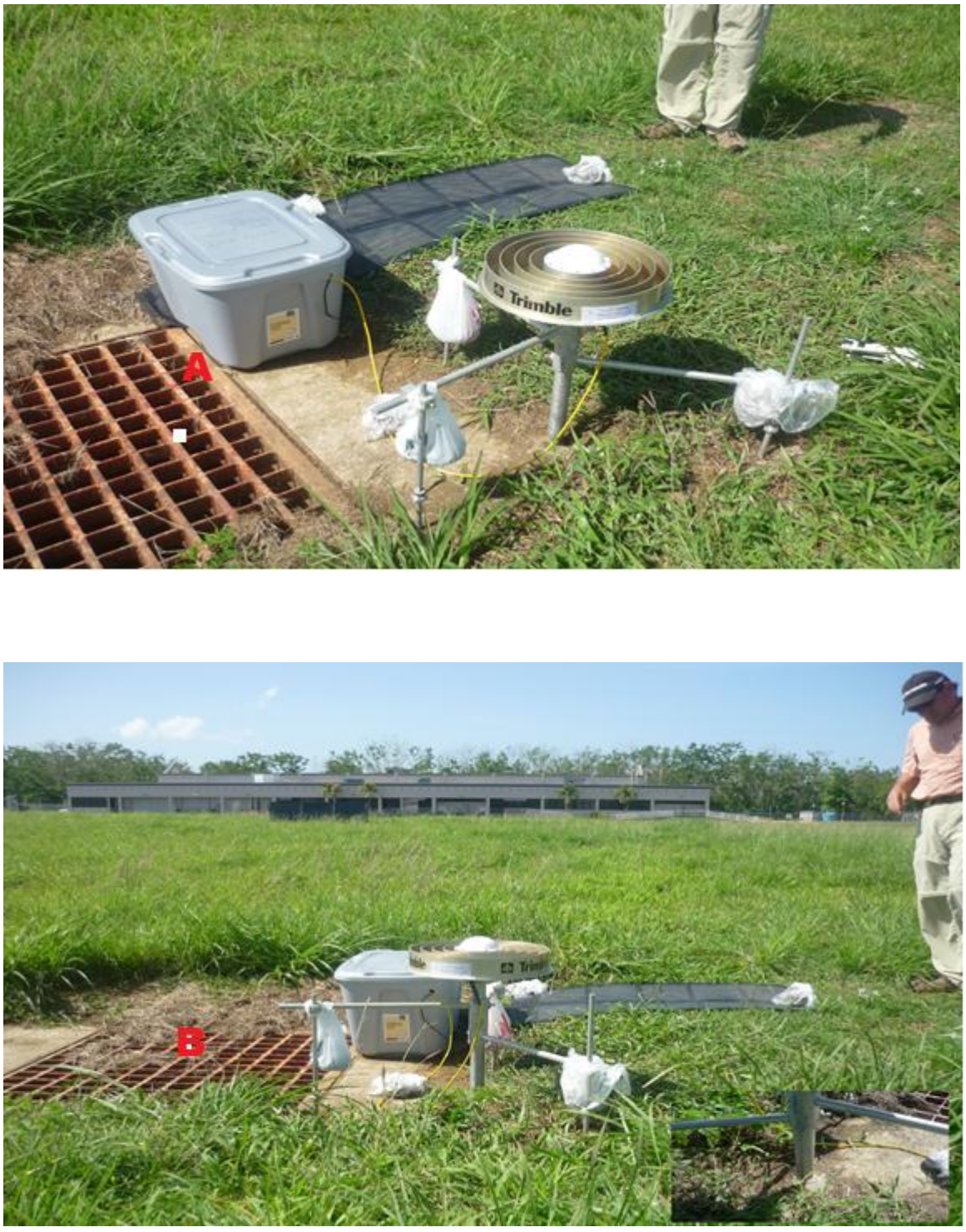

Figure A10. Photographs of site MAZC acquired during May 2011 campaign (A) Photoview of the antenna set up right beside the drainage system (B) Photoview facing north and the inset photo shows the pin location.

Figure A11.Photographs of site VEGB acquired during June 2011 campaign (A) Photoview facing south. (B) Photoview facing northwest on top of the abandoned fire building.

Figure A12. Photographs of site ZSUB acquired during May/June 2011 campaign (A) Photoview of the site right in front of the weather building. (B) Photoview facing east around the car park area.

APPENDIX B

PLATE INVERSION OUTPUT RESULTS

***********INVERSION RESULTS***** - Chuck DeMets *******
Plate inversion output results data used to define CA-ITRF05 results from GCCM program of C. DeMets

>> File header is Rigid plate site velocities - ITRF2005

```
----------- INPUT DATA STATISTICS ------------

# PLATES:  2 # of DATA:  128 DOF: 125
Fixed plate is ca
Optimal angular velocities are in file fort.7

 Covariances are in file format

----------- BEGIN ITERATIVE SEARCH ------------

Results from Iteration 0
-------------------------
> Trial angular velocities
>   it      0.000      0.000    1.0000

> Chi**2   Reduced Chi**2
   ********    *******

> Convergence criteria are:  0.016810457 0.003882895 0.002558442

Results from Iteration 1
-------------------------
> Trial angular velocities
>   it    -33.026     80.600    0.2690

> Chi**2   Reduced Chi**2
    228.312     1.8265

> Convergence criteria are:  0.000000000 0.000000000 0.000000000

----------- END ITERATIVE SEARCH ------------

 The best fitting angular velocities are:
 plate id     Lat      Long     W deg/Myr
 ----- --  ------  ------   ------
    ca       0.0     0.0      .00
    it     -33.026  80.600   0.2690

Final chi**2 and reduced chi**2 are 228.312 and 1.8265

 2D 1-sigma error ellipse and 1D 1-sigma angular velocity uncertainty
 Plate   Ellipse axes azimuth of major axis rot. rate
   id    major   minor   (CCW  from east)      uncert.
   --    -----   -----   ----------------      -------
   it     2.03    0.37          19.77         0.0105
```

Data Type	# Data	Chi**2	Data Importance
Rates	0	0.00	0.00
Transforms	0	0.00	0.00
Slip vectors	0	0.00	0.00
Baselines	0	0.00	0.00
Vn/Ve pairs	128	228.31	2.98

Plate ID	Data Type	Lat	Long	Datum	S.D	Pred wt.	Res.	imp	Pred. az	Site
ca	vn	15.67	296.38	1.71	0.14	1.467	1.746	0.010	90	AVES
ca	ve	15.67	296.38	1.33	0.26	1.021	1.208	0.004	0	AVES
ca	vn	13.09	300.39	1.57	0.10	1.606	-0.348	0.039	90	BARB
ca	ve	13.09	300.39	1.22	0.19	1.152	0.356	0.010	0	BARB
ca	vn	14.51	274.29	0.69	0.18	0.594	0.539	0.059	90	CMP1
ca	ve	14.51	274.29	1.19	0.33	0.968	0.680	0.003	0	CMP1
ca	vn	17.76	295.42	1.34	0.04	1.433	-2.445	0.111	90	CRO1
ca	ve	17.76	295.42	1.09	0.05	0.925	3.297	0.081	0	CRO1
ca	vn	14.73	298.85	1.75	0.16	1.554	1.242	0.013	90	FSD0
ca	ve	14.73	298.85	1.25	0.29	1.077	0.602	0.003	0	FSD0
ca	vn	14.73	298.85	1.80	0.19	1.554	1.317	0.009	90	FSD1
ca	ve	14.73	298.85	1.61	0.25	1.077	2.116	0.004	0	FSD1
ca	vn	15.03	273.93	0.68	0.21	0.579	0.476	0.042	90	GLCO
ca	ve	15.03	273.93	0.93	0.52	0.942	-0.024	0.001	0	GLCO
ca	vn	15.98	298.30	1.63	0.07	1.535	1.422	0.063	90	HOUE
ca	ve	15.98	298.30	1.11	0.08	1.022	1.090	0.035	0	HOUE
ca	vn	14.92	273.62	0.76	0.15	0.565	1.342	0.094	90	MNTO
ca	ve	14.92	273.62	1.24	0.47	0.947	0.628	0.001	0	MNTO
ca	vn	17.90	288.33	1.06	0.11	1.168	-1.026	0.021	90	ROJO
ca	ve	17.90	288.33	1.17	0.22	0.870	1.391	0.004	0	ROJO
ca	vn	12.52	278.27	0.78	0.06	0.762	0.319	0.372	90	SANA
ca	ve	12.52	278.27	1.49	0.10	1.074	4.285	0.043	0	SANA
ca	vn	14.97	273.76	0.60	0.14	0.571	0.203	0.099	90	SFDP
ca	ve	14.97	273.76	1.29	0.38	0.945	0.906	0.002	0	SFDP
ca	vn	12.57	274.63	0.58	0.33	0.608	-0.087	0.017	90	PRT1
ca	ve	12.57	274.63	1.00	0.54	1.063	-0.116	0.001	0	PRT1
ca	vn	14.04	276.62	0.64	0.39	0.693	-0.135	0.010	90	PUEC
ca	ve	14.04	276.62	0.74	0.62	0.998	-0.417	0.001	0	PUEC
ca	vn	12.92	274.78	0.81	0.15	0.615	1.337	0.083	90	RIOB
ca	ve	12.92	274.78	0.70	0.64	1.046	-0.541	0.001	0	RIOB
ca	vn	12.41	274.19	0.74	0.15	0.590	0.988	0.081	90	TEUS
ca	ve	12.41	274.19	0.87	0.18	1.069	-1.088	0.013	0	TEUS
ca	vn	18.73	295.67	1.50	0.06	1.442	0.938	0.046	90	ABVI
ca	ve	18.73	295.67	0.92	0.08	0.885	0.412	0.028	0	ABVI
ca	vn	18.17	293.20	1.45	0.09	1.352	1.113	0.016	90	ADJN
ca	ve	18.17	293.20	0.80	0.14	0.891	-0.639	0.010	0	ADJN
ca	vn	18.73	295.67	1.54	0.11	1.442	0.892	0.014	90	ANEG
ca	ve	18.73	295.67	0.95	0.16	0.885	0.397	0.008	0	ANEG
ca	vn	18.35	293.25	1.51	0.11	1.354	1.407	0.010	90	AOPR
ca	ve	18.35	293.25	0.84	0.14	0.883	-0.300	0.010	0	AOPR
ca	vn	18.35	293.25	1.23	0.06	1.354	-2.031	0.033	90	ARC1
ca	ve	18.35	293.25	0.87	0.08	0.883	-0.158	0.030	0	ARC1

ca	vn	18.34	293.25	1.19	0.10	1.354	-1.639	0.012	90	ARC2
ca	ve	18.34	293.25	0.95	0.152	0.884	0.437	0.009	0	ARC2
ca	vn	18.41	293.84	1.47	0.085	1.376	1.111	0.018	90	BYSP
ca	ve	18.41	293.84	0.83	0.085	0.885	-0.646	0.028	0	BYSP
ca	vn	18.12	293.84	1.43	0.177	1.376	0.308	0.004	90	CAYE
ca	ve	18.12	293.84	0.70	0.366	0.898	-0.540	0.002	0	CAYE
ca	vn	18.08	293.42	1.43	0.071	1.360	0.984	0.025	90	CCM5
ca	ve	18.08	293.42	0.87	0.107	0.896	-0.245	0.018	0	CCM5
ca	vn	18.21	292.86	1.31	0.068	1.339	-0.433	0.027	90	CIDE
ca	ve	18.21	292.86	0.76	0.094	0.886	-1.345	0.023	0	CIDE
ca	vn	18.31	294.72	1.48	0.105	1.408	0.689	0.015	90	CUPR
ca	ve	18.31	294.72	0.91	0.104	0.896	0.134	0.017	0	CUPR
ca	vn	18.38	292.52	1.24	0.123	1.327	-0.706	0.008	90	DSCH
ca	ve	18.38	292.52	0.79	0.181	0.876	-0.477	0.006	0	DSCH
ca	vn	18.38	294.38	1.43	0.069	1.395	0.503	0.029	90	FAJA
ca	ve	18.38	294.38	0.90	0.100	0.890	0.096	0.021	0	FAJA
ca	vn	18.21	292.86	1.27	0.042	1.339	-1.654	0.070	90	GEOL
ca	ve	18.21	292.86	0.87	0.058	0.886	-0.283	0.061	0	GEOL
ca	vn	18.47	292.95	1.34	0.127	1.343	-0.022	0.008	90	ISAB
ca	ve	18.47	292.95	0.68	0.250	0.876	-0.782	0.003	0	ISAB
ca	vn	18.08	292.95	1.62	0.087	1.343	3.186	0.016	90	LAJ1
ca	ve	18.08	292.95	0.85	0.120	0.893	-0.357	0.014	0	LAJ1
ca	vn	18.04	292.93	1.42	0.095	1.342	0.820	0.014	90	LAJ2
ca	ve	18.04	292.93	0.77	0.128	0.894	-0.972	0.012	0	LAJ2
ca	vn	17.99	292.89	1.09	0.125	1.341	-2.005	0.008	90	LAJ3
ca	ve	17.99	292.89	1.19	0.186	0.896	1.579	0.006	0	LAJ3
ca	vn	18.22	292.84	1.52	0.204	1.339	0.889	0.004	90	MAYZ
ca	ve	18.22	292.84	0.65	0.175	0.886	-1.348	0.005	0	MAYZ
ca	vn	18.25	292.85	1.30	0.092	1.339	-0.425	0.015	90	MAZC
ca	ve	18.25	292.85	0.70	0.163	0.885	-1.132	0.008	0	MAZC
ca	vn	17.89	293.47	1.43	0.094	1.362	0.724	0.015	90	MIPR
ca	ve	17.89	293.47	0.97	0.107	0.905	0.608	0.017	0	MIPR
ca	vn	18.11	292.09	1.15	0.122	1.311	-1.318	0.008	90	MONA
ca	ve	18.11	292.09	0.90	0.227	0.885	0.065	0.004	0	MONA
ca	vn	18.08	292.07	1.27	0.110	1.310	-0.364	0.011	90	MOPR
ca	ve	18.08	292.07	0.81	0.123	0.886	-0.622	0.013	0	MOPR
ca	vn	18.08	293.42	1.40	0.091	1.360	0.438	0.016	90	P780
ca	ve	18.08	293.42	0.84	0.094	0.896	-0.598	0.023	0	P780
ca	vn	17.97	292.96	1.54	0.065	1.343	3.028	0.029	90	PARG
ca	ve	17.97	292.96	0.97	0.088	0.898	0.821	0.026	0	PARG
ca	vn	18.08	293.63	1.33	0.095	1.368	-0.399	0.017	90	PR4N
ca	ve	18.08	293.63	0.88	0.088	0.898	-0.202	0.022	0	PR4N
ca	vn	18.45	293.35	1.40	0.159	1.358	0.267	0.007	90	PRAR
ca	ve	18.45	293.35	0.60	0.147	0.879	-1.901	0.007	0	PRAR
ca	vn	18.05	293.19	1.53	0.206	1.352	0.866	0.003	90	PRGY
ca	ve	18.05	293.19	1.09	0.245	0.896	0.792	0.003	0	PRGY

ca	vn	18.38	293.85	1.47	0.221	1.376	0.426	0.005	90	PRHL
ca	ve	18.38	293.85	0.44	0.158	0.886	-2.825	0.004	0	PRHL
ca	vn	18.34	293.00	1.41	0.201	1.345	0.325	0.005	90	PRJC
ca	ve	18.34	293.00	0.63	0.159	0.882	-1.583	0.005	0	PRJC
ca	vn	18.19	294.13	1.44	0.16	1.386	0.334	0.006	90	PRLP
ca	ve	18.19	294.13	0.71	0.18	0.897	-1.032	0.006	0	PRLP
ca	vn	18.06	292.81	1.35	0.26	1.338	0.049	0.008	90	PRLT
ca	ve	18.06	292.81	0.47	0.12	0.893	-3.409	0.003	0	PRLT
ca	vn	17.97	292.95	1.19	0.07	1.343	-2.315	0.033	90	PRMI
ca	ve	17.97	292.95	0.89	0.06	0.898	-0.123	0.046	0	PRMI
ca	vn	18.08	293.63	1.41	0.16	1.368	0.262	0.007	90	PRN4
ca	ve	18.08	293.63	0.68	0.14	0.898	-1.601	0.008	0	PRN4
ca	vn	18.46	292.93	1.29	0.04	1.342	-1.301	0.077	90	PUR3
ca	ve	18.46	292.93	0.84	0.07	0.876	-0.536	0.046	0	PUR3
ca	vn	18.46	292.93	1.36	0.07	1.342	0.249	0.024	90	PUR5
ca	ve	18.46	292.93	0.83	0.08	0.876	-0.581	0.032	0	PUR5
ca	vn	18.03	293.77	1.34	0.12	1.373	-0.275	0.009	90	SALN
ca	ve	18.03	293.77	0.74	0.18	0.901	-0.910	0.007	0	SALN
ca	vn	18.34	295.03	1.45	0.10	1.419	0.321	0.016	90	STVI
ca	ve	18.34	295.03	1.00	0.12	0.897	0.879	0.015	0	STVI
ca	vn	18.15	294.16	0.77	0.19	1.387	-3.249	0.004	90	UPRH
ca	ve	18.15	294.16	0.91	0.28	0.899	0.040	0.003	0	UPRH
ca	vn	18.40	293.95	1.17	0.09	1.380	-2.409	0.017	90	UPRR
ca	ve	18.40	293.95	1.03	0.12	0.886	1.208	0.014	0	UPRR
ca	vn	18.45	293.61	1.14	0.13	1.367	-1.695	0.007	90	VEGB
ca	ve	18.45	293.61	0.89	0.17	0.881	0.049	0.007	0	VEGB
ca	vn	18.12	294.56	1.42	0.23	1.402	0.080	0.003	90	VIEN
ca	ve	18.12	294.56	0.65	0.34	0.903	-0.744	0.002	0	VIEN
ca	vn	18.13	294.49	1.64	0.23	1.399	1.065	0.003	90	VIEQ
ca	ve	18.13	294.49	0.47	0.37	0.902	-1.158	0.001	0	VIEQ
ca	vn	17.72	295.20	1.37	0.08	1.425	-0.705	0.028	90	VIKH
ca	ve	17.72	295.20	1.09	0.08	0.925	2.086	0.030	0	VIKH
ca	vn	18.34	295.03	1.45	0.06	1.419	0.503	0.039	90	VITH
ca	ve	18.34	295.03	0.88	0.07	0.897	-0.231	0.037	0	VITH
ca	vn	18.43	294.01	1.41	0.05	1.382	0.565	0.052	90	ZSU1
ca	ve	18.43	294.01	0.83	0.06	0.885	-1.006	0.068	0	ZSU1
ca	vn	18.43	294.01	1.03	0.12	1.382	-3.007	0.010	90	ZSUA
ca	ve	18.43	294.01	1.06	0.16	0.885	1.105	0.008	0	ZSUA
ca	vn	18.43	294.01	1.84	0.10	1.382	4.773	0.014	90	ZSUB
ca	ve	18.43	294.01	0.61	0.14	0.885	-1.925	0.010	0	ZSUB

***********INVERSION RESULTS – Chuck DeMets *******
>> File header is Rigid plate site velocities - ITRF2005

```
---------- INPUT DATA STATISTICS ------------

# PLATES:  3 # of DATA:  128 DOF: 122
Fixed plate is   ca
Optimal angular velocities are in file fort.7

 Covariances are in file format

---------- BEGIN ITERATIVE SEARCH ------------

Results from Iteration 0
------------------------
> Trial angular velocities
>   it      0.000      0.000    1.0000
>   pr      0.000      0.000    1.0000

> Chi**2   Reduced Chi**2
   ********    *******

> Convergence criteria are:  0.016528325 0.003104702 0.001662713


Results from Iteration 1
------------------------
> Trial angular velocities
>   it    -36.820     78.418    0.2637
>   pr     11.342    -66.877    0.1652

> Chi**2   Reduced Chi**2
    186.310     1.5271

> Convergence criteria are:  0.000000000 0.000000000 0.000000000

---------- END ITERATIVE SEARCH ------------

 The best fitting angular velocities are:
 plate id     Lat     Long     W deg/Myr
 ----- --  ------  ------   ------
    ca       0.0     0.0      .00
    it     -36.820  78.418   0.2637
    pr      11.342 -66.877   0.1652



Final chi**2 and reduced chi**2 are 186.310 and 1.5271
```

2D 1-sigma error ellipse and 1D 1-sigma angular velocity uncertainty

Plate id	Ellipse axes major	minor	azimuth of major axis (CCW from east)	rot. rate uncert.
it	2.38	0.80	28.61	0.0109
pr	5.01	1.20	87.21	0.0800

Data Type	# Data	Chi**2	Data Importance
Rates	0	0.00	0.00
Transforms	0	0.00	0.00
Slip vectors	0	0.00	0.00
Baselines	0	0.00	0.00
Vn/Ve pairs	128	186.31	5.99

Plate ID	Data Type	Lat	Long	Datum	S.D	Pred wt.	Res.	imp	Pred. az	Site
ca	vn	15.67	296.38	1.71	0.139	1.445	1.905	0.038	90	AVES
ca	ve	15.67	296.38	1.33	0.256	1.193	0.534	0.016	0	AVES
ca	vn	13.09	300.39	1.57	0.104	1.571	-0.013	0.103	90	BARB
ca	ve	13.09	300.39	1.22	0.190	1.318	-0.514	0.031	0	BARB
ca	vn	14.51	274.29	0.69	0.178	0.643	0.266	0.063	90	CMP1
ca	ve	14.51	274.29	1.19	0.326	1.137	0.164	0.010	0	CMP1
ca	vn	17.76	295.42	1.34	0.038	1.414	-1.945	0.474	90	CRO1
ca	ve	17.76	295.42	1.09	0.050	1.103	-0.253	0.409	0	CRO1
ca	vn	14.73	298.85	1.75	0.158	1.524	1.432	0.038	90	FSD0
ca	ve	14.73	298.85	1.25	0.288	1.246	0.013	0.013	0	FSD0
ca	vn	14.73	298.85	1.80	0.187	1.524	1.477	0.027	90	FSD1
ca	ve	14.73	298.85	1.61	0.252	1.246	1.443	0.017	0	FSD1
ca	vn	15.03	273.93	0.68	0.213	0.628	0.242	0.046	90	GLCO
ca	ve	15.03	273.93	0.93	0.523	1.112	-0.347	0.004	0	GLCO
ca	vn	15.98	298.30	1.63	0.067	1.506	1.843	0.201	90	HOUE
ca	ve	15.98	298.30	1.11	0.081	1.195	-1.044	0.156	0	HOUE
ca	vn	14.92	273.62	0.76	0.145	0.616	0.992	0.101	90	MNTO
ca	ve	14.92	273.62	1.24	0.467	1.116	0.266	0.005	0	MNTO
ca	vn	17.90	288.33	1.06	0.105	1.172	-1.062	0.050	90	ROJO
ca	ve	17.90	288.33	1.17	0.216	1.048	0.566	0.022	0	ROJO
ca	vn	12.52	278.27	0.78	0.057	0.798	-0.315	0.421	90	SANA
ca	ve	12.52	278.27	1.49	0.097	1.238	2.597	0.123	0	SANA
ca	vn	14.97	273.76	0.60	0.141	0.622	-0.153	0.105	90	SFDP
ca	ve	14.97	273.76	1.29	0.381	1.114	0.462	0.007	0	SFDP

ca	vn	12.57	274.63	0.58	0.329	0.656	-0.231	0.018	90	PRT1
ca	ve	12.57	274.63	1.00	0.538	1.226	-0.420	0.004	0	PRT1
ca	vn	14.04	276.62	0.64	0.389	0.734	-0.241	0.011	90	PUEC
ca	ve	14.04	276.62	0.74	0.618	1.165	-0.688	0.003	0	PUEC
ca	vn	12.92	274.78	0.81	0.146	0.662	1.014	0.090	90	RIOB
ca	ve	12.92	274.78	0.70	0.640	1.210	-0.798	0.003	0	RIOB
ca	vn	12.41	274.19	0.74	0.152	0.639	0.667	0.087	90	TEUS
ca	ve	12.41	274.19	0.87	0.183	1.232	-1.978	0.035	0	TEUS
pr	vn	18.73	295.67	1.50	0.062	1.502	-0.035	0.319	90	ABVI
pr	ve	18.73	295.67	0.92	0.084	0.829	1.080	0.041	0	ABVI
pr	vn	18.17	293.20	1.45	0.088	1.343	1.221	0.024	90	ADJN
pr	ve	18.17	293.20	0.80	0.142	0.851	-0.358	0.013	0	ADJN
pr	vn	18.73	295.67	1.54	0.110	1.502	0.344	0.095	90	ANEG
pr	ve	18.73	295.67	0.95	0.163	0.829	0.740	0.011	0	ANEG
pr	vn	18.35	293.25	1.51	0.111	1.346	1.479	0.015	90	AOPR
pr	ve	18.35	293.25	0.84	0.144	0.838	0.014	0.012	0	AOPR
pr	vn	18.35	293.25	1.23	0.061	1.346	-1.899	0.048	90	ARC1
pr	ve	18.35	293.25	0.87	0.083	0.838	0.386	0.037	0	ARC1
pr	vn	18.34	293.25	1.19	0.100	1.346	-1.558	0.018	90	ARC2
pr	ve	18.34	293.25	0.95	0.152	0.839	0.732	0.011	0	ARC2
pr	vn	18.41	293.84	1.47	0.085	1.384	1.010	0.025	90	BYSP
pr	ve	18.41	293.84	0.83	0.085	0.838	-0.094	0.035	0	BYSP
pr	vn	18.12	293.84	1.43	0.177	1.384	0.259	0.006	90	CAYE
pr	ve	18.12	293.84	0.70	0.366	0.859	-0.435	0.002	0	CAYE
pr	vn	18.08	293.42	1.43	0.071	1.357	1.029	0.032	90	CCM5
pr	ve	18.08	293.42	0.87	0.107	0.859	0.103	0.023	0	CCM5
pr	vn	18.21	292.86	1.31	0.068	1.320	-0.153	0.055	90	CIDE
pr	ve	18.21	292.86	0.76	0.094	0.845	-0.908	0.029	0	CIDE
pr	vn	18.31	294.72	1.48	0.105	1.441	0.370	0.048	90	CUPR
pr	ve	18.31	294.72	0.91	0.104	0.852	0.557	0.021	0	CUPR
pr	vn	18.38	292.52	1.24	0.123	1.298	-0.473	0.025	90	DSCH
pr	ve	18.38	292.52	0.79	0.181	0.830	-0.223	0.008	0	DSCH
pr	vn	18.38	294.38	1.43	0.069	1.419	0.157	0.067	90	FAJA
pr	ve	18.38	294.38	0.90	0.100	0.844	0.557	0.026	0	FAJA
pr	vn	18.21	292.86	1.27	0.042	1.320	-1.200	0.146	90	GEOL
pr	ve	18.21	292.86	0.87	0.058	0.845	0.424	0.076	0	GEOL
pr	vn	18.47	292.95	1.34	0.127	1.326	0.108	0.014	90	ISAB
pr	ve	18.47	292.95	0.68	0.250	0.827	-0.588	0.004	0	ISAB
pr	vn	18.08	292.95	1.62	0.087	1.326	3.376	0.031	90	LAJ1
pr	ve	18.08	292.95	0.85	0.120	0.856	-0.047	0.019	0	LAJ1
pr	vn	18.04	292.93	1.42	0.095	1.325	1.000	0.026	90	LAJ2
pr	ve	18.04	292.93	0.77	0.128	0.858	-0.691	0.017	0	LAJ2
pr	vn	17.99	292.89	1.09	0.125	1.322	-1.859	0.016	90	LAJ3
pr	ve	17.99	292.89	1.19	0.186	0.862	1.765	0.008	0	LAJ3
pr	vn	18.22	292.84	1.52	0.204	1.319	0.985	0.009	90	MAYZ
pr	ve	18.22	292.84	0.65	0.175	0.844	-1.111	0.006	0	MAYZ
pr	vn	18.25	292.85	1.30	0.092	1.320	-0.215	0.031	90	MAZC
pr	ve	18.25	292.85	0.70	0.163	0.842	-0.873	0.010	0	MAZC

pr	vn	17.89	293.47	1.43	0.094	1.360	0.743	0.019	90	MIPR
pr	ve	17.89	293.47	0.97	0.107	0.873	0.904	0.025	0	MIPR
pr	vn	18.11	292.09	1.15	0.122	1.270	-0.984	0.041	90	MONA
pr	ve	18.11	292.09	0.90	0.227	0.847	0.232	0.005	0	MONA
pr	vn	18.08	292.07	1.27	0.110	1.269	0.012	0.052	90	MOPR
pr	ve	18.08	292.07	0.81	0.123	0.849	-0.320	0.017	0	MOPR
pr	vn	18.08	293.42	1.40	0.091	1.357	0.474	0.020	90	P780
pr	ve	18.08	293.42	0.84	0.094	0.859	-0.202	0.029	0	P780
pr	vn	17.97	292.96	1.54	0.065	1.327	3.278	0.054	90	PARG
pr	ve	17.97	292.96	0.97	0.088	0.864	1.207	0.036	0	PARG
pr	vn	18.08	293.63	1.33	0.095	1.371	-0.427	0.021	90	PR4N
pr	ve	18.08	293.63	0.88	0.088	0.861	0.221	0.029	0	PR4N
pr	vn	18.45	293.35	1.40	0.159	1.352	0.300	0.009	90	PRAR
pr	ve	18.45	293.35	0.60	0.147	0.831	-1.574	0.009	0	PRAR
pr	vn	18.05	293.19	1.53	0.206	1.342	0.913	0.005	90	PRGY
pr	ve	18.05	293.19	1.09	0.245	0.860	0.941	0.004	0	PRGY
pr	vn	18.38	293.85	1.47	0.221	1.385	0.385	0.007	90	PRHL
pr	ve	18.38	293.85	0.44	0.158	0.840	-2.533	0.005	0	PRHL
pr	vn	18.34	293.00	1.41	0.201	1.330	0.400	0.009	90	PRJC
pr	ve	18.34	293.00	0.63	0.159	0.837	-1.301	0.006	0	PRJC
pr	vn	18.19	294.13	1.44	0.161	1.403	0.230	0.010	90	PRLP
pr	ve	18.19	294.13	0.71	0.181	0.856	-0.808	0.007	0	PRLP
pr	vn	18.06	292.81	1.35	0.255	1.317	0.129	0.018	90	PRLT
pr	ve	18.06	292.81	0.47	0.124	0.856	-3.113	0.004	0	PRLT
pr	vn	17.97	292.95	1.19	0.066	1.326	-2.065	0.061	90	PRMI
pr	ve	17.97	292.95	0.89	0.062	0.864	0.425	0.064	0	PRMI
pr	vn	18.08	293.63	1.41	0.161	1.371	0.245	0.009	90	PRN4
pr	ve	18.08	293.63	0.68	0.136	0.861	-1.328	0.010	0	PRN4
pr	vn	18.46	292.93	1.29	0.040	1.325	-0.874	0.149	90	PUR3
pr	ve	18.46	292.93	0.84	0.067	0.827	0.187	0.058	0	PUR3
pr	vn	18.46	292.93	1.36	0.072	1.325	0.487	0.047	90	PUR5
pr	ve	18.46	292.93	0.83	0.079	0.827	0.032	0.041	0	PUR5
pr	vn	18.03	293.77	1.34	0.120	1.380	-0.330	0.012	90	SALN
pr	ve	18.03	293.77	0.74	0.177	0.865	-0.708	0.009	0	SALN
pr	vn	18.34	295.03	1.45	0.097	1.461	-0.114	0.070	90	STVI
pr	ve	18.34	295.03	1.00	0.117	0.852	1.262	0.018	0	STVI
pr	vn	18.15	294.16	0.77	0.190	1.405	-3.342	0.007	90	UPRH
pr	ve	18.15	294.16	0.91	0.279	0.859	0.181	0.003	0	UPRH
pr	vn	18.40	293.95	1.17	0.087	1.391	-2.544	0.026	90	UPRR
pr	ve	18.40	293.95	1.03	0.119	0.840	1.601	0.018	0	UPRR
pr	vn	18.45	293.61	1.14	0.134	1.369	-1.711	0.009	90	VEGB
pr	ve	18.45	293.61	0.89	0.174	0.833	0.326	0.009	0	VEGB
pr	vn	18.12	294.56	1.42	0.228	1.431	-0.047	0.007	90	VIEN
pr	ve	18.12	294.56	0.65	0.340	0.865	-0.631	0.002	0	VIEN
pr	vn	18.13	294.49	1.64	0.226	1.426	0.946	0.007	90	VIEQ
pr	ve	18.13	294.49	0.47	0.373	0.863	-1.055	0.002	0	VIEQ
ca	vn	17.72	295.20	1.37	0.078	1.407	-0.471	0.121	90	VIKH
ca	ve	17.72	295.20	1.09	0.079	1.103	-0.160	0.151	0	VIKH

pr	vn	18.34	295.03	1.45	0.062	1.461	-0.179	0.168	90	VITH
pr	ve	18.34	295.03	0.88	0.074	0.852	0.373	0.047	0	VITH
pr	vn	18.43	294.01	1.41	0.050	1.395	0.296	0.084	90	ZSU1
pr	ve	18.43	294.01	0.83	0.055	0.838	-0.142	0.086	0	ZSU1
pr	vn	18.43	294.01	1.03	0.117	1.395	-3.121	0.015	90	ZSUA
pr	ve	18.43	294.01	1.06	0.158	0.838	1.406	0.010	0	ZSUA
pr	vn	18.43	294.01	1.84	0.096	1.395	4.633	0.023	90	ZSUB
pr	ve	18.43	294.01	0.61	0.143	0.838	-1.593	0.013	0	ZSUB

REFERENCES

Blewitt, G., Heflin, M.B., Webb, F.H., Lindqwister, U.J., and Malla, R.P., 1992*, Global coordinates with centimeter accuracy in the International Terrestrial Reference Frame using GPS*: Geophysical Research Letters, v. 19, p. 853–856.

Boysee, P., Andreieff, P.,Richard, M., Baubron, J., Mascle, A., Mauray,R.& Westercamp, D. 1985*. Aves Swell and northern Lesser Antilles Rigde: rock dredging results from Arcante 3 cruise: in Mascle*, A. (ed), Geodynamiques des caribres, Symposium, Paris, 5-8 Fevrier. Editions Technip, Paris, 65-75.

Byrne, D.B., Suarez, G., and McCann, W.R., 1985, *Muertos Trough Subduction—Microplate tectonics in the northern Caribbean*: Nature, v. 317, p. 420–421.

Cox, D.F., Marvin, F.R, M' Gonigle, J.W., McIntyre, D.H. & Rogers, C. 1977, *Potassium-argon chronology of some metamorphic, igneous and hydrothermal events in Puerto Rico and Virgin Island*. USGS Journal of Research, 5, 689-703.

DeMets, C., Jansma, P., Mattioli, G., Dixon, T., Farina, F., Bilham, R., Calais, E., and Mann, P., 2000*, GPS geodetic constraints on Caribbean–North America plate motion: Implications for plate rigidity and oblique plate boundary convergence*: Geophysical Research Letters, v. 27, p. 437–440, doi: 10.1029/1999GL005436.

Deng, J., and Sykes, L.R., 1995, *Determination of Euler pole for contemporary relative motion of Caribbean and North American plates using slip vectors of interplate earthquakes*: Tectonics, v. 14, p. 39–53, doi: 10.1029/ 94TC02547.

Dixon, T.H., Farina, F., DeMets, C., Jansma, P., Mann, P., and Calais, E., 1998, *Caribbean–North American plate relative motion and strain partitioning across the northern Caribbean plate boundary zone from a decade of GPS observations:* Journal of Geophysical Research, v. 103, p. 15,157–15,182, doi: 10.1029/97JB03575.

Draper, G., and Bartel, J.M. 1990, *Development of cleavage in the Cretaceous rocks of St. Croix, U.S.V.I., and some tectonic implications*. Geological Society of America, Abstract with programs, 22, A337

Erickson, J.P., Pindell, J.L. & Larue, D.K. 1989, *Mid Eocene-early Oligocene sinistral transcurrent faulting in Puerto – Rico associated with formation of the northern Caribbean Plate Boundary Zone*. Journal of Geology, 98, p365-384.

Erikson, J., Pindell, J., and Larue, D., 1990, *Tectonic evolution of the south central Puerto Rico region: Evidence for transpressional tectonism*: Journal of Geology, v. 98, p. 365–368.

Erikson, J., Pindell, J., and Larue, D., 1991*, Fault zone deformational constraints on Paleogene tectonic evolution in southern Puerto Rico*: Geophysical Research Letters, v. 18, p. 569–572.

Frankel, A., McCann, W.R., and Murphy, A.J., 1980*, Observations from a seismic network in the Virgin Islands region: Tectonic structures and earthquake swarms*: Journal of Geophysical Research, v. 85, p. 2,669–2,678.

Glover, L., III, 1971, *Geology of the Coama area, Puerto Rico and its relation to the volcanic arc-trench association*: U.S. Geological Survey Professional Paper 636, p. 102.

Glover, L., III, and Mattson, P., 1960, Successive thrust and transcurrent faulting during the early Tertiary in south-central Puerto Rico: U.S. Geological Survey Professional Paper 400-B, 363–365.

Grindlay, N.R., Mann, P., and Dolan, J.F., 1997, *Researchers investigate submarine faults north of Puerto Rico*: Eos (Transactions, American Geophysical Union), v. 78, p. 404.

Heflin, M., Bertiger, W., Blewitt, G., Freedman, A., Hurst, K., Lichten, S., Lindqwister, U., Vigue, Y., Webb, F., Yunck, T., and Zumberge, J., 1992, *Global geodesy using GPS without fiducial sites*: Geophysical Research Letters, 19, p. 131.

Helsey, C.E. 1960, *Geology of the British Virgin Islands*, unpublished Ph.D. thesis, Princeton University, p. 219.

Holcombe, T.L., Fisher, C.G., and Bowles, F.A., 1989, *Gravity-flow deposits from the St. Croix Ridge; depositional history*: Geo-Marine Letters, v. 9, p. 11–18.

James, Stephen, 2008, *Volcanic Process Inferred from GPS Geodesy*, Dominica, Lesser Antilles. MS Thesis. University of Arkansas, Arkansas, p. 9-12.

Jansma, P., Mattioli, G., Lopez, A., DeMets, C., Dixon, T., Mann, P., and Calais, E., 2000, *Neotectonics of Puerto Rico and the Virgin Islands, northeastern Caribbean from GPS geodesy*: Tectonics, v. 19, p. 1021–1037.

Jansma, P.E., and G.S. Mattioli, G.S., 2005, *GPS results from Puerto Rico and the Virgin Islands: Constraints on tectonic setting and rates of active faulting*, in Mann, P., ed., Active tectonics and seismic hazards of Puerto Rico, the Virgin Islands, and offshore areas: Geological Society of America Special Paper 385, p. 13–30.

Jany, I., Mauffret, A., Bouysse, P., Mascle, A., Mercier de Lépinay, B.,Renard, V., and Stephan, J.F., 1987, *Relevé bathymétrique Sea beam et tectonique en décrochement au sud des Iles Vierges (Nord-Est Caraibes):*Comptes Rendus de l'Académie des Sciences, Serie II, Mecanique,Physique, Chimie, Sciences de l'Univers: Sciences de la Terre, v. 304,p. 527–532.

Jordan, T.H. 1975, *The present day motions of the Caribbean Plate*. Journal of geophysical research, 80, 4433-4440 Ladd, J.W., Worzel, J.L., and Watkins, J.S., 1977, *Multifold seismic reflection records from the northern Venezuela Basin and the north slope of MuertosTrench,* in Talwani, M., and Pitman, W.C., eds., Island arcs, deep-sea trenches and back-arc basins: Washington, D.C., American Geophysical Union, p. 41–56.

Ladd, J.W., and Watkins, J.S., 1978, *Active margin structures within the north slope of the Muertos Trough*: Geologie en Mijnbouw, v. 57, p. 225–260. (Larue, D.K., and Ryan, H.F., 1990, Extensional tectonism in the Mona Passage, Puerto Rico and Hispaniola: a preliminary study: Transactions of the Caribbean Geological Conference, v. 12, p. 301–313).

Larue, D.K., and Ryan, H.F., 1998, *Seismic reflection profiles of the Puerto Rico Trench; shortening between the North American and Caribbean plates*, in Lidiak, E.G., and Larue, D.K., eds., Tectonics and geochemistry of the northeastern Caribbean: Geological Society of America Special Paper 322, p. 193–210.

Lewis, J.F. and Draper, G (with Bourdon, C., Bowin, C., Mattson, P., Maurrasse, F., Nagle, F., & Pardo, G.) 1990. *Geology and tectonic evolution of the northern Caribbean margin*: in Dengo, G. & Case, J.E. The Caribbean region, 77-140. GSA (Geologic Society of America).

Mann, P., Taylor, F., Edwards, L., and Ku, T., 1995, *Actively evolving microplate formation by oblique collision and sideways motion along strike slip faults*: an example from the northeastern Caribbean plate margin: Tectonophysics, v. 246, p. 1–69, doi: 10.1016/0040-1951(94)00268-E.

Mao, A., Harrison, C.G.A., and Dixon, T.H., 1999, *Noise in GPS coordinate time series*: Journal of Geophysical Research, v. 104, p. 2,797–2,816. Masson, D.G., and Scanlon, K.M., 1991, The neotectonic setting of Puerto Rico: Geological Society of America Bulletin, v. 103, p. 144–154.

Matson, Shane, E., 2007, *Arc Kinematics of the Northern Lesser Antilles from GPS Geodesy* MS Thesis, University of Arkansas, Arkansas, p. 1-3, 13, 38-41.

Mauffret, A., and Jany, I., 1990, *Collision et tectonique d'expulsion le long de la frontiere Nord-Caraibe*: Oceanologica Acta, v. 10, p. 97–116.

McCann, W.R., 1985, *On the earthquake hazards of Puerto Rico and the Virgin Islands*: Bulletin of the Seismological Society of America, v. 75, p. 251–262.

McCann, W.R., 2002, *Micro earthquake data elucidate details of Caribbean Subduction zone*: Seismological Research Letters, v. 73, p. 25–32.

McCann, W.R., and Pennington, W.D., 1990, *Seismicity, large earthquakes, and the margin of the Caribbean plate,* in Dengo, G., and Case, J., eds.,The Geology of North America, The Caribbean Region: Geological Society of America: Boulder, Colorado, Geology of North America, v. H, p 291-306.

Murphy, A.J., and McCann, W.R., 1979*, Preliminary results from a new seismic network in the northeastern Caribbean*: Bulletin of the Seismological Society of America, v. 69, p. 1497–1513.

Officer, C.B., Ewing, J.I.,Hennion, D.G., Harkrider, D.G. & Miller, D.E. 1959, *Geophysical investigations of the eastern Caribbean: Venezuela Basin, Antilles island arc, and PRT*.

Pacheco J.F., and Sykes, L.R., 1992, Seismic moment catalog of large shallow earthquakes, 1900 to 1989: Bulletin of the Seismological Society of America, v. 82, p. 1306–1349.

Reid, J., Plumley, P., and Schellekens, J., 1991, *Paleomagnetic evidence for late Miocene counterclockwise rotation of the North Coast carbonate sequence, Puerto Rico*: Geophysical Research Letters, v. 18, p. 565–568.

Seiglie, G.A. and Moussa, M.T 1984, *Late Oligocene-Pliocene transgressive-regressive cycles of sedimentation in northwestern Puerto – Rico international unconformity and hydrocarbon accumulatio*n. AAPG memoir, p. 36, 89-96.

Turner, Henry, III, 2003, *Strain/Slip partitioning along the Middle American Trench in Nicaraqua: Constrained by GPS Geodesy*, M.S. Thesis. University of Arkansas, Arkansas, p. 19-30.

Van Gestel, J., Mann, P., Dolan, J., and Grindlay, N., 1998, *Structure and tectonics of the upper Cenozoic Puerto Rico–Virgin Islands carbonate platform as determined from seismic reflection studies*: Journal of Geophysical Research, v. 103, p. 30,505, doi: 10.1029/98JB02341.

Weber, J.C., Dixon, T., DeMets, C., Ambeh, W.B., Jansma, P., Mattioli, G.,Saleh, J., Sella, G., Bilham, R., and Pérez, O., 2001*, A GPS estimate of relative motion between the Caribbean and South American plates and geologic implications for Trinidad and Venezuela*: Geology, v. 29,p. 75–78, doi: 10.1130/0091-7613(2001)0292.

Whetten, J.T., 1966, *Geology of St. Croix, U.S. Virgin Islands*: in Hess, H.H (ed), Carribean Geological Investigation. Geological Society of America Memoir, 98, 177-239.

Zumberge, J.F., Heflin, M., Jefferson, D., Watkins, M., and Webb, F., 1997*, Precise point positioning for efficient and robust analysis of GPS data from large networks*, Journal of Geophysical Research, v. 102, p. 5,005–5,017.

BIOGRAPHICAL INFORMATION

Desmond Ihemedu has a bachelor's degree in Applied Geophysics from Obafemi Awolowo University Ile-Ife, Nigeria. He worked for three years with Hypergear Services before relocating to the United States. At UTA, he worked with Prof. Glen S. Mattioli on his master's thesis research and earned a master's degree in Geology (Petroleum geosciences option) 2011 at the University of Texas at Arlington. He is presently prepared to take up the challenges of a long time career in the petroleum industry.